

## CHAPTER VI

### Cell-Mediated Matrix Stiffening Accompanies Capillary Morphogenesis In Ultra-Soft Amorphous Hydrogels

© 2019 Elsevier Ltd. All rights reserved

#### 6.1 ABSTRACT

There is a critical need for biomaterials that support robust neovascularization for a wide-range of clinical applications. Here we report how cells alter tissue-level mechanical properties during capillary morphogenesis using a model of endothelial-stromal cell co-culture within poly(ethylene glycol) (PEG) based hydrogels. After a week of culture, we observed substantial stiffening in hydrogels with very soft initial properties. Endothelial cells or stromal cells alone, however, failed to induce hydrogel stiffening. This stiffening tightly correlated with degree of vessel formation but not with hydrogel compaction or cellular proliferation. Despite a lack of fibrillar architecture within the PEG hydrogels, cell-generated contractile forces were essential for hydrogel stiffening. Upregulation of alpha smooth muscle actin and collagen-1 was also correlated with enhanced vessel formation and hydrogel stiffening. Blocking cell-mediated hydrogel degradation abolished stiffening, demonstrating that matrix metalloproteinase (MMP)-mediated remodeling is required for stiffening to occur. These results highlight the dynamic reciprocity between cells and their mechanical microenvironment during capillary morphogenesis and provide important insights for the rational design of materials for vasculogenic applications.

#### 6.2 INTRODUCTION

Biomaterials that support capillary formation are critical for wide ranging regenerative medicine applications (1, 246). To date, most studies of 3D capillary morphogenesis have used biologically-derived extracellular matrix (ECM) hydrogels such as fibrin, collagen and Matrigel (93). Synthetic, proteolytically degradable poly(ethylene glycol) (PEG) hydrogel ECMs also have attracted interest because of their biocompatibility and versatile macromer chemistry (94). However, the extent of capillary morphogenesis is significantly restricted in PEG hydrogels compared with biologically-derived ECMs (114, 231, 247). To overcome this limitation, a range of strategies have emerged to modulate initial hydrogel properties (221, 248) and to incorporate proangiogenic biological cues into PEG hydrogels to enhance their angiogenic potential (133, 225, 247, 249). Despite this interest, relatively few studies have investigated how cellular remodeling of these minimalist PEG matrices accompanies microvascular morphogenesis (221).

Biophysical and biochemical cues in the ECM guide cellular remodeling, which in turn, alters the mechanical and biochemical microenvironment (250). This dynamic and reciprocal relationship between cells and their ECM occurs throughout capillary morphogenesis. While many biochemical cues have been established (2), the relationship between microvascular cells and their mechanical microenvironment also plays a critical role. In fibrillar ECMs, mechanical tension helps guide endothelial migration and sprouting (6, 68) and fiber recruitment plays an important role in this process both in 2D (66) and 3D (64). Stiffening of initially soft fibrillar hydrogels occurs both locally and globally as capillary morphogenesis proceeds (64, 251). However, whether soft or stiff fibrillar ECMs best support vessel formation depends on the model system used (13).

In PEG hydrogels, the pericellular microenvironment has an amorphous nano-scale architecture that is distinct from fibrillar ECMs (219) which alters how force transmission

occurs. In contrast to conflicting reports regarding stiffness effects in fibrillar ECMs, in PEG hydrogels capillary morphogenesis is inversely related to initial modulus (114, 133, 221, 230). Though differences in matrix degradability (91) and diffusion (114) likely contribute to these effects, whether cell-mediated mechanical cues contribute to enhanced capillary morphogenesis in these soft amorphous matrices, which lack the fibrous architecture needed to support long-range force propagation, remains poorly understood. Moreover, whether cell-mediated matrix stiffening occurs in amorphous PEG hydrogels and associates with capillary morphogenesis is unknown.

To address these questions, we generated PEG hydrogels with a range of initial moduli and measured how the extent of capillary morphogenesis and bulk stiffening correlated. Using this model, we then interrogated the relative contributions of cell generated traction, ECM deposition, and cell-mediated remodeling on stiffening behavior to better understand the mechanisms underpinning cell-mediated changes to hydrogel mechanics and enhanced capillary morphogenesis in soft amorphous hydrogels.

## **6.3 MATERIALS AND METHODS**

### **6.3.1 Cell culture**

All reagents were obtained from Thermo Fisher Scientific (Waltham, MA) unless specified. Endothelial and stromal cell sources in this study were chosen to provide continuity with our prior work (231). Human umbilical vein endothelial cells (ECs) were harvested from fresh umbilical cords (obtained from the University of Michigan's Mott's Children's Hospital via an IRB-exempt process, without any identifying information provided to the researchers) and cultured in fully supplemented Vasculife VEGF Endothelial Medium (Lifeline Cell Technology LLC, Frederick, MD) as previously described (172). ECs were used between passages 2-4.

Normal human dermal fibroblasts (DFs, Lonza, Walkersville, MD) were cultured in Dulbecco's modified Eagle medium (DMEM, Life Technologies, Grand Island, NY) supplemented with 10% fetal bovine serum (FBS, Life Technologies) and 1% penicillin streptomycin (Life Technologies) and were used up to passage 15. Both cell types were cultured at 37 °C and 5% CO<sub>2</sub> with thrice weekly medium exchanges. Cells were harvested below 80% confluence using 0.05% trypsin-EDTA (Life Technologies).

### **6.3.2 PEG-VS hydrogel formation.**

Hydrogels were formed from 4-arm poly(ethylene glycol) vinyl sulfone (PEG-VS; 20 kDa, Jenkem USA, Allen TX) and a combination of a thiol containing adhesive peptide and a protease-sensitive crosslinking peptide adapted from published protocols (114, 127). Hydrogels were functionalized with CGRGDS peptide ("RGD", Genscript, Piscataway, NJ) and crosslinked with Ac-GCRDVPMS↓MRGGDRCG-NH<sub>2</sub> ("VPMS", Genscript, cleavage site indicated by ↓), which contains an N-terminal acetylation and a C-terminal amidation. These peptides were chosen to provide continuity with our previous work (231). All reagents were prepared in batches of single-use aliquots. Peptides, dissolved in 25 mM acetic acid, and PEG-VS, dissolved in ultrapure water, were 0.22 μm filtered, lyophilized, and stored desiccated at -20 °C. Precise thiol content of each batch of peptide aliquots was determined using Ellman's reagent. Immediately before use, all reagents were dissolved in HEPES (100 mM, pH 8.4) to achieve final desired concentrations. RGD was reacted with the PEG-VS for 30 min to achieve a constant final concentration of 400 μM for all gel formulations. After RGD conjugation, VPMS was added to the PEG-VS solution, gently mixed, and 50 μl samples were dispensed into sterile 1 mL syringes with the needle end cut off. Hydrogels polymerized for 1 h at 37 °C in a sealed 50 mL conical tube. Polymerized hydrogels were punched into phosphate buffered saline (PBS). An

optimal thiol:vinyl sulfone ratio (typically 0.8-0.9), achieved by varying crosslinker concentration to yield the maximum hydrogel shear modulus for acellular hydrogels, was determined for each batch and used for subsequent vasculogenesis assays.

### **6.3.3 Vasculogenesis assays and drug inhibitor studies**

A 3D co-culture model of vasculogenesis, in which endothelial and stromal cells distributed in a hydrogel matrix self-assemble into a vascular network, was used as previously described (231). Briefly, hydrogels were formed as above except that a cell pellet was resuspended just before adding the crosslinking peptide to achieve a final cell seeding density of  $2 \times 10^6$  cells/mL of each cell type ( $1 \times 10^5$  ECs and/or  $1 \times 10^5$  DFs per 50  $\mu$ l gel). Hydrogels were formed with 27, 32, and 40 mg/mL PEG-VS corresponding to 2.7%, 3.2%, and 4% (w/v PEG-VS). For quantification of gel compaction, a solution of Fluoresbrite Polychromatic Red microspheres ( $2.1 \pm 0.018$   $\mu$ m diameter, 2.6% solids, Polysciences Inc, Warrington, PA) was additionally incorporated into hydrogels by substituting a 5% volume of HEPES for microsphere solution. Samples of the resulting suspension were dispensed and polymerized as above. Each hydrogel was cultured in 2 mL Vasculife VEGF medium in a 12-well plate for 7 d. For most conditions, medium was exchanged on days 1, 3, and 5. Blebbistatin (Calbiochem) and GM6001 (Calbiochem) were delivered in a 500x dilution of DMSO vehicle. Blebbistatin was delivered at a final concentration of 30  $\mu$ M for all conditions and GM6001 was delivered to achieve the indicated final concentrations. 24-hour exposure to blebbistatin was achieved by spiking it into the culture media on day 6 of culture. Daily exposures to blebbistatin and GM6001 were achieved by exchanging culture media and inhibitors daily to maintain vehicle concentrations and inhibitor activities. All inhibitor conditions were compared to their appropriate vehicle controls. Experiments with 24-hour exposure to blebbistatin were performed with both 27

mg/mL and 32 mg/mL PEG hydrogels. Experiments in which blebbistatin and GM6001 were included throughout culture were performed with 32 mg/mL PEG hydrogels.

#### **6.3.4 Mechanical characterization of PEG-VS hydrogels**

Hydrogel shear moduli were obtained for all conditions on day 1 after allowing for hydrogel swelling and on day 7. Hydrogels were mounted on an AR-G2 rheometer (TA Instruments, New Castle, DE) between an 8-mm measurement head and a Peltier stage, each covered with P800 sandpaper. Shear storage modulus ( $G'$ ) was determined at 0.05 N normal force, 5% strain amplitude, and 1 rad/sec frequency and averaged over a 1-minute time sweep.

#### **6.3.5 Fluorescent image quantification methods**

On day 7, co-cultures were fixed with Z-fix (Anatech, Battle Creek, MI). All PEG-VS hydrogels were cut longitudinally down the cylinder midline prior to staining, yielding two halves. For quantification of vessel and nuclei density and cell spreading, samples were stained with rhodamine-conjugated lectin from *Ulex europaeus* (UEA, Vector Laboratories, Burlingame, CA, specific for endothelial cells, 1:200), 4', 6-diamidino-2-phenylindol (DAPI, 1  $\mu$ g/mL, Sigma), and AlexaFluor 488 phalloidin (1:200). PEG-hydrogels were imaged on the cut side to ensure images were representative of cellular behavior within the hydrogels. Images were acquired using an Olympus IX81 microscope equipped with a disk scanning unit (DSU, Olympus America, Center Valley, PA) and Metamorph Premier software (Molecular Devices, Sunnyvale, CA). For all analyses, confocal z-stacks were acquired using the DSU. Z-series were collapsed into maximum intensity projections prior to analyses. Quantifications of vessel and nuclei densities were performed on 300  $\mu$ m stacks (30  $\mu$ m/slice) imaged at 4x (2.16 x 1.65 mm). Total vessel length per region of interest (ROI) was quantified from UEA images using the Angiogenesis Tube Formation module in Metamorph and reported as vessel length per volume

of ROI. Total nuclei per ROI were quantified from DAPI images using a custom ImageJ script as previously described (231), and reported as counts per volume. A custom ImageJ script (script and example included in supplement) was used to determine the fraction of UEA-negative nuclei. Briefly, binary DAPI projections were masked with their associated binary UEA projections and the fraction of DAPI stained area excluded from UEA-stained regions was calculated. Cell body circularity and projected cell area per volume of ROI were quantified from 30  $\mu\text{m}$  thick stacks (3  $\mu\text{m}$ /slice) of phalloidin images acquired at 10x (0.86 x 0.65 mm) and processed with a custom ImageJ script (included in supplement). Microbead density, as a measure of gel compaction, was calculated from 10  $\mu\text{m}$  thick stacks (1  $\mu\text{m}$ /slice) imaged at 20x (0.44 x 0.34 mm). Bead densities on day 0 were acquired before gel swelling. For each independent experiment, a value for each metric was determined by averaging multiple ROIs (4 for vessel and nuclei density, 6 for cell coverage and circularity, and 12 for bead densities). Only the final value of each parameter from each independent experiment (N=3-7) was subsequently analyzed in our statistical analysis.

### **6.3.6 Immunofluorescent staining and imaging**

Following tissue construct fixation and bisection, hydrogels were permeabilized with 0.5% v/v TritonX-100 in tris-buffered saline (TBS) for 30 minutes then blocked overnight at 4°C in TBS with 2% w/v bovine serum albumin (BSA, Sigma-Aldrich) and 0.1% v/v Tween 20. Primary antibodies for alpha smooth muscle actin (Abcam, mouse IgG<sub>2b</sub> isotype, 1:200 dilution), collagen-1 (Santa Cruz Biotech, mouse IgG<sub>1</sub> isotype, 1:200 dilution), fibronectin (Santa Cruz Biotech, mouse IgG<sub>2b</sub> isotype, 1:200 dilution), collagen-IV (Invitrogen, mouse IgG<sub>1</sub> isotype, 1:500 dilution), or laminin beta-1 (Invitrogen, rabbit IgG, 1:500 dilution) were incubated with samples overnight at 4°C. Samples were then washed several times and incubated overnight at

4°C with appropriate secondary antibodies (Invitrogen, either AlexaFluor 488 goat-anti-mouse IgG<sub>H+L</sub> or goat-anti-rabbit IgG<sub>H+L</sub>, 1:200 dilutions). Samples were again washed then stained with DAPI and either UEA or AlexaFluor 568 phalloidin as indicated and stored in TBS.

Representative images were acquired at 10x and 20x magnification using the DSU and presented as maximum intensity projections of 30 µm thick stacks (3 µm/slice).

### **6.3.7 Gene expression analysis**

Hydrogels (2-3 per experimental replicate, pooled) were rinsed in PBS, cut into 4 pieces per gel, and incubated under constant gentle rotation in Collagenase IV (200 U/mL) at 37 °C for 30-40 min until gels were dissociated. The suspension was centrifuged at 500 × g for 3 min. The resulting cell pellet was lysed and RNA purified using an RNeasy Mini Kit (Qiagen, Venlo, Netherlands). RNA was reverse transcribed to cDNA using a High Capacity cDNA Reverse Transcription Kit (Applied Biosystems, Thermo Fisher Scientific). PCR amplifications were performed on a 7500 Fast Real-Time PCR System (Applied Biosystems) using Taqman Gene Expression reagents (20 ng cDNA per PCR reaction). The primer probe sets for the following genes were utilized (Taqman Assay ID indicated): GAPDH (Glyceraldehyde 3-phosphate dehydrogenase, Hs04420566\_g1); TGFB1 (transforming growth factor β1, Hs00998133); PDGFRB (platelet derived growth factor receptor-β, Hs01019589\_m1); PDGFB (platelet derived growth factor-β, Hs00966522\_m1); ANTXR2 (capillary morphogenesis gene 2 protein, Hs00292467\_m1); KDR (vascular endothelial growth factor receptor 2, Hs00911700\_m1); ACTA2 (α-smooth muscle actin, Hs00426835\_g1); COL1A1 (Collagen I, alpha 1 chain, Hs00164004\_m1); LAMB1 (Laminin, Beta 1 chain, Hs01055960\_m1); FN1 (Fibronectin 1, Hs01549976\_m1); COL4A1 (Collagen IV, alpha 1 chain, Hs00266237\_m1); MMP2 (matrix metalloproteinase 2, Hs01548724\_m1); MMP9 (matrix metalloproteinase 9, Hs00957562\_m1);



MMP14 (membrane type 1 matrix metalloproteinase, Hs01037009\_g1). The  $\Delta\Delta C_t$  method was used to determine relative gene expression with GAPDH as the internal control.

### 6.3.8 Statistics

Statistical analysis was performed using GraphPAD Prism (La Jolla, CA). Unless noted, data are represented as mean  $\pm$  standard deviation of at least 3 independent experiments. Data were analyzed using one- or two-way ANOVA with Tukey post-hoc testing with matching when possible and pre-specified comparisons between conditions on a given day and between days for a given condition. Correlations were determined by linear regression and  $R^2$  and  $p$  value for the correlation coefficient reported. Statistics for gene expression data was performed in the  $C_t$  domain. A value of  $\alpha < 0.05$  was considered significant.

## 6.4 RESULTS

### 6.4.1 Vessel density and hydrogel stiffening both depend on initial PEG composition and are tightly correlated

We first confirmed that initial PEG composition affects cellular morphogenetic processes including vessel formation, changes in cell density, and cell spreading consistent with previous work with EC-DF co-cultures (231). We then characterized the expression of pro-angiogenic genes and the evolution of tissue-level physical properties including stiffening and compaction depending on PEG composition. Lower PEG concentration at gel polymerization supported increased vessel density at 7 d (**Figure 6.1A and 6.1D**), with a 2-fold higher vessel density in 27 mg/mL gels compared with 40 mg/mL ( $p < 0.001$ ). The baseline shear moduli of hydrogels formed from 27, 32, and 40 mg/mL PEG were  $59 \pm 27$  pa,  $114 \pm 27$  pa, and  $209 \pm 50$  pa, respectively (**Figure 6.1B**), confirming that changes in PEG composition led to differences in

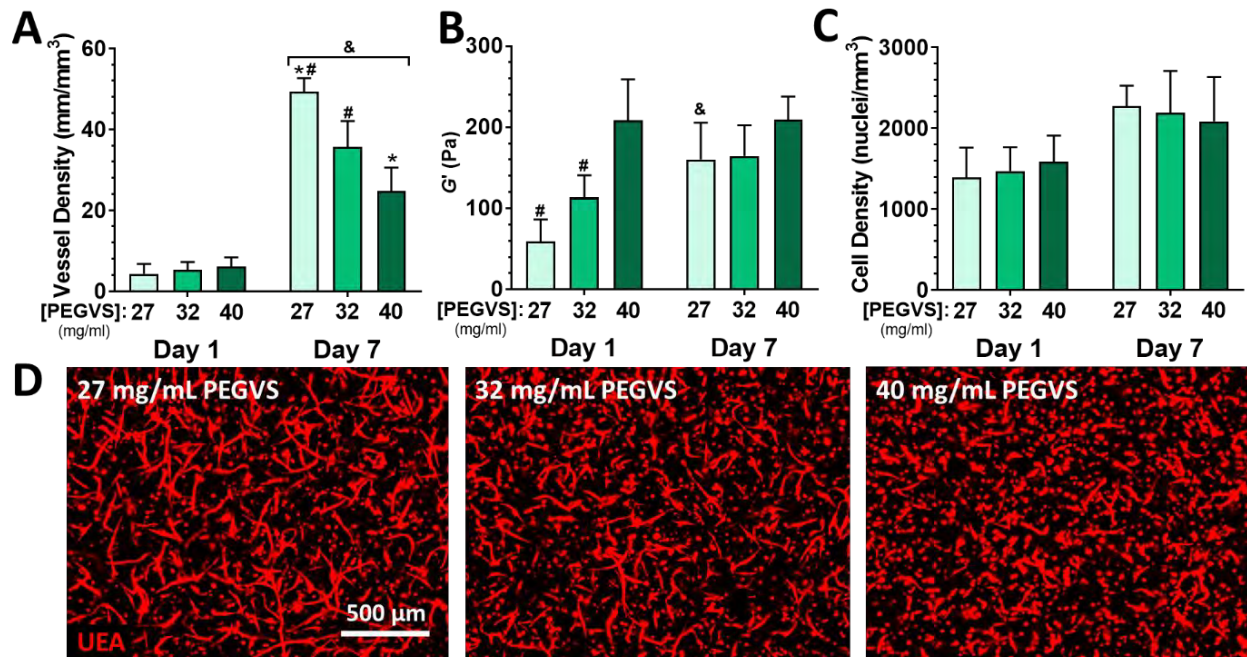


**Figure 6.1: Lower concentration of PEGVS at the time of crosslinking results in higher vessel density at 7 d and induces gel stiffening without altering cell density.** A) Hydrogel constructs were formed with a range of concentrations of PEGVS and cultured for 7 d. Vessel density in the bulk of the constructs was estimated as described in the methods. B) The shear storage modulus ( $G'$ ) of constructs was determined after overnight culture (Day 1) and at 7 d. C) Cell density in the constructs after 1 d and 7 d was quantified from DAPI stained images. Two-way ANOVA: time  $p < 0.001$ , PEG  $p > 0.99$ , interaction  $p = 0.60$ . D) Representative images of maximum intensity projections of confocal sections ( $z$  height = 300  $\mu\text{m}$ ) for ECs stained with UEA at 7 d from constructs with a range of PEGVS compositions. #:  $p < 0.05$ , relative to 40 mg/mL PEGVS (same day); \*:  $p < 0.05$ , relative to 32 mg/mL PEGVS (same day); &:  $p < 0.05$  relative to day 1 (same PEGVS composition),  $N=4-7$ .

bulk shear storage moduli on day 1 (after swelling). These PEG densities were empirically chosen to interrogate the softest formulation which would consistently gel (27 mg/mL), the softest formulation which did not exhibit any stiffening behavior (40 mg/mL), and an intermediate formulation (32 mg/mL). Despite significant differences in vessel formation, we did not observe composition dependent differences in gene expression for a panel of angiogenesis-associated genes (**Supplemental, Figure 6.9 A-E**). After 7 d, 27 mg/mL hydrogels stiffened 2.7-fold ( $p < 0.01$ ) and 32 mg/mL hydrogels stiffened 1.5-fold (NS), while the shear moduli of 40 mg/mL gels remained unchanged. Cell density did not vary with PEG composition at 1 d or 7 d, though there was a modest  $\sim 1.4$ -fold increase in total cell density for all gel compositions over

the 7 d culture (**Figure 6.1C & Supplemental, Figure 6.10**), Two-way ANOVA: time  $p < 0.001$ , PEG  $p > 0.99$ , interaction  $p = 0.60$ ). Cell density after 1 d was  $\sim 1.4 \times 10^6$  cell/mL (compared with  $4 \times 10^6$  cell/mL at seeding), reflecting swelling of the gels after casting. There was a strong inverse correlation of the shear storage modulus at 1 d with vessel density at 7 d (**Supplemental, Figure 6.11A**,  $R^2 = 0.762$ ,  $p < 0.0001$ ), but no correlation with cell density (**Supplemental, Figure 6.11B**,  $R^2 = 0.002$ ,  $p = 0.956$ ). We noted a positive correlation between the degree of stiffening observed in each experiment and the ultimate vessel density at 7 d (**Supplemental, Figure 6.11C**,  $R^2 = 0.480$ ,  $p = 0.0087$ ).

We also assessed spreading of all cells using both individual cell circularity and projected area covered by all cells in phalloidin stained samples. No differences in circularity or spreading were noted 1 d after seeding (**Supplemental, Figure 6.12**). After 7 d, average circularity decreased in all gels (**Supplemental, Figure 6.12A**,  $p < 0.0001$ ) and area coverage increased (**Supplemental, Figure 6.12B**,  $p < 0.005$ ), but this effect was most pronounced in 27 mg/mL gels ( $p = 0.033$  relative to 40 mg/mL).

In contrast to co-culture experiments, ECs cultured in the absence of DFs did not undergo capillary morphogenesis (**Figure 6.2A**). The shear moduli of EC or DF mono-cultures in 27 mg/mL hydrogels were statistically unchanged after 7 d, similar to controls (**Figure 6.2B**). EC mono-culture cell densities significantly decreased 2.7-fold (**Figure 6.2C**,  $p < 0.01$ ) and cell bodies remained rounded (**Fig 6.2D**), whereas DF mono-culture cell densities significantly increased 1.6-fold (**Figure 6.2C**,  $p < 0.01$ ) and cell bodies appeared well spread (**Figure 6.2E**).

In addition to stiffening accompanying capillary morphogenesis, we observed that soft hydrogel constructs changed shape macroscopically, suggesting possible gel compaction (**Supplemental, Figure 6.13**). To investigate whether compaction could account for the apparent

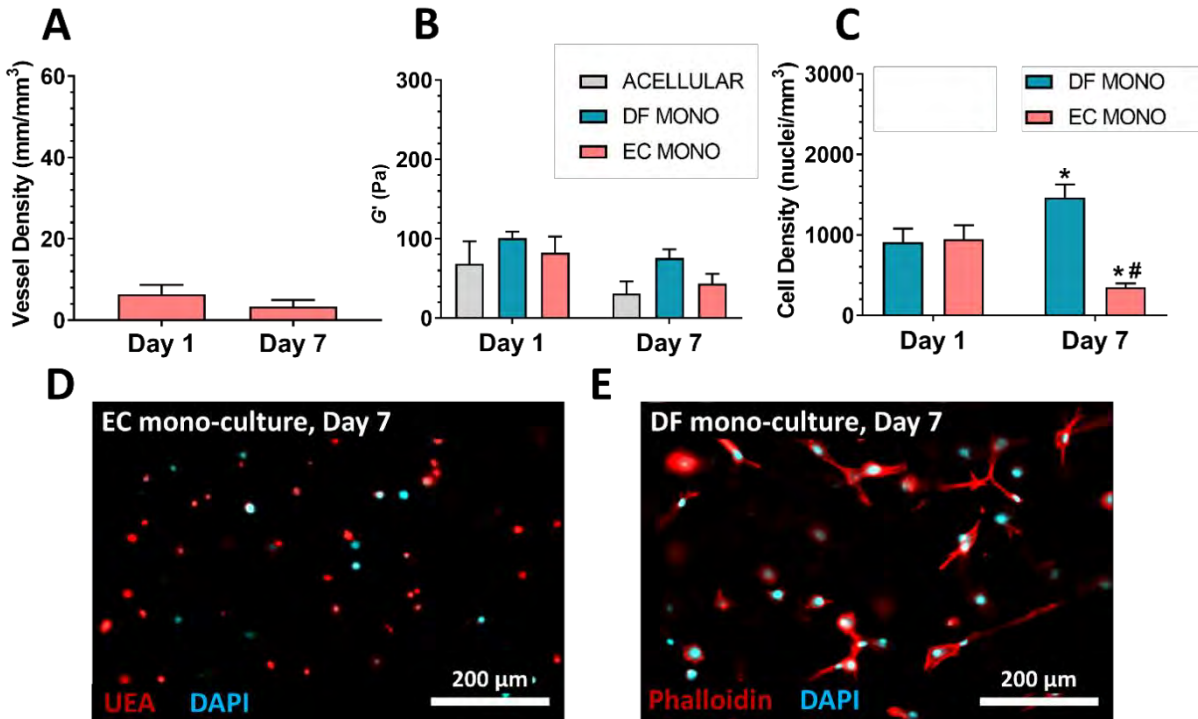


**Figure 6.2: Co-culture of ECs with DFs is necessary for capillary morphogenesis and hydrogel stiffening.** A) ECs cultured in the absence of DFs in 27 mg/mL PEGVS did not develop capillary networks. B) The shear storage modulus ( $G'$ ) of 27 mg/mL constructs which were acellular or contained mono-cultures of either DFs or ECs did not show any significant differences between conditions on a given day or between days for a given condition. C) Mono-cultures of ECs in 27 mg/mL hydrogels demonstrated a significant decrease in nuclei density over a 7 d culture period and cell bodies remained rounded as visualized with UEA for cell bodies and DAPI for nuclei (D). Mono-cultures of DFs in 27 mg/mL hydrogels demonstrated a significant increase in nuclei density over a 7 d culture period (C) and cell bodies appeared well spread as visualized with phalloidin staining for cell bodies and DAPI for nuclei (E). \*:  $p < 0.05$ , relative to Day 1 (same cellular condition). #:  $p < 0.05$ , relative to DF mono (same day); . Y-axes were scaled to match Fig. 1

changes in modulus and vessel density, we entrapped 2  $\mu$ m beads within the hydrogel network as fiduciary markers, allowing us to infer changes in hydrogel density from changes in bead density specifically in the centers of the gels where capillary density was measured. Incorporation of beads did not substantially alter initial hydrogel mechanical properties nor stiffening behavior (Supplemental, Figure 6.14A). As expected, after overnight swelling we observed a decrease in bead density to  $34 \pm 6$  % of reference gels (Supplemental, Figure 6.14B), where density was quantified immediately after gelation. This result corresponded closely with the observed

changes in cell density after gel swelling and confirmed the validity of the technique. Despite the suggestion of hydrogel compaction from macroscopic images for 27 mg/mL hydrogels, no significant differences in bead density (measured locally inside of the gels) were observed as a function of gel composition during the 7 d culture (**Supplemental, Figure 6.14B**), though a weak inverse correlation was noted between initial gel modulus and change in bead density from 1 d to 7 d (**Supplemental, Figure 6.14C**,  $R^2 = 0.3935$ ,  $p = 0.016$ ).

#### **6.4.2 Active cellular contraction significantly contributes to hydrogel stiffening**

To investigate the contribution of cell-generated forces to hydrogel stiffening, we blocked cell-mediated contractility with the myosin II inhibitor, blebbistatin. Only 27 and 32 mg/mL hydrogels were assessed because 40 mg/mL hydrogels did not stiffen. Gels were incubated with 30  $\mu$ M blebbistatin for the final 24 h of a 7 d culture period to inhibit traction forces (252) and minimize confounding effects from changes in vessel density, nuclei density, and cell spreading that occur with long-term blebbistatin treatment (171, 253). This treatment caused a significant decrease in measured modulus of  $36 \pm 6\%$  and  $30 \pm 11\%$  for 27 and 32 mg/mL hydrogels, respectively ( $p < 0.030$ , **Figure 6.3A**). Interestingly, the 32 mg/mL hydrogels relaxed back to their initial shear moduli whereas the 27 mg/mL hydrogels did not (**Figures 6.1B, 6.3A**), suggesting our softest gels may incur some degree of permanent remodeling. 24-hour treatment with blebbistatin did not cause any changes in vessel density (**Figure 6.3B**), nuclei density (**Figure 6.3C**), or cell-spread coverage (**Figure 6.3D**), but did cause a modest increase in circularity in 27 mg/mL hydrogels ( $p = 0.015$ , **Figure 6.3E**), suggesting some retraction of cellular protrusions occurred without significantly altering average cell size. 24-hour blebbistatin treatment did not affect gel density as assessed by microbead density (**Figure 6.3F**). In contrast, supplementing blebbistatin daily over the entire 7d culture period resulted in the dissolution of

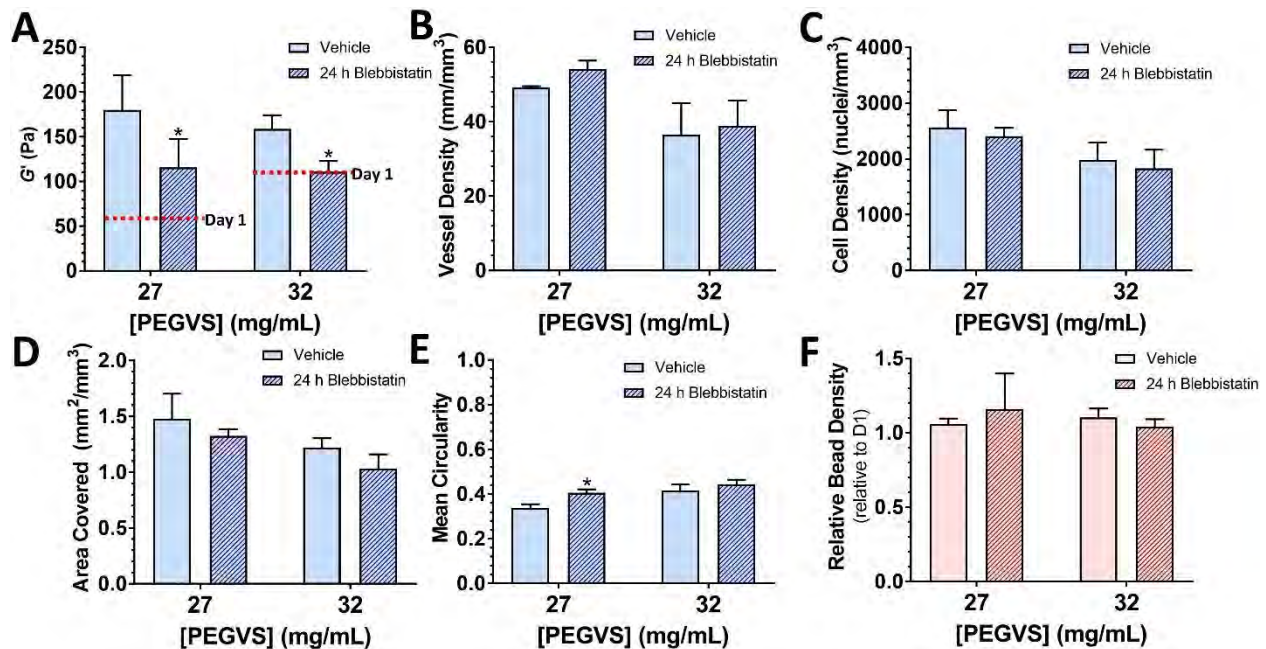


**Figure 6.3: Cell contractility partly contributes to construct stiffening.** Hydrogel constructs with either 27 or 32 mg/mL PEGVS were cultured for 6 d and then were incubated with 30  $\mu$ M blebbistatin or vehicle during the final 24 h of culture. The shear storage modulus ( $G'$ ) at 7 d was measured in each condition (A). Average stiffness at 1 d is shown in red on each graph for reference. 24 h treatment with blebbistatin did not affect vessel density (B), the cell density (C), or cell area covered (D). Blebbistatin induced a slight increase in cell circularity in 27 mg/mL PEGVS constructs (E). Blebbistatin did not alter the density of microbeads (F). \*:  $p < 0.05$ , relative to vehicle control,  $N=3$ .

27 mg/mL gels and significant softening for 32 mg/mL gels ( $p = 0.0015$ , **Supplemental, Figure 6.15A**), as well as significantly reduced vessel density and cell density ( $p \leq 0.017$ , **Supplemental, Figure 6.15B-D**).

To investigate if initial matrix stiffness alters cell phenotypes associated with increased cellular contractility (254), we measured ACTA2 ( $\alpha$ -smooth muscle actin,  $\alpha$ SMA) gene expression. The expression of  $\alpha$ SMA was significantly upregulated in all constructs during culture, but the increase was most significant for the 27 mg/mL gels ( $p = 0.017$  relative to 40 mg/mL, **Figure 6.4A**). Immunofluorescent staining showed that  $\alpha$ SMA was expressed exclusively in UEA negative fibroblasts, which were often present in the perivascular space (**Figure 6.4B**) and appeared in all gel formulations (**Supplemental, Figure 6.16**). The pooled



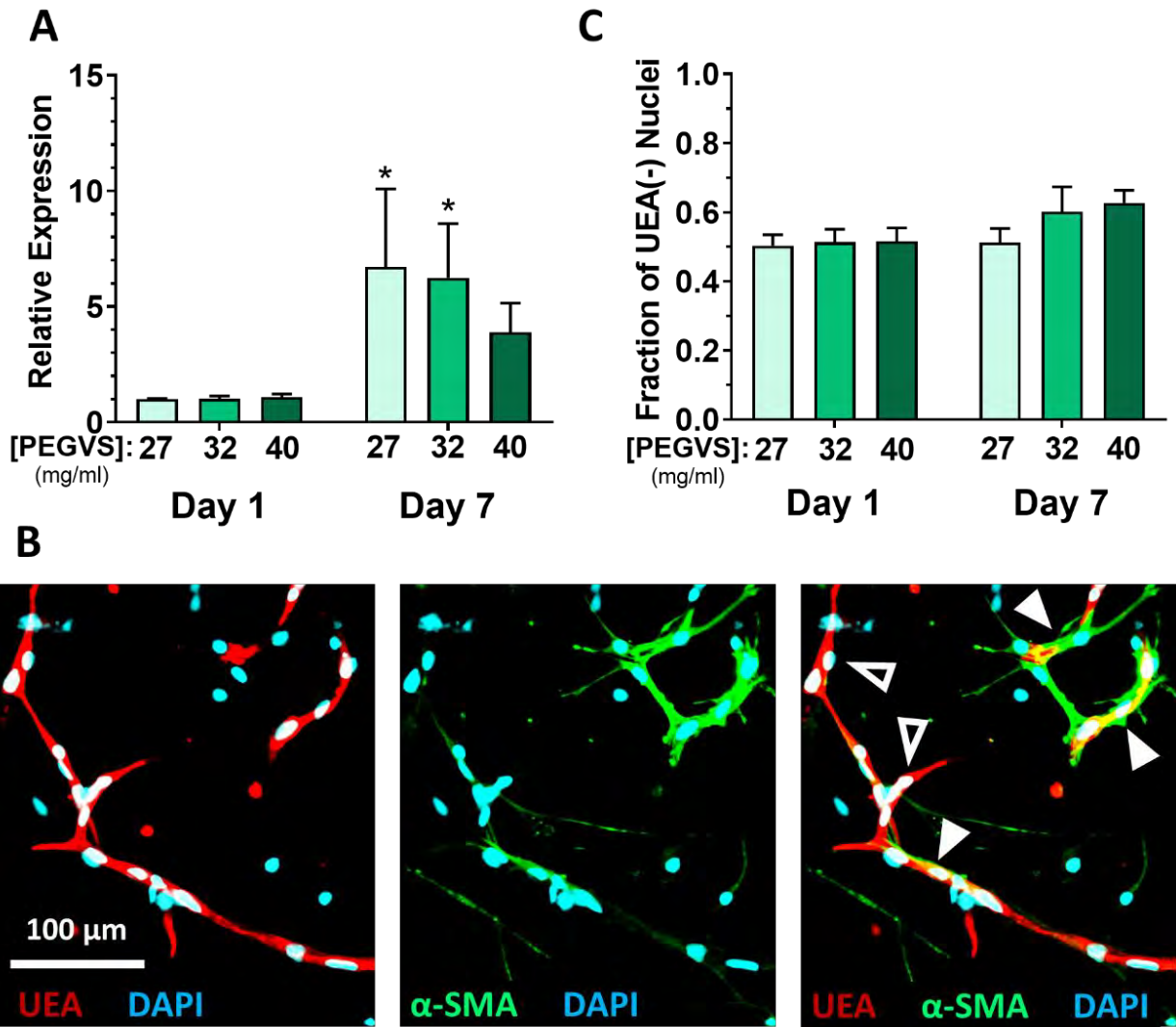


**Figure 6.4: Smooth muscle actin is upregulated by fibroblasts in soft hydrogels.** A) Expression of  $\alpha$  smooth muscle actin ( $\alpha$ SMA, gene: ACTA2) was measured from RNA collected from constructs after 1 d or 7 d using real time RT-PCR. Expression levels were normalized to GAPDH in each sample and then to expression in 27 mg/mL PEGVS at 1 d ( $\Delta\Delta C_t$  method). \*:  $p < 0.05$ , relative to 40 mg/mL PEGVS, N=3. B) Only fibroblasts display significant  $\alpha$ -smooth muscle actin protein expression. Representative image in an intermediate stiffness construct showing immunofluorescent staining for ( $\alpha$ SMA), counterstained with UEA to highlight endothelium, and DAPI. Note the tight association of  $\alpha$ SMA+ fibroblasts with UEA+ microvessels (solid arrowheads) but lack of  $\alpha$ SMA staining in UEA+ microvessels themselves (open arrowhead). Scale bar = 100  $\mu$ m. C) The proportion of UEA(-) nuclei (representing fibroblasts) in stiff constructs after 7 d was quantified as described in the supplemental methods.

RNA contained transcripts from both cell types but  $\alpha$ SMA is only expressed in fibroblasts.

Therefore, the measured increase in  $\alpha$ SMA expression could either represent an increase in  $\alpha$ SMA per fibroblast or a higher proportion of fibroblasts contributing to the RNA pool. To differentiate these possibilities, we estimated the proportion of fibroblasts in our samples by

quantifying the number of nuclei excluded from UEA stained regions. There was not an increased proportion of fibroblasts in soft hydrogel formulations (**Figure 6.4C**), demonstrating that soft hydrogels supported higher levels of  $\alpha$ SMA expression in fibroblasts.

### **6.4.3 Enhanced deposition of collagen I and downregulation of MMP expression associates with hydrogel stiffening in ultra-soft hydrogels**

The observation that blebbistatin inhibition of cell-mediated contractility did not result in a return to initial mechanical properties in 27 mg/mL gels suggested deposition of new matrix may contribute to stiffening. To assess this possibility, we quantified mRNA levels of collagen I alpha 1 chain (COL1A1), fibronectin (FN1), laminin beta 1 chain (LAMB1), and collagen IV alpha 1 chain (COL4A1) in pooled RNA collected from both cell populations in the gels. No differences in expression level were detected between hydrogels on day 1 (**Figure 6.5**). However, after 7 d of culture, we observed a 1.8-fold increase in collagen I expression in 27 mg/mL hydrogels compared with 40 mg/mL hydrogels ( $p = 0.0007$ , **Figure 6.5**). We also observed fibronectin expression in all gels was increased from 1 d to 7 d (Two-way ANOVA: time  $p = 0.0002$ , PEG  $p = 0.11$ , interaction  $p = 0.0094$ ) but was most strongly upregulated in 40 mg/mL at day 7 ( $p \leq 0.0009$ ). Expression of transcripts for the basement membrane component laminin beta 1 chain was unchanged during culture for the 27 mg/mL gels but was modestly upregulated 1.3-fold in 40 mg/mL gels ( $p \leq 0.0021$ ). Collagen IV alpha 1 was upregulated after 7 d but did not depend on PEG composition.

We further analyzed the deposition of proteins encoded by these transcripts using immunostaining. Collagen I and fibronectin were deposited around both UEA negative fibroblasts and UEA positive vessels (**Figure 6.6 & Supplemental, Figure 6.17A**). Compared



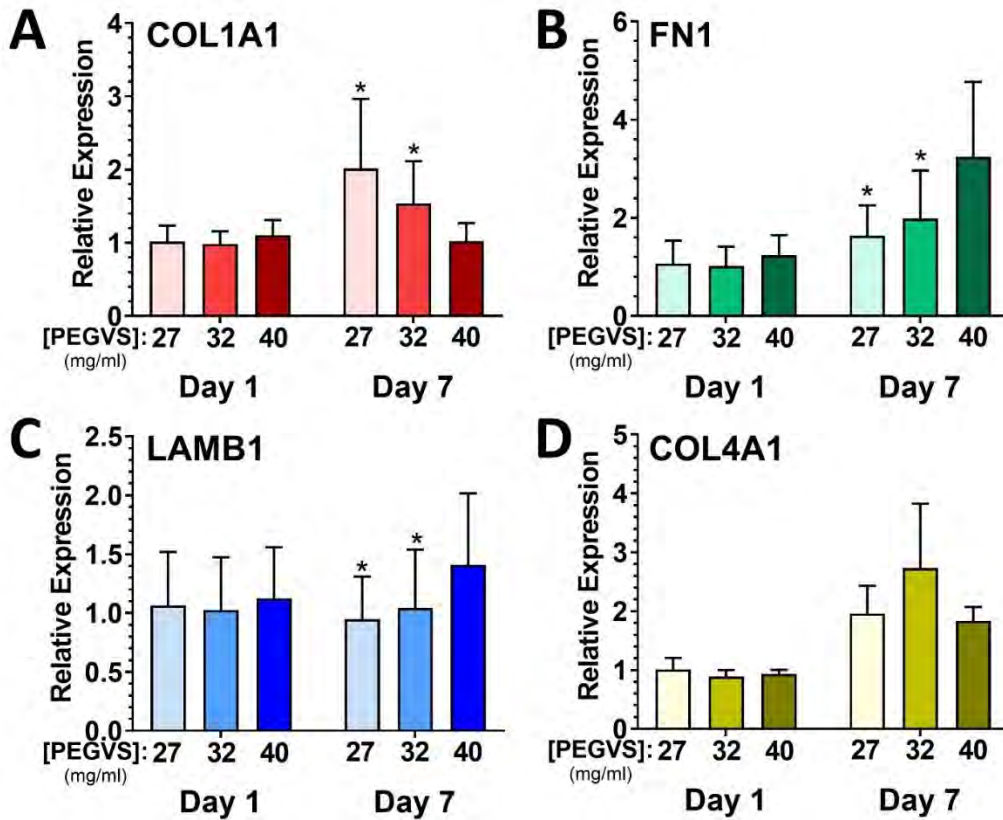


**Figure 6.5: Collagen I alpha 1 chain expression is upregulated in soft hydrogels.** RNA was collected from constructs after 1 d and 7 d, purified, and expression determined using real time RT-PCR. Expression of collagen I  $\alpha$ 1 chain (COL1A1, A), fibronectin (FN1, B), laminin  $\beta$ 1 chain (LAMB1, C), and collagen IV  $\alpha$ 1 chain (COL4A1, D) was measured. Expression levels were normalized to glyceraldehyde 3-phosphate dehydrogenase (GAPDH) in each sample and then to expression in 27 mg/mL PEGVS at 1 d ( $\Delta\Delta C_t$  method). \*:  $p < 0.05$ , relative to 40 mg/mL PEGVS same day, N=3.

with 27 mg/mL gels, we noted a qualitative decrease in Collagen I deposition in 40 mg/mL hydrogels, consistent with the expression analysis. Fibronectin deposition was observed not only around vessel like structures but also surrounding rounded cells which did not spread. In contrast to deposition of collagen I and fibronectin, the basement membrane proteins laminin (beta 1 chain) and collagen IV (which reacts with both alpha 1 and alpha 2 chains) were tightly associated with UEA+ vessel-like structures and were less prominently expressed in UEA negative fibroblasts (**Supplemental, Figure 6.17B, C**). To assess the spatial distribution of ECM protein deposition relative to the encapsulated cells, we co-stained phalloidin with collagen I or

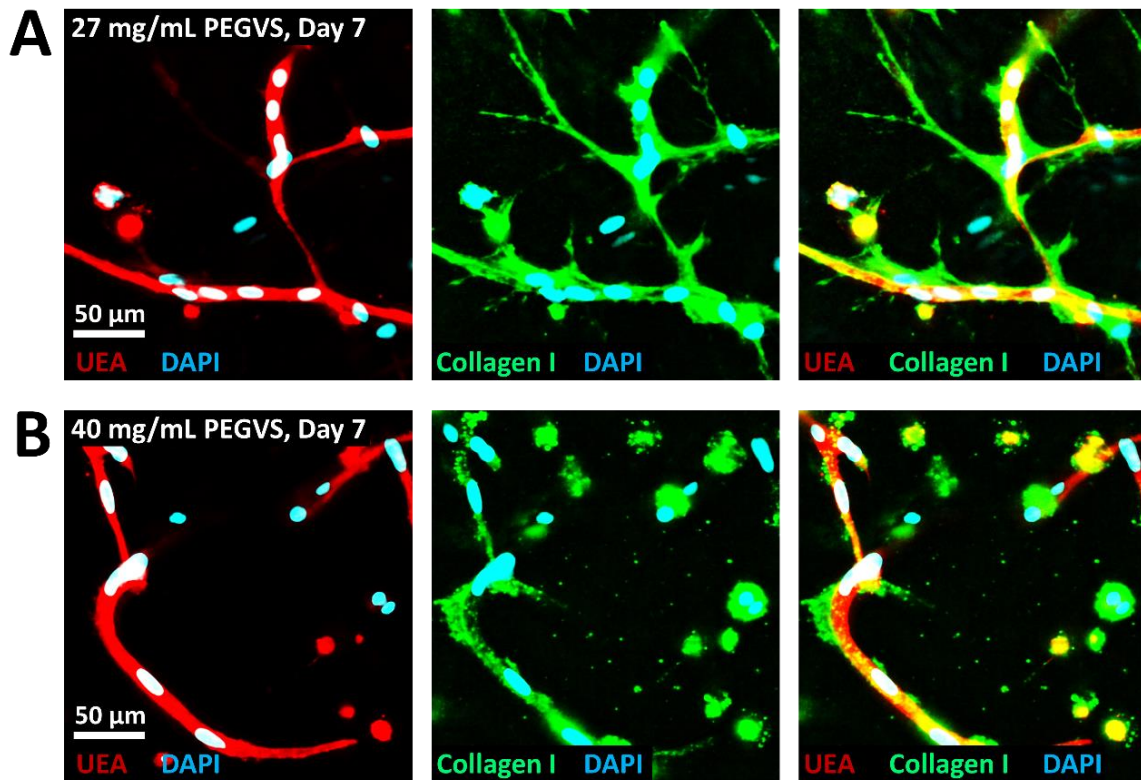


**Figure 6.6: Collagen I deposition around vessels is more robust in soft hydrogels.** 27 mg/mL (A) or 40 mg/mL (B) PEGVS constructs were fixed at 7d and stained for collagen I and counterstained with UEA and DAPI. There was a clear increase in collagen I deposition in 27 mg/mL constructs compared with 40 mg/mL.

fibronectin. In 27 mg/mL gels we observed very little ECM protein deposition in the hydrogel bulk distant from cells, with nearly all ECM deposited within  $\sim 30 \mu\text{m}$  of cells (**Supplemental, Figure 6.18**). We also noted areas of extensive ECM deposition devoid of actin but adjacent to nearby cells, suggesting active cellular remodeling in these regions followed by migration (**Supplemental, Figure 6.18**, arrowheads). Fibronectin expression surrounding poorly spread cells never extended more than a few microns from the nuclei.

Concurrent with our observation of enhanced matrix deposition in ultra-soft hydrogel formulations, we also observed downregulation of MT1-MMP and MMP2 in 27 mg/mL hydrogels compared to 40 mg/mL hydrogels on day 7 (**Figure 6.7A, B**,  $p \leq 0.014$ ). However,

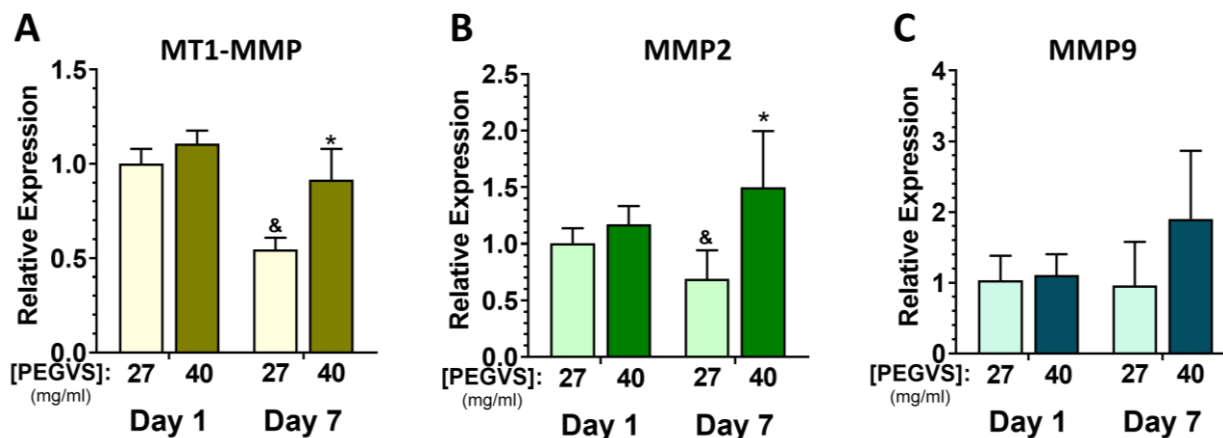


**Figure 6.7: MMP expression is downregulated in ultra-soft hydrogel formulations.** RNA was collected from constructs after 1 d and 7 d, purified, and expression determined using real time RT-PCR. Expression of matrix type-1 MMP (MT1-MMP, A), MMP2 (B) and MMP9 (C) was measured. Expression levels were normalized to glyceraldehyde 3-phosphate dehydrogenase (GAPDH) in each sample and then to expression in 27 mg/mL PEGVS at 1 d ( $\Delta\Delta C_t$  method). \*:  $p < 0.05$ , relative to 27 mg/mL (same day); &:  $p < 0.05$  relative to day 1 (same composition). N=3.

there was no significant change in MMP9 expression over time regardless of formulation

(Figure 6.7C).

#### 6.4.4 Inhibition of MMP-mediated proteolysis reduces hydrogel stiffening and correlates with decreased cell spreading but not changes in cell number

We have previously shown that inhibition of MMPs with the broad-spectrum MMP inhibitor GM6001 severely restricts capillary morphogenesis in VPMS crosslinked hydrogels (231). Given that our results to this point suggested stiffening behavior was due to cell contractility and pericellular matrix remodeling, we reasoned that blocking cell-mediated hydrogel degradation, needed for cell spreading and endothelial tube assembly, would also abolish gel stiffening. Closely mirroring the decrease in vessel density with GM6001 which we previously reported (231), we observed a robust and dose-dependent loss of gel stiffening with GM6001 (Figure 6.8A) in comparatively soft 32 mg/mL hydrogels ( $30 \pm 8$  Pa on day 1). Notably, GM6001 did not significantly alter cell density in the gels, indicating changes in

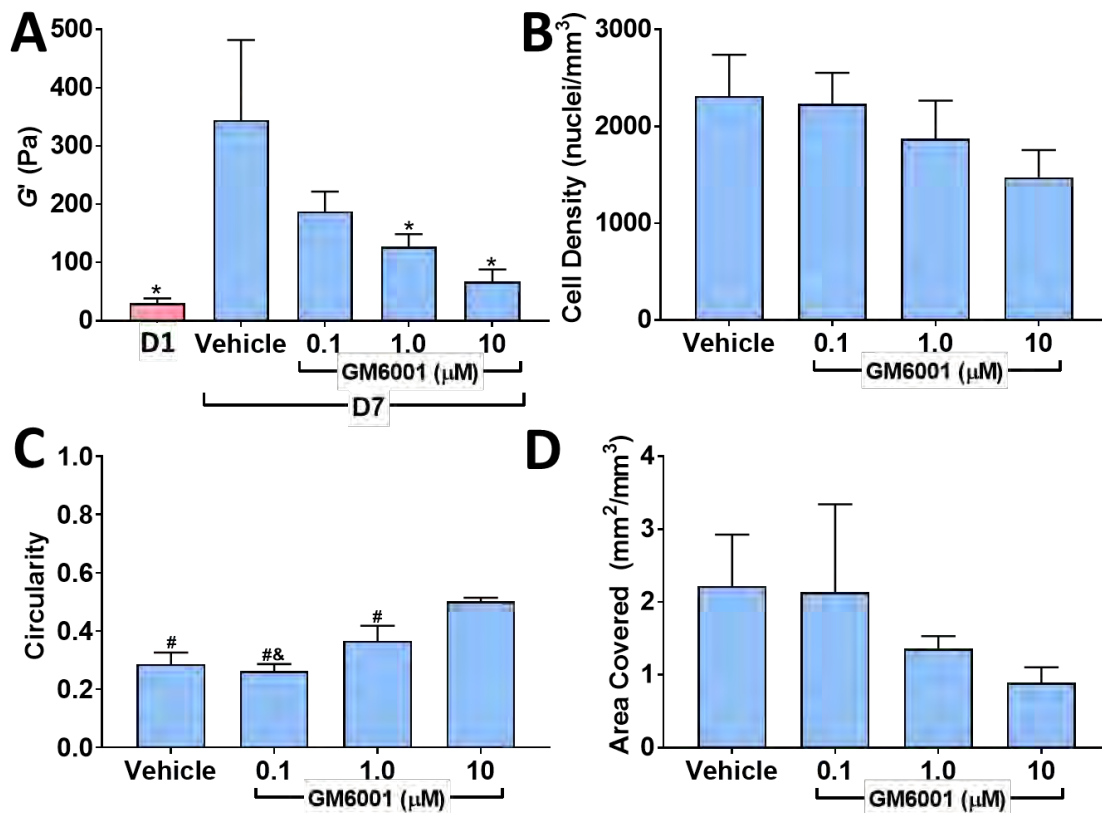


**Figure 6.8. Inhibition of MMP-mediated matrix degradation abolishes gel stiffening and blocks cell spreading.** 32 mg/mL PEGVS constructs were incubated with the broad-spectrum MMP inhibitor GM6001 for 7 d. The shear storage modulus ( $G'$ ) at 7 d was measured in each condition (A, \*:  $p < 0.05$ , relative to vehicle 7 d). There was a modest trend toward lower cell density with increasing GM6001 concentration but did not reach statistical significance (B, ANOVA:  $p = 0.0734$ ). Average cell circularity, a measure of cell spreading, increased with GM6001 concentration (C, #:  $p < 0.01$ , relative to 10  $\mu\text{M}$  GM6001; &:  $p < 0.05$ , relative to 1  $\mu\text{M}$  GM6001, lower values of circularity reflect greater irregularly shaped spreading). Projected cell area covered also decreased with GM6001 concentration but did not reach statistical significance (D, ANOVA:  $p = 0.1417$ ).  $N=3$ .

stiffening were not due to reduced cell density over time (**Figure 6.8B**). We measured a significant rise in circularity with increasing doses of GM6001 (ANOVA:  $p < 0.0001$ , **Figure 6.8C**) and a non-significant trend toward lower cell coverage (**Figure 6.8D**), both suggesting reduced cell spreading with GM6001.

## 6.5 DISCUSSION

While the effects of stiffness on capillary morphogenesis have been studied extensively (13), how cells, in turn, alter the mechanical properties of their surrounding ECM during this

process has received less attention (251). A clear understanding of the dynamic and reciprocal relationship between cells and their mechanical microenvironment is critical to engineer synthetic materials for regenerative medicine applications because these mechanical changes may in turn affect the differentiation and function of co-encapsulated functional cell types (250). Protease-susceptible PEG hydrogels are prototypical synthetic materials and have been widely utilized for their ability to support and control populations of single cells in 3D (255, 256). However, the impact of their amorphous structure, which is distinct from native fibrillar ECMs, on complex multicellular morphogenetic processes remains less understood. Consistent with several previous reports in other synthetic hydrogels, including protein-synthetic hybrid systems (202, 229) and polysaccharide-synthetic systems (89, 230), we observed enhanced vessel formation with reduced PEG crosslinking density (91, 114, 133, 221). Interestingly, this enhanced vessel formation in softer gel formulations was not correlated with differential expression of pro-angiogenic genes. However, the more surprising observation was that ultra-soft amorphous gels significantly stiffened over time as capillary morphogenesis occurred. We then used a combination of inhibitor studies and molecular expression analyses to provide evidence that both cell-mediated contractility and ECM deposition, but not hydrogel compaction, contribute to this stiffening. We then demonstrated that inhibition of cell-mediated degradation inhibited cellular spreading and severely attenuated gel stiffening.

We recently reported that fibrin matrices stiffen on both the microscale and the macroscale as capillary morphogenesis occurs (251), but it was not clear if this phenomenon required a fibrillar matrix to transduce cell-generated forces and thereby alter the mechanical microenvironment. The strain stiffening properties of fibrous materials such as fibrin and collagen allow cell-mediated tension to transmit mechanical forces over long distances, perhaps

serving as a cue to guide network organization (6, 68, 257). However, the nanoscale, amorphous architecture of PEG hydrogels is distinctly different from fibrin or collagen (219). Such synthetic hydrogels generally display linear elastic deformation (257), which limits the distance mechanical forces can propagate relative to strain-stiffening fibrous materials.

To our knowledge, stiffening behavior in a purely synthetic matrix material during capillary morphogenesis has not been previously reported. Cell-mediated changes to hydrogel mechanics have, however, been more extensively studied in the context of fibrosis and wound healing, and engineering of load bearing tissues such as cartilage and bone (258). Fibroblast-mediated stiffening of fibrous materials is well documented in fibrin (251) and collagen (259), is dependent on cellular contractility, and results in hydrogel compaction (260). Dermal fibroblasts have also been shown to stiffen and compact PEG-fibrinogen composites (261). However, we did not observe a significant change in marker bead density over time depending on gel formulation, suggesting that gel compaction was not necessarily associated with stiffening in our system. These observations suggest the bulk of PEG gels are not significantly reorganized, unlike collagen or fibrin which restructure into more compact fibrous architectures (175). Distinct from fibrillar ECM or PEG-fibrinogen composite hydrogels, we also observed that stiffening depended on the co-culture of ECs with DFs. In the absence of capillary morphogenesis, DFs failed to stiffen ultra-soft hydrogel formulations. In contrast, others have reported that fibroblasts in unmodified alginate (262) and endothelial colony forming cells in RGD modified hyaluronan crosslinked with MMP degradable peptides (263) soften over time. These differences in the evolution of hydrogel mechanics depending on cell culture system demonstrate a complex interplay between cell types and ECM identity in dictating changes to hydrogel mechanics over time.

The cellular networks that formed throughout the bulk of the hydrogel may themselves be mediating the stiffening effects via cell-mediated contractility. To test this hypothesis, we included a saturating dose of blebbistatin, which inhibits the action of myosin II (264), in our culture medium for the final 24 hours of culture. This treatment reversed about half of the observed stiffening in the 27 mg/mL and all the stiffening seen in the 32 mg/mL gels, implicating cytoskeletal tension as a major contributor to the observed stiffening behavior. We previously demonstrated that long term inhibition of cell-mediated contractility severely attenuated endothelial sprouting in fibrin (171). Likewise, we observed that exposure to blebbistatin throughout the 7 d culture period not only reduced capillary morphogenesis, but resulted in gel softening over time. Matrix stiffness itself may also directly impact the degree of cellular contractility. Mabry *et al.* observed that valvular interstitial cells exhibited a more contractile phenotype in soft materials and that this phenotype could be reversed by changing matrix mechanics in situ (265). Likewise, we observed an increase in the expression of  $\alpha$ -smooth muscle actin in fibroblasts within our soft hydrogel constructs during capillary morphogenesis.

Since 24-hour exposure to blebbistatin did not fully reverse stiffening in the softest gels, the contributions of matrix deposition to the observed stiffening behavior were also assessed. We observed that collagen I alpha 1 chain was upregulated in pooled RNA samples from the soft hydrogels. Collagen I alpha chain is one of the key secreted proteins from fibroblasts that induce capillary morphogenesis in coculture with endothelial cells and its deposition contributes to progressive stiffening of fibrin (52). Deposition of ECM proteins by chondrocytes in alginate has similarly been correlated with progressive hydrogel stiffening (266). We noted collagen I near both vessels and fibroblasts but not within the bulk of the PEG hydrogels, suggesting deposition was highly localized. Fibronectin was also upregulated in all gel formulations and was deposited

in a clear pericellular distribution around cells, similar to that of collagen I, as has been reported previously (221). We also observed decreased expression of MT1-MMP and MMP2 in ultra-soft hydrogels which would shift ECM dynamics toward deposition over degradation.

Combined, the tight association of ECM proteins with invading cells, lack of change in the bulk hydrogel density, and the dependence of stiffening on cell contractility suggested a model in which networks of cells deposit an interconnected fibrillar architecture in soft hydrogels. Such a network also provides a mechanism for long-range force transmission that may help to facilitate network organization in the otherwise amorphous material. This network could result in a composite with properties increasingly dominated by a relatively stiff network of cells and their pericellular ECM rather than the adjacent soft amorphous hydrogel material. Cell-mediated tension may contribute to hydrogel mechanics by propagating through this newly deposited ECM and possibly through endothelial tubules themselves, which has been suggested in fibrin hydrogels (253). This suggests that co-culture of ECs and DFs in PEG may be necessary to induce formation of a sufficiently interconnected network through which traction forces can propagate.

In support of our hypothesis that cellular network formation is necessary to allow hydrogel stiffening, we also observed a profound loss of stiffening behavior in co-cultures containing the MMP inhibitor GM6001, which inhibits MMP-mediated proteolysis necessary for cell spreading. Cell-mediated matrix degradation is required for an interconnected network of cells to form and deposit ECM. MMPs are required for capillary morphogenesis in natural ECMs (5, 55) and MMP-degradable PEG hydrogels (114, 231), but our findings here show they are also required for stiffening in a synthetic hydrogel. This effect may be MMP-specific because inhibition of plasmin-mediated degradation in PEG-fibrinogen hydrogels was necessary to



permit stiffening (261). Moreover, our results suggest that cellular growth and deposition of new ECM outpaces global proteolytic hydrogel degradation in this model tissue.

Reciprocal crosstalk between ECM stiffness and cell-mediated remodeling to adjust the cellular microenvironment has been suggested in the progression of tumors (250) and may also partially regulate the process of neovascularization. Here we demonstrate a correlation between gel stiffening and capillary morphogenesis, suggesting that localized cellular remodeling around networks of fibroblasts and ECs is necessary for both processes to occur. Therefore, these data suggest that the initial mechanical properties of the cellular microenvironment may not directly dictate capillary morphogenesis *per se*, but instead create a permissive environment that can be readily remodeled by the cells themselves. This hypothesis is supported by observations by Sokic *et al.* that capillary morphogenesis is significantly enhanced in PEG hydrogels with similar initial mechanical properties but with MMP degradability controlled by crosslinking peptide sequence (91). Counterintuitively, this suggests that enhancing MMP degradability may also result in enhanced hydrogel stiffening.

In summary, this study highlights the critical importance of cell-mediated remodeling on the evolution of tissue-level mechanical properties during the complex multicellular process of capillary morphogenesis in 3D. ECM mechanics affect the differentiation and function of many target cell types in engineered tissues beyond ECs and fibroblasts, such as osteoblasts, neurons, hepatocytes, and renal epithelium (162, 267). Thus, dynamic changes in matrix properties are a particularly important consideration in the design of functional vascularized tissues formed from multiple cell types to ensure the mechanical environment is permissive both for the morphogenesis of vascular structures and for tissue function. Characterizing cell-mediated changes to hydrogel mechanics provides an essential framework for understanding, and

ultimately controlling, the evolution of tissue mechanics when applied for regenerative medicine applications.

## 6.6 SUPPLEMENTAL FIGURES

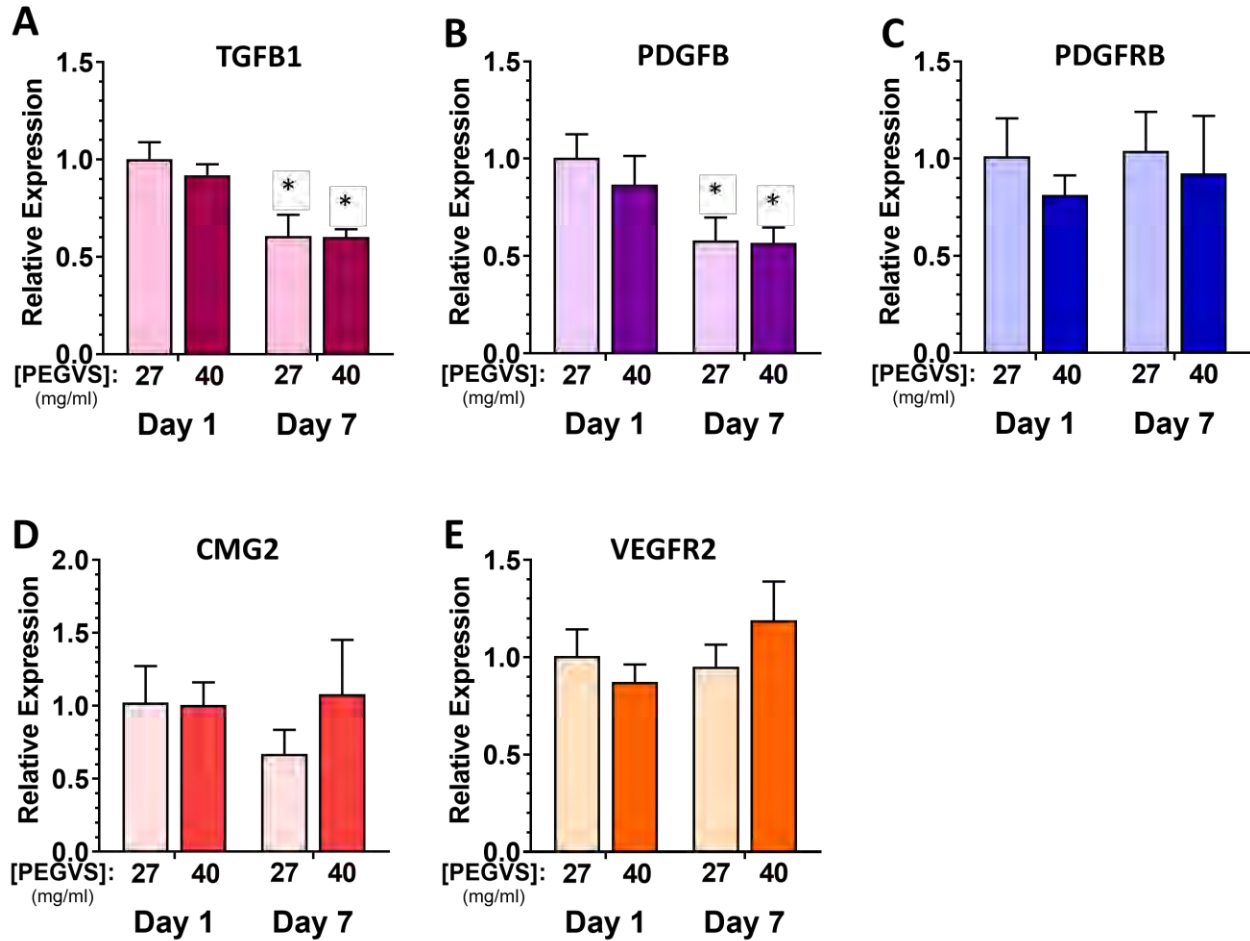


**Figure 6.9: Hydrogel formulation does not affect pro-angiogenic gene expression.** RNA was collected from constructs after 1 d and 7 d, purified, and expression determined using real time RT-PCR. Expression of transforming growth factor  $\beta$ 1 (TGFB1, A), platelet derived growth factor- $\beta$  (PDGFB, B), platelet derived growth factor receptor- $\beta$  (PDGFRB, C), capillary morphogenesis gene 2 protein (CMG2, D), and vascular endothelial growth factor receptor 2 (VEGFR2, E) was measured. Expression levels were normalized to glyceraldehyde 3-phosphate dehydrogenase (GAPDH) in each sample and then to expression in 27 mg/mL PEGVS at 1 d ( $\Delta\Delta C_t$  method). \*:  $p < 0.05$ , relative to day 1, N=3.

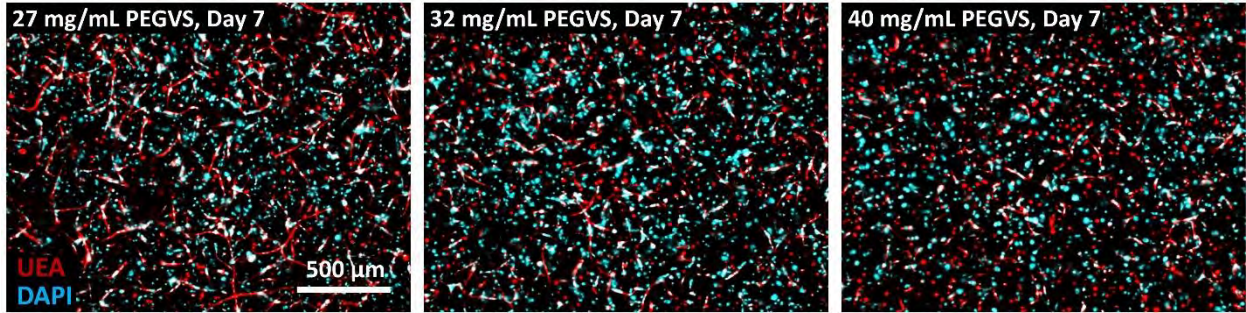


**Figure 6.10: Representative images of constructs with various PEGVS compositions showing similar overall cell density in each construct.** Maximum intensity projections from confocal sections are shown ( $z$  height = 300  $\mu\text{m}$ ) for ECs stained with UEA and all cellular nuclei stained with DAPI.

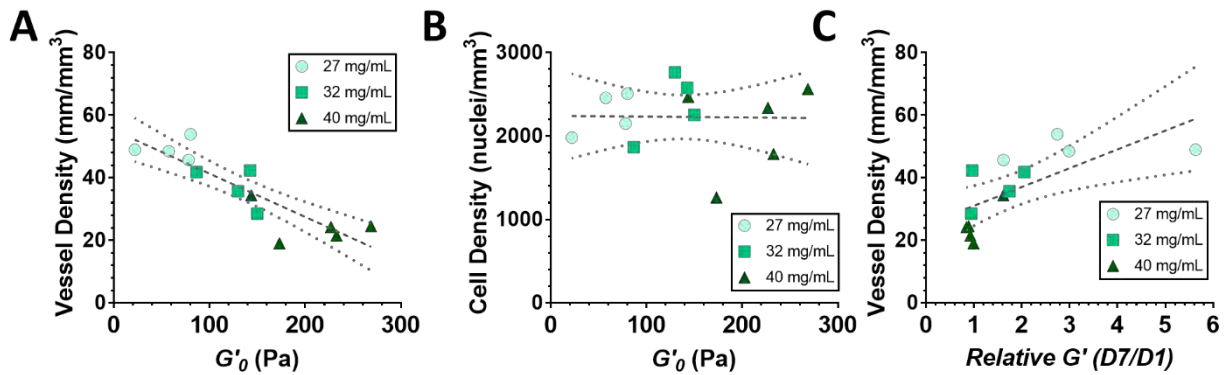


**Figure 6.11: Scatter plots showing the correlations between vessel densities, cell densities and hydrogel moduli** (shown as linear regression  $\pm$  95% confidence interval) for A) vessel density at 7 d vs  $G'$  at 1 d ( $R^2 = 0.762$ ,  $p < 0.0001$ ), B) cell density at 7 d vs  $G'$  at 1 d ( $R^2 = 0.0002$ ,  $p = 0.9562$ ), C) vessel density vs relative  $G'$  (defined as  $G'$  at 7 d divided by  $G'$  at 1 d,  $R^2 = 0.480$ ,  $p = 0.0087$ ). Each independent experiment is plotted separately, with the color and shape used to show PEGVS composition.

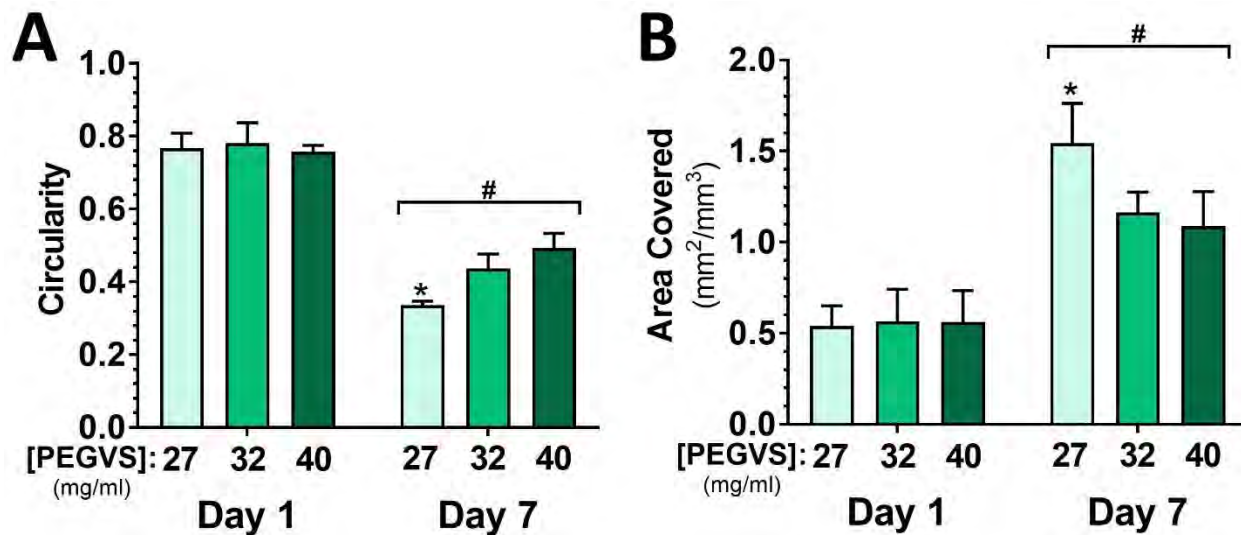


**Figure 6.12: Soft hydrogels facilitate cell spreading.** Average cell circularity (A) and area covered (B) after 1 d and 7 d of culture for various PEGVS compositions. Measurements were made as described in the Materials and Methods. #:  $p < 0.05$ , relative to Day 1 (same composition); \*:  $p < 0.05$ , relative to 40 mg/mL PEGVS (same day). N=3-7.

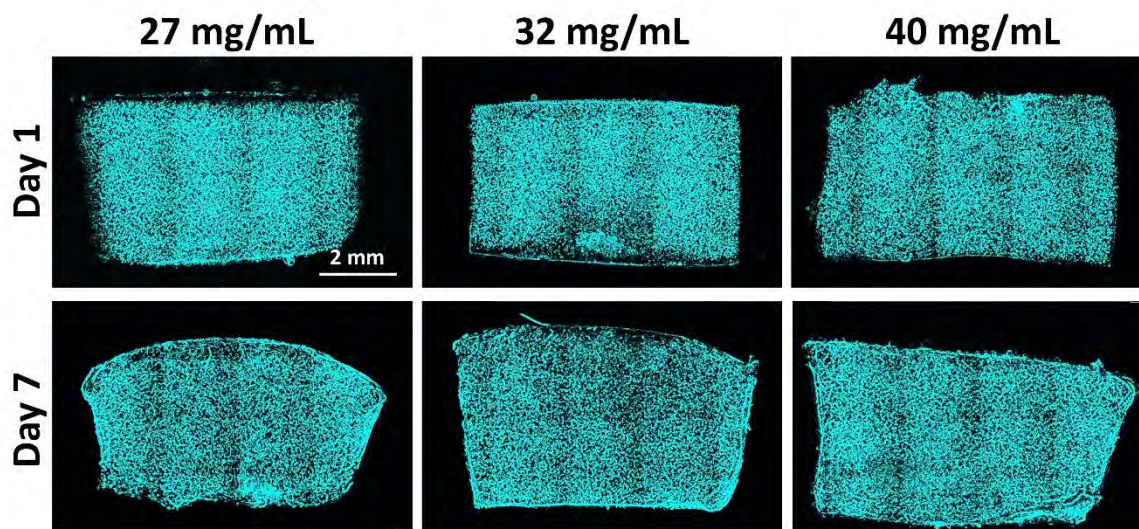


**Figure 6.13: Soft hydrogels change shape during culture.** Representative wide field images (reconstructed from tiled 4X images) of constructs of various compositions at 1 d and 7 d. Samples cut along the cylinder diameter, stained with DAPI, and imaged on the cut face (shown).

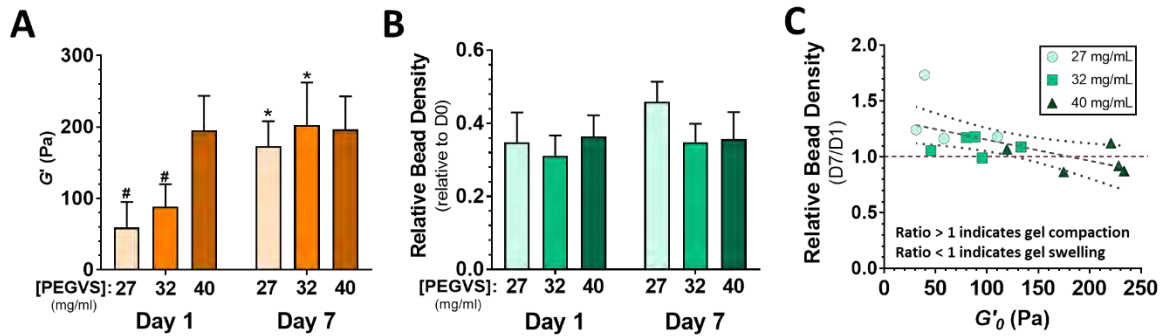


**Figure 6.14: Measurement of hydrogel compaction depending on hydrogel formulation.** A) Microbead incorporation into constructs does not alter stiffening behavior. The shear storage modulus of constructs was determined after 1 d and at 7 d. Note the pattern is similar to that shown in Figure 1. \*:  $p < 0.05$ , relative to Day 1 (same composition); #:  $p < 0.05$ , relative to 40 mg/mL PEGVS (same day),  $N=4-5$ . B) Microbead density does not significantly change during culture depending on PEGVS composition. Relative bead density was determined immediately after casting hydrogels and after 1 d or 7 d of culture. Relative bead density  $< 1$  reflects hydrogel swelling after casting.  $N=3-4$ . C) Scatter plots showing the correlation between ratio of microbeads at 7 d to 1 d and the initial shear storage modulus ( $G'_0$ ), shown as linear regression ( $\pm 95\%$  confidence interval,  $R^2 = 0.394$ ,  $p = 0.0163$ ). A ratio  $> 1$  indicated relative compaction of bead density (above red line); a ratio  $< 1$  indicates swelling (below red line). Each independent experiment is plotted separately with the color and shape used to show PEGVS composition. PEGVS composition was not taken into account for linear regression analysis.



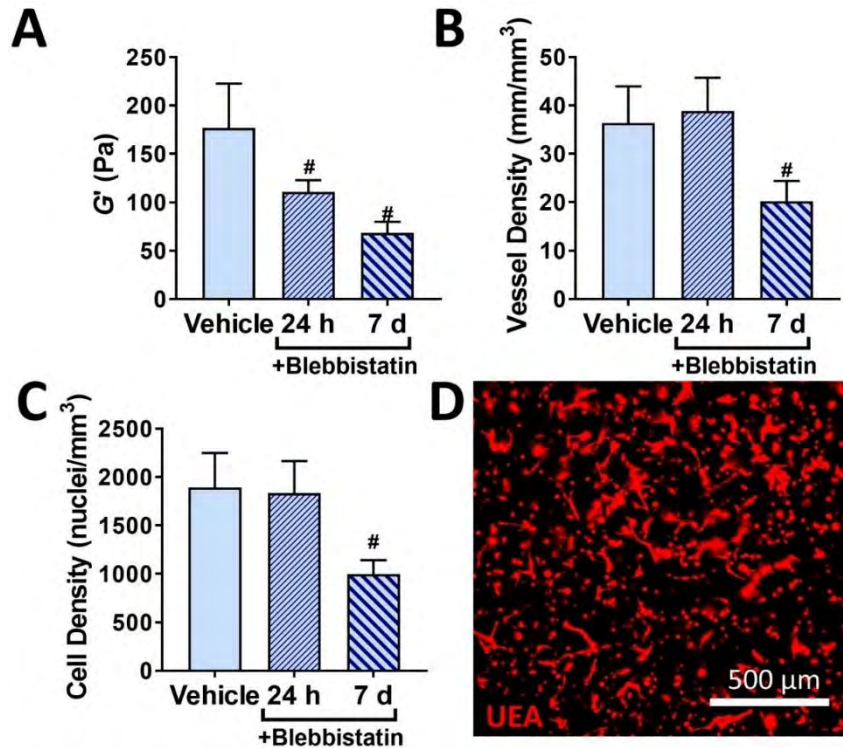


**Figure 6.15: Prolonged culture with blebbistatin abolishes stiffening, reduces capillary morphogenesis, and results in decreased cell density.** Hydrogel constructs with 32 mg/mL PEGVS were cultured with 30 μM blebbistatin for all 7 d of culture. Data from Figure 3 are replicated for comparison. The vehicle control was cultured with vehicle for 24 h. Shear storage modulus ( $G'$ , A), vessel density (B), and cell density (C) were measured at 7 d. A representative maximum intensity projection of a UEA stained sample incubated with blebbistatin for 7 d is shown (D). #:  $p < 0.05$  relative to vehicle, N=3-6.

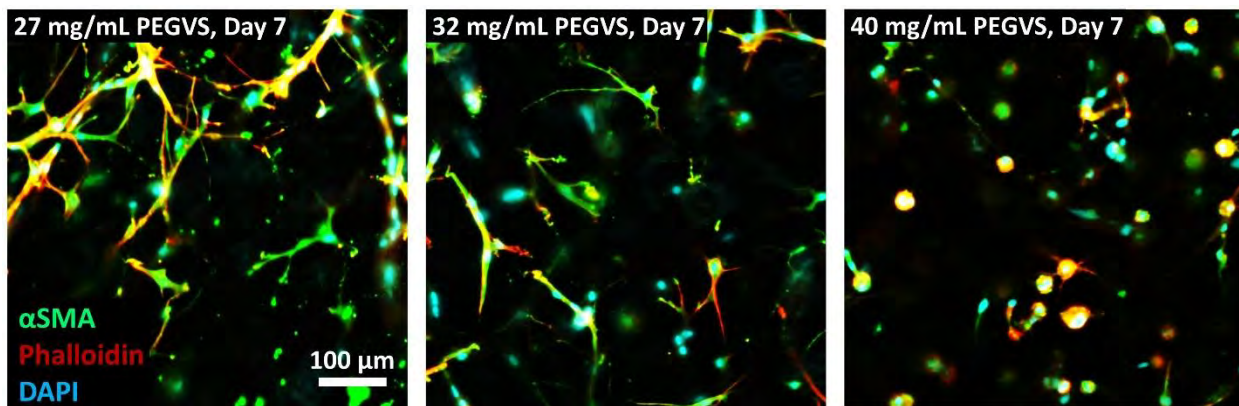


**Figure 6.16: Smooth muscle actin is expressed by fibroblasts in all PEGVS constructs.** Representative images of constructs showing immunofluorescent staining for ( $\alpha$ SMA), counterstained with phalloidin and DAPI.

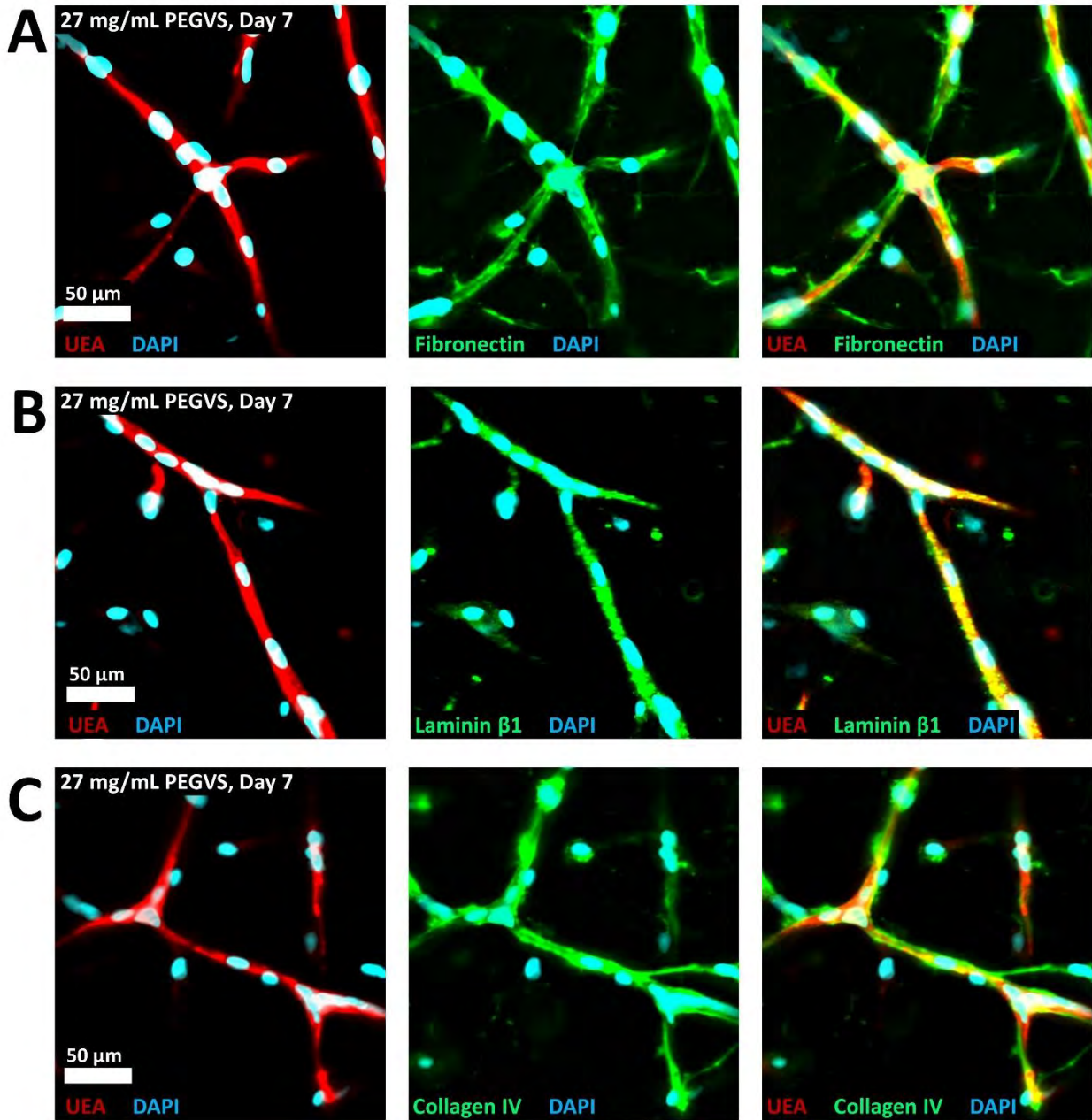


**Figure 6.17: Deposition of all assessed ECM components occurred around UEA+ vessels.** 27 mg/mL PEGVS constructs were fixed at 7d and stained for fibronectin (A), laminin  $\beta$ 1 chain (B), and collagen IV (C) and counterstained with UEA and DAPI. The basement membrane components collagen IV and laminin  $\beta$ 1 chain were deposited tightly around UEA+ vessels.

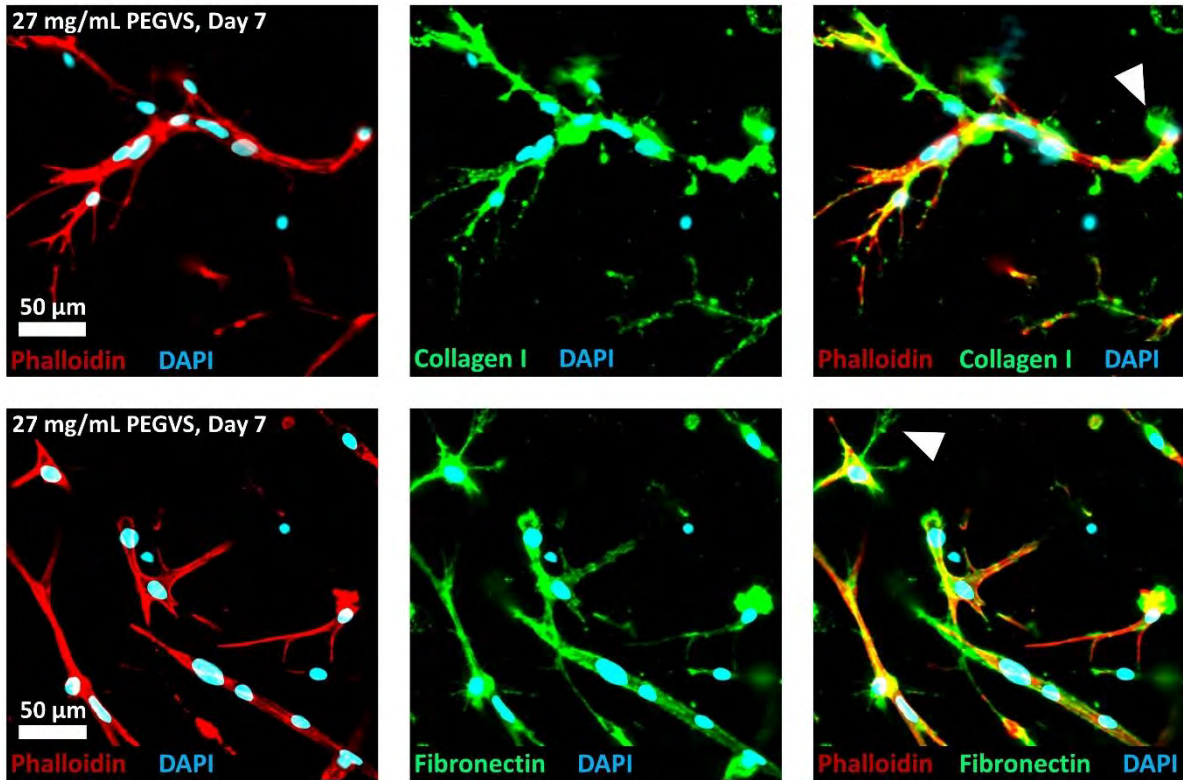


**Figure 6.18: Collagen I and fibronectin are deposited predominantly in focal areas near cells.** 27 mg/mL PEGVS constructs were fixed at 7 d and stained for collagen I and fibronectin and counterstained with phalloidin (to mark cell bodies) and DAPI. There are multiple clearly defined areas of collagen I and fibronectin deposition without superimposed nearby phalloidin staining (arrowheads).



## CHAPTER VII

### **Dermal Fibroblasts Support Enhanced Vessel Formation and Increased Hydrogel Stiffening Compared to Mesenchymal Stem Cells in Fibrin and PEG Hydrogels**

#### **7.1 ABSTRACT**

Formation of an extensive microvascular network within engineered tissue constructs is essential for numerous tissue engineering applications. Combination of endothelial cells (ECs) and appropriate stromal cells is a convenient means of encouraging neovascularization through angiogenic or vasculogenic network formation. Although multiple stromal cell types are capable of supporting neovascular network formation, there is little consensus as to the relative benefits depending on choice of stromal cell type. Within this chapter, morphogenetic behavior in the presence of either dermal fibroblasts (DFs) or bone marrow derived mesenchymal stem cells (MSCs) was compared in fibrin- and PEG-based models of microvascular network formation. Rheological properties of hydrogels were tracked over time as an easily obtainable surrogate metric indicative of matrix remodeling. DF supported cultures consistently supported more extensive network formation and increased hydrogel stiffening in both fibrin and PEG hydrogels compared to MSCs. Increased stiffening in the presence of DFs may be indicative of enhanced extracellular matrix (ECM) deposition or enhanced cellular contractility. DF and MSC co-cultures both upregulated alpha smooth muscle actin ( $\alpha$ SMA) over time in fibrin and PEG hydrogels, with more  $\alpha$ SMA positive cells tending to associate with vessels in PEG hydrogels than in fibrin, but there were no noticeable differences between stromal cell type. The data

presented in this chapter is intended to help generate hypotheses regarding differences in ECM remodeling depending on stromal cell type that facilitate neovascularization.

## 7.2 INTRODUCTION

A major hurdle for many tissue engineering applications is the formation of an extensive microvascular network in tissue constructs to support their long-term viability and function.

Although larger scale vessels can be fabricated (116), and arteriole scale conduits can be printed into a tissue scaffold (112, 268), techniques to induce the formation of a microvascular capillary bed rely on either angiogenic or vasculogenic morphogenesis of endothelial cells (ECs) (16, 87).

Extensive endothelial capillary morphogenesis typically relies on co-culture with a supportive stromal cell such as mesenchymal stem cells (MSCs) (56, 99, 100), adipose derived cells (10, 101, 102), various fibroblasts (11, 52, 103, 104), or smooth muscle cells (53, 91, 105). Despite numerous studies demonstrating the capacity of various stromal cells to support capillary morphogenesis, there are relatively few studies directly comparing morphogenetic behavior between potential stromal cell choices. Direct comparative studies of morphogenetic behavior depending on stromal cell choice can provide valuable insights for their judicious selection to elicit preferred morphogenetic outcomes.

Our lab has previously demonstrated that fibroblasts stimulate more rapid vessel formation compared to MSCs, but MSCs promote improved barrier function both *in vitro* (10) and *in vivo* (11) and are more capable of acting as pericytes (7) in fibrin hydrogels. Differences in proteolytic matrix remodeling was proposed as a possible explanation for the difference in rate, and possibly quality, of observed vessel formation. In this chapter, measurement of cell-mediated changes to matrix mechanics depending on stromal cell choice is used as surrogate metric for assessing differences in extracellular matrix (ECM) remodeling. Cellular remodeling

processes that affect the dynamics of hydrogel mechanics include proteolytic degradation (231), deposition of ECM proteins (52, 266), and active cellular contractility (175, 238), however, the relative contribution of each process was not deconvoluted in this work. As such, the preliminary data presented in this chapter showing differences in hydrogel stiffening depending on stromal cell type during capillary morphogenesis in fibrin and poly(ethylene glycol) (PEG) hydrogels is intended to be hypothesis generating for future work.

## **7.3 MATERIALS AND METHODS**

### **7.3.1 Cell culture**

All reagents were obtained from Thermo Fisher Scientific (Waltham, MA) unless specified. Human umbilical vein endothelial cells (ECs) were harvested from fresh umbilical cords and cultured in fully supplemented EGM2 (Lonza, Walkersville, MD) or Vasculife VEGF Endothelial Medium (Lifeline Cell Technology LLC, Frederick, MD) as previously described (172). ECs were used between passages 2-4. Normal human dermal fibroblasts (DFs, Lonza) were cultured in Dulbecco's modified eagle medium (DMEM) supplemented with 10% fetal bovine serum (FBS) and 1% penicillin streptomycin and were used up to passage 15. Bone marrow mesenchymal stem cells (MSCs, RoosterBio, Frederick, MD) were cultured in RoosterNourish-MSC medium (RoosterBio) and used up to passage 5. All cells were cultured at 37 °C and 5% CO<sub>2</sub> with thrice weekly medium exchange.

### **7.3.2 Fibrin-based angiogenic sprouting assay**

A three-dimensional cell culture model of capillary morphogenesis was assembled following adapted protocols as previously described (92, 172, 176). Briefly, EC-coated microbeads were embedded in 2.5 mg/mL fibrin gels with DFs or MSCs either embedded or overlaid on the gel as a monolayer. For a more detailed description of the procedure please refer

to **Chapter 3**. For conditions in which the stromal cells were embedded within the fibrin gel (“embedded”) a suspension of DFs or MSCs was added to the fibrinogen at a final concentration of  $2.5 \times 10^4$  cells/mL; for the other conditions, an equal volume of EGM2 was added instead. Microbeads were added to the solution at 50 beads/mL. After gelation, 2 mL of EGM2 per 1 mL of fibrin gel was overlaid for all gels. For conditions in which the stromal fibroblasts were cultured on top of the gel (“overlay”), DFs or MSCs were introduced in the overlaid EGM2 at a concentration of  $2.5 \times 10^4$  cells/mL of fibrin gel to achieve equal stromal cell numbers per gel for both overlay and embedded conditions. For the presented experiment, 6 gels were cast for each time point (3 gels for rheology, 3 gels for image analysis). Gel constructs (0.5 mL total volume) were fabricated in 24-well tissue culture plates (Corning Inc).

### **7.3.3 Fibrin-based vasculogenesis assay**

A 3D model of capillary morphogenesis was adapted from our previously described protocol (77) as follows. ECs ( $3 \times 10^5$  cells/mL) and either DFs or MSCs ( $3 \times 10^5$  cells/mL) were distributed in 0.5 mL fibrin hydrogels formed in a 24-well culture plate from 2.5 mg/mL of 0.22  $\mu\text{m}$  filtered bovine fibrinogen (Sigma-Aldrich, St Louis, MO) dissolved in serum free DMEM and polymerized with 1 U/mL bovine thrombin (Sigma). After gelation, 1 mL of Vasculife VEGF Endothelial Medium (Lifeline Cell Technology LLC, Frederick, MD) was added to the hydrogel.

### **7.3.4 PEG-based vasculogenesis assay**

Hydrogels were formed from 4-arm poly(ethylene glycol) vinyl sulfone (PEG-VS; 20 kDa, Jenkem USA, Allen TX) and a combination of thiol containing adhesive and protease-sensitive peptides adapted from published protocols (114, 127) and covered in detail in **Chapter 4** and **Chapter 6**. Immediately before use, PEG-VS was dissolved in HEPES (100 mM, pH 8.4)

and CGRGDS peptide (RGD, Genscript, Piscataway, NJ) was reacted with the PEG-VS for 30 min at a final concentration of 500  $\mu$ M. All hydrogels contained a 1:1 ratio of ECs to stromal cells. In rapid succession, a cell pellet was resuspended in the dithiol peptide solution to achieve the indicated final cell density (either  $3 \times 10^6$  cells/mL or  $5 \times 10^6$  cells/mL of each cell type), this solution was then added to the PEG-VS solution, gently mixed, and 50  $\mu$ l was dispensed into a sterile 1 mL syringe with the needle end cut off, and allowed to polymerize for 1 h at 37 °C in a sealed 50 mL conical tube. Crosslinking peptides included: Ac-GCRDVPMS↓MRGGDRCG-NH<sub>2</sub> (“VPMS”) and Ac-GCRDVPMS↓MRGGVPMS↓MRGGDRCG-NH<sub>2</sub> (“2xVPMS”) each containing an N-terminal acetylation and a C-terminal amidation (Genscript, cleavage sites indicated by ↓). Polymerized hydrogels were punched into 2 mL of Vasculife VEGF medium in a 24-well plate. Media was exchanged on day 1 then on alternate days thereafter up to 7 or 14 days. At the end of the experiment, hydrogels were fixed with Z-fix (Anatech, Battle Creek, MI) for 1 hr, rinsed 4x in PBS, and then stored at 4 °C.

#### **7.3.4 Mechanical characterization of fibrin and PEG hydrogels**

The bulk mechanical properties of fibrin and PEG hydrogels were measured via parallel plate shear rheology using an AR-G2 rheometer (TA Instruments, New Castle, DE) equipped with an 8 mm diameter measurement head and a Peltier stage maintained at 37 °C. A detailed description of rheological assessment of fibrin hydrogels is available in **Chapter 3**, but briefly, oscillatory shear measurements of 6% strain amplitude and a frequency of 1 rad/sec were performed on the specified days directly in multi-well tissue culture. Cell culture media was aspirated before measurements, with a small volume left to ensure the gel remained wet. A protocol was developed whereby the top platen was lowered until it made initial contact with the hydrogel, followed by measurements of shear modulus ( $G'$ ) taken at 200  $\mu$ m intervals while

closing the gap between platen and stage. Gels exhibited a plateau in  $G'$  as the gap was progressively decreased after making contact, the peak  $G'$  measured of 3 gap heights after contacting the gel was used as our reported value for the given hydrogel.

Free floating PEG hydrogels were removed from their culture plate, mounted on the AR-G2 rheometer between an 8-mm measurement head and a Peltier stage, each covered with P800 sandpaper. Shear storage modulus ( $G'$ ) was determined at 0.05 N normal force, 5% strain amplitude, and 1 Hz frequency and averaged over a 1-minute time sweep.

### 7.3.5 Fluorescent image quantification methods

On the indicated days, hydrogels were fixed with Z-fix (Anatech, Battle Creek, MI). All PEG-VS hydrogels were cut longitudinally down the cylinder midline prior to staining, yielding two halves. For quantification of vessel and nuclei density and to visualize cell spreading, samples were stained with rhodamine-conjugated lectin from *Ulex europaeus* (UEA, Vector Laboratories, Burlingame, CA, specific for endothelial cells, 1:200), 4', 6-diamidino-2-phenylindol (DAPI, 1  $\mu\text{g}/\text{mL}$ , Sigma), and AlexaFluor 488 phalloidin (1:200). PEG-hydrogels were imaged on the cut side to ensure images were representative of cellular behavior within the hydrogels. Images were acquired using an Olympus IX81 microscope equipped with a disk scanning unit (DSU, Olympus America, Center Valley, PA) and Metamorph Premier software (Molecular Devices, Sunnyvale, CA). For all analyses, confocal z-stacks were acquired using the DSU. Z-series were collapsed into maximum intensity projections prior to analyses.

Quantifications of network length per bead for the angiogenesis assay was performed as detailed in **Chapter 3**. Quantification of nuclei density for the angiogenesis assay was performed on stacks spanning the full thickness of the hydrogel imaged at 4x (2.16 x 1.65 mm). The full thickness of the gel was imaged to allow comparison of nuclei densities between overlay and

embedded conditions. Stacks used to quantify nuclei densities were taken in regions that did not include any endothelial cells and thus solely represent stromal cell densities.

Quantification of vessel densities for the fibrin and PEG based vasculogenesis assays were performed on 200  $\mu\text{m}$  stacks (50  $\mu\text{m}$ /slice) imaged at 4x (2.16 x 1.65 mm). Total vessel length per region of interest (ROI) was quantified from UEA images using the Angiogenesis Tube Formation module in Metamorph and reported as vessel length per volume of ROI. Total nuclei per ROI were quantified from DAPI images using a custom ImageJ script as previously described (231), and reported as counts per volume.

### **7.3.6 Immunofluorescent staining and imaging of $\alpha$ -smooth muscle actin in fibrin and PEG based vasculogenesis assays**

Following tissue construct fixation (and bisection for PEG hydrogels), hydrogels were permeabilized with 0.5% v/v TritonX-100 in tris-buffered saline (TBS) for 30 minutes then blocked overnight at 4°C in TBS with 2% w/v bovine serum albumin (BSA, Sigma-Aldrich) and 0.1% v/v Tween 20. Primary antibodies for alpha smooth muscle actin ( $\alpha\text{SMA}$ , Abcam, mouse IgG<sub>2b</sub> isotype, 1:200 dilution) were incubated with samples overnight at 4°C. Samples were then washed several times and incubated overnight at 4°C with the appropriate secondary antibody. Samples were again washed then stained with DAPI and UEA and stored in TBS. Representative images were acquired at 10x magnification using the DSU and presented as maximum intensity projections of 50  $\mu\text{m}$  thick stacks (5  $\mu\text{m}$ /slice).

### **7.3.7 Gene expression analysis of $\alpha$ -smooth muscle actin in fibrin and PEG based vasculogenesis assays**

At the indicated time points, hydrogels were washed with PBS and then disrupted to allow recovery of encapsulated cells. Fibrin hydrogels were dislodged from their well using a

small spatula and then dissolved using 500  $\mu$ L of Nattokinase (1000 U/mL, Japan Bio Science Laboratory Co., Osaka City, Japan) and incubated at 37 °C for 45 min. PEG hydrogels were cut into small pieces with surgical scissors, and incubated under constant gentle rotation in 500  $\mu$ L Collagenase IV (200 U/mL) at 37 °C for 30-40 min until gels were dissociated. Solutions were pooled from 2 hydrogels, and the dissociated hydrogel suspensions were centrifuged at 500  $\times$  g for 3 min. The resulting cell pellet was lysed and RNA purified using an RNeasy Mini Kit (Qiagen, Venlo, Netherlands). RNA was reverse transcribed to cDNA using a High Capacity cDNA Reverse Transcription Kit (Applied Biosystems, Thermo Fisher Scientific). PCR amplifications were performed on a 7500 Fast Real-Time PCR System (Applied Biosystems) using Taqman Gene Expression reagents (20 ng cDNA per PCR reaction). The primer probe sets for the following genes were utilized (Taqman Assay ID indicated): GAPDH (Glyceraldehyde 3-phosphate dehydrogenase, Hs04420566\_g1); ACTA2 ( $\alpha$ -smooth muscle actin, Hs00426835\_g1); The  $\Delta\Delta C_t$  method was used to determine relative gene expression with GAPDH as the internal control.

### **7.3.8 Western blot analysis of $\alpha$ -smooth muscle actin in vasculogenesis assays**

Cell pellets were recovered on day 7 as described for gene expression analysis. Cell pellets were lysed and protein concentrations were determined using a Pierce BCA protein assay kit. Western blot analysis for  $\alpha$ SMA was then conducted on the purified protein solutions. After boiling samples, equal amounts of protein (5  $\mu$ g) from each respective sample was electrophoresed in a 10% Tris glycine gel (Invitrogen) under reducing conditions and transferred to a PVDF membrane. The PVDF membrane was then probed in a 5% BSA blocking solution with primary antibodies for alpha smooth muscle actin ( $\alpha$ SMA, Abcam, mouse IgG<sub>2b</sub> isotype, 1:200 dilution). The PVDF membrane was placed inside a 50 mL conical tube with the transfer



side facing inward and incubated for 1.5 hours at room temperature with 5 mL of primary antibody solution on a rotary rack and subsequently washed 6× with TBS-T for 5 min. After washing, the membrane was incubated in TBS-T with horseradish peroxidase (HRP)-conjugated anti-mouse secondary antibody (1:10,000, Pierce Biotechnology) and pre-conjugated GAPDH HRP (1:2000, Santa Cruz Biotechnologies, Santa Cruz, CA). Protein expression was visualized using an enhanced chemiluminescence detection system. Bands were identified by comparing to a molecular mass ladder (Pierce Biotechnology).

### 7.3.8 Statistics

Statistical analysis was performed using GraphPAD Prism (La Jolla, CA) for vasculogenesis assays performed in PEG hydrogels for which 3-4 replicates were collected. Data are represented as mean ± standard deviation. Data were analyzed using two-way ANOVA with Tukey post-hoc testing. A value of  $\alpha < 0.05$  was considered significant. Statistical analysis was not performed for the fibrin-based angiogenesis and vasculogenesis assays because only 1 replicate was collected. Error bars represent the standard deviation between 3 identical hydrogels cast from the same stock of reagents, representing the intra-experimental variability.

## 7.4 RESULTS

### 7.4.1 DFs appear more proliferative and induce more hydrogel stiffening than MSCs in a fibrin-based model of angiogenic sprouting.

This preliminary study compared endothelial sprouting from an EC-coated microcarrier bead embedded in fibrin either in the presence of DFs or MSCs. DFs and MSCs were either overlaid on the hydrogel as a monolayer or embedded in the hydrogel (**Fig 7.1A**). Both stromal cell types supported a similar average network length per bead when the supportive stromal cell was overlaid on top of the matrix (**Fig 7.1B**). In this overlay model, stromal cells are spatially

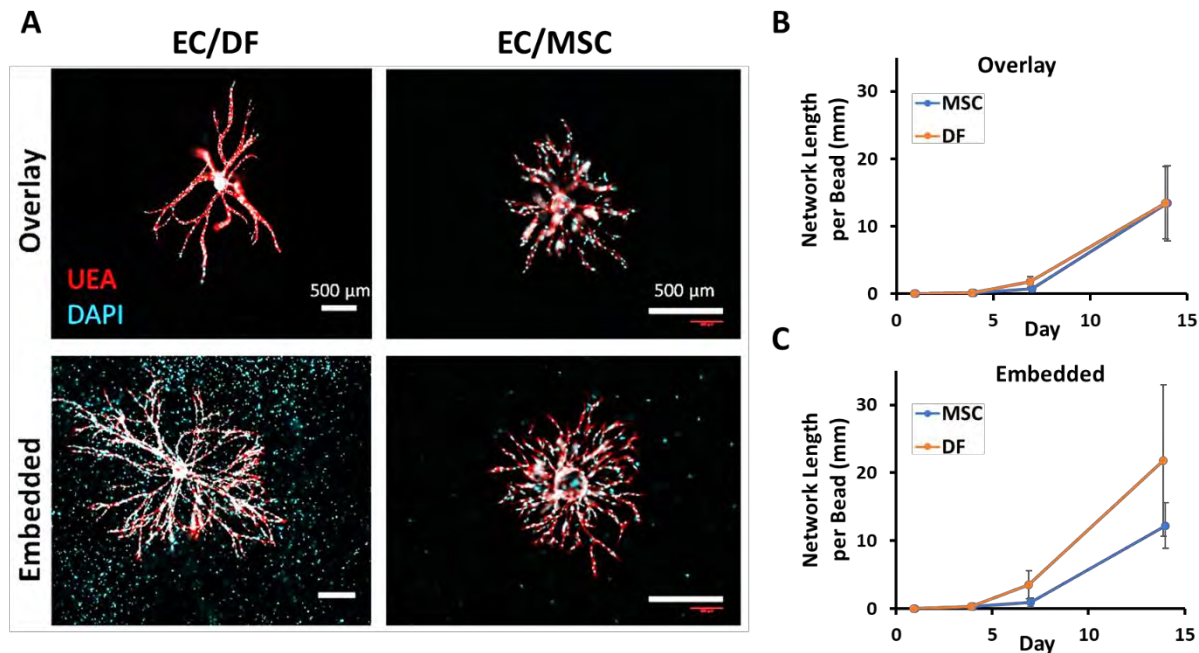


**Figure 7.1: DFs support more extensive network formation than MSCs when embedded, but not overlaid, in a fibrin-based angiogenic sprouting model.** The “Overlay” condition involves culturing DFs or MSCs on top of the fibrin gel, whereas they are distributed throughout the fibrin gel in the “Embedded” condition. A) Representative images from each condition on day 14. UEA and DAPI staining indicate ECs and total cell nuclei, respectively. Scale bars = 500  $\mu\text{m}$ . Quantified average network length per bead is shown in the presence of either DFs (orange) or MSCs (blue) for both Overlay (B) and Embedded (C) conditions. 8-40 beads per hydrogel were quantified, error bars represent the standard deviation of average network length per bead between 3 hydrogels cast from the same precursor solutions for MSC conditions, representing the intra-experimental variability. DF data is reproduced from figure 3.1 and error bars represent interexperimental variability ( $n = 3$ )

isolated from the sprouting ECs. When stromal cells were embedded in the matrix, however, DFs appeared to support more extensive network formation than MSCs (Fig 7.1C).

In the overlay condition, pronounced hydrogel stiffening was observed for both DF and MSC supported cultures. DFs appeared to promote enhanced hydrogel stiffening compared to MSCs, with apparent differences as early as day 4 (Fig 7.2A). DFs similarly appeared to promote enhanced hydrogel stiffening in the embedded condition, with a noticeable difference compared to MSCs only on day 14 (Fig 7.2B). Enhanced hydrogel stiffening in DF supported cultures was

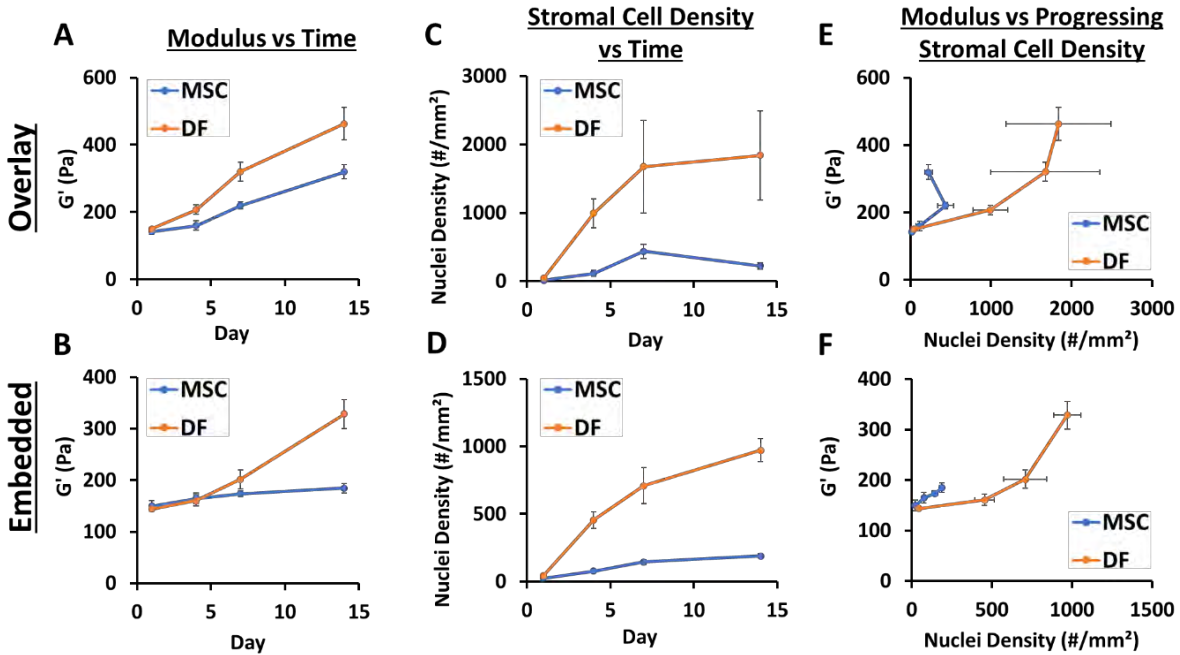


**Figure 7.2: DFs induce increased hydrogel stiffening and increased nuclei densities compared to MSCs in a fibrin-based model of angiogenic sprouting.** Bulk rheology on days 1,4, 7, and 14 is shown in the presence of either DFs or MSCs for both Overlay (A) and Embedded (B) conditions. The nuclei density, quantified from maximum intensity projections of DAPI stained images, is shown for DFs and MSCs for the Overlay (C) and Embedded (D) conditions on days 1,4, 7, and 14. Multiple maximum intensity projections were taken per hydrogel in regions without EC vessels, such that the quantification solely represents stromal cell nuclei. Overlay and embedded conditions were both seeded with  $1.25 \times 10^4$  total stromal cells per hydrogel. The hydrogel modulus is plotted against the stromal cell density on progressive days (1,4, 7, 14) for the Overlay (E) and Embedded (F) conditions. Data from (A) and (C) is plotted in (E), whereas data from (B) and (D) is plotted in (F). These graphs help illustrate the change in modulus relative to change in nuclei density. Error bars on all graphs represent intra-experimental variability between 3 hydrogels cast from the same stock of reagents.

accompanied by pronounced increases in DF nuclei density compared to MSC in both the overlay (**Fig 7.2C**) and embedded (**Fig 7.2D**) conditions. Plots of hydrogel modulus versus progressive nuclei densities on days 1, 4, 7, and 14 suggest that although DFs induce more aggregate hydrogel stiffening, MSCs may mediate more hydrogel stiffening per cell in both the overlay (**Fig 7.2E**) and embedded (**Fig 7.2F**) conditions.

#### 7.4.2 DFs support enhanced vessel formation and induce increased hydrogel stiffening compared to MSCs when co-cultured with ECs in a fibrin-based model of vasculogenesis.

This preliminary study compared capillary network self-assembly and hydrogel stiffening in a fibrin-based vasculogenesis model containing EC monocultures, EC/DF co-cultures, and EC/MSC co-cultures. All culture conditions resulted in some degree of vessel-like network formation after 7 days (**Fig 7.3A**). Although substantial hydrogel volume remained unoccupied in EC monocultures, DFs and MSCs both spread to occupy the majority of hydrogel volume in co-culture conditions (**Fig 7.3B**). Quantification of vessel densities on day 7 for each condition shows that co-culture improves vessel formation compared to monoculture, and DFs support more extensive vessel formation than MSCs (**Fig 7.4A**). The total nuclei densities for all conditions on day 1 is higher than expected (EC:  $1086 \pm 35$ , EC/MSC:  $1441 \pm 174$ , EC/DF:  $1808 \pm 149$ ) given the total cell seeding densities of  $3 \times 10^5$  cells/mL for EC monocultures and  $6 \times 10^5$  cells/mL for co-cultures, suggesting hydrogel compaction during the first day of culture (**Fig**

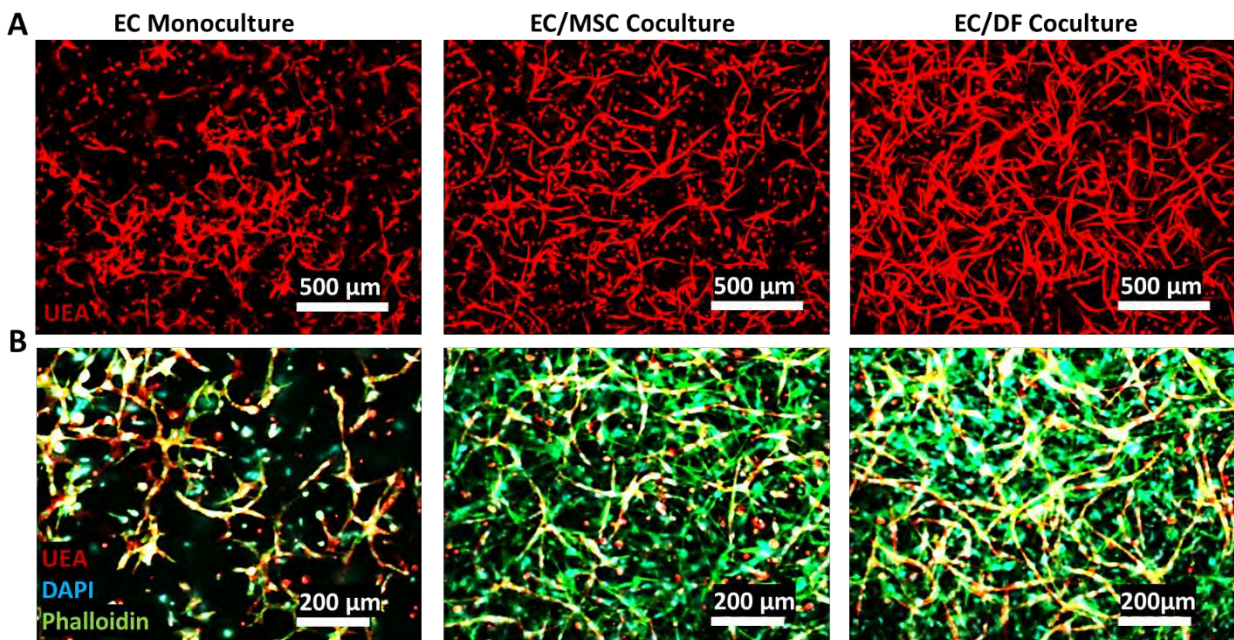


**Figure 7.3: Representative images of capillary network formation and overall cell spreading in a vasculogenic model of capillary self-assembly in 2.5 mg/mL fibrin.** A) Representative images of for ECs stained with UEA at 7 d from constructs containing an EC mono-culture ( $3 \times 10^5$  cells/mL seeded), EC/DF co-culture or EC/MSC co-culture (co-cultures seeded with  $3 \times 10^5$  cells/mL of each cell type). B) Representative images of each culture condition shown stained with UEA (red), phalloidin (green) and DAPI (cyan) Stromal cells in the co-culture conditions are phalloidin positive but UEA negative. Maximum intensity projections of confocal sections ( $z$  height = 200 μm).

7.4B). In the absence of stromal cells there was no noticeable change in EC nuclei densities over time. However, both EC/MSC and EC/DF cocultures exhibited increases in total nuclei densities, suggesting either further hydrogel compaction or cellular proliferation (Fig 7.4B). Day 1 hydrogel mechanics were noticeably higher in this vasculogenic model (Fig 7.4C) than in the angiogenesis model with embedded stromal cells (Fig 7.2B), but this is consistent with the observation that hydrogel shear modulus on day 1 for an embedded mono-culture of DFs increased with increasing cell seeding density (Supplemental, Fig S1). Hydrogel shear modulus increased from day 1 to day 7 for all 3 culture conditions but had the largest increase for EC/DF co-cultures (Fig 7.4C).

Nuclei densities and hydrogel shear moduli for monocultures of DFs and MSCs were also collected. Representative images of DFs and MSCs after 7 days in culture are shown in Fig 7.5A. Both DFs and MSCs had similar nuclei densities on day 1 (MSC:  $978 \pm 54$ , DF:  $926 \pm$

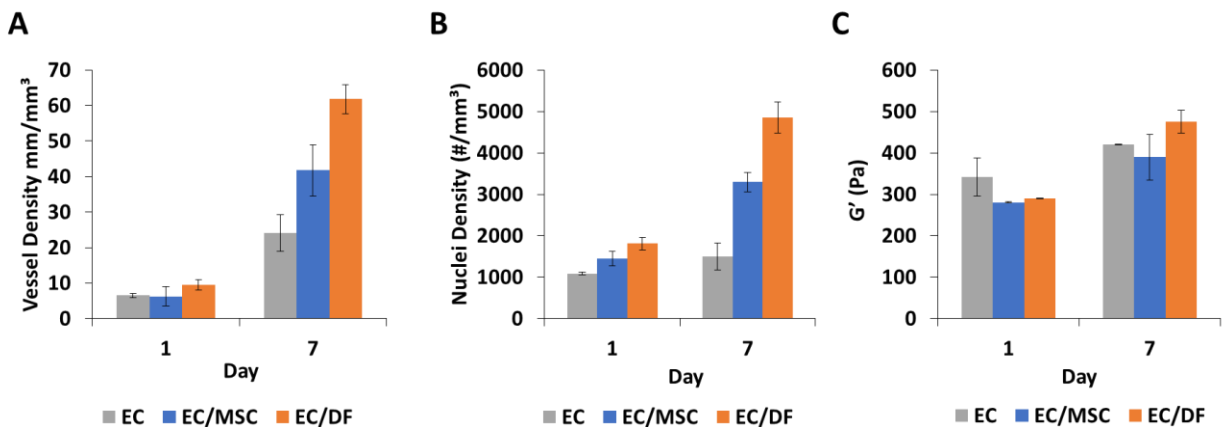


**Figure 7.4: EC/DF co-cultures support increased vessel densities, nuclei densities, and hydrogel stiffening compared to EC mono-cultures and EC/MSC co-cultures in 2.5 mg/mL fibrin.** Vessel density (A), total nuclei density (B), and shear modulus ( $G'$ )(C) were quantified for EC mono-cultures, EC/MSC co-cultures, and EC/DF co-cultures on days 1 and 7 as described in the methods. All cultures were seeded with  $3 \times 10^5$  ECs/mL, co-cultures contained an additional  $3 \times 10^5$  stromal cells/mL. Vessel density (A) and nuclei density (B) were quantified from confocal stacks ( $z$  height = 200  $\mu$ m). Error bars for all metrics represent intra-experimental variability between the average values obtained from 3 hydrogels.



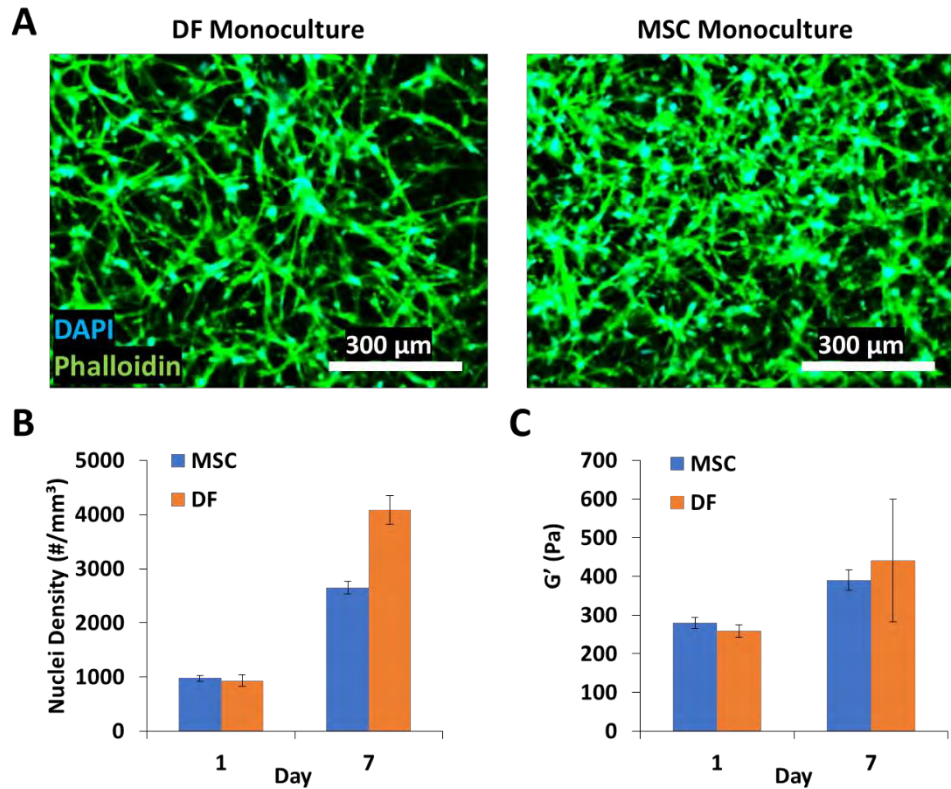


**Figure 7.5: DF monocultures had increased nuclei densities compared to MSC monocultures on day 7 in fibrin, but both cell types showed a similar degree of hydrogel stiffening.** A) Representative maximum intensity projections of confocal sections ( $z$  height =  $200\ \mu\text{m}$ ) of DFs and MSCs stained with DAPI (cyan) and phalloidin (green) on day 7 from constructs seeded with  $3 \times 10^5$  stromal cells/mL. B) Nuclei densities were quantified from maximum intensity projections, both conditions had similar nuclei densities on day 1, but DF cultures had higher nuclei densities on day 7. C) Both cell types demonstrated a similar increase in shear modulus ( $G'$ ) from day 1 to day 7. Error bars for both metrics represent intra-experimental variability between the average values obtained from 3 hydrogels.

109) (Fig 7.5B), higher than expected based on the seeding densities of  $3 \times 10^5$  cells/mL, suggesting hydrogel compaction for both cell types during the first day of culture. However, on day 7 DF cultures had higher nuclei densities than MSC cultures (Fig 7.5B). As opposed to co-cultures, monocultures of DFs and MSCs in fibrin appeared to stiffen a similar amount over 7 days (Fig 7.5C). These results suggest there may be a cooperative contribution to hydrogel stiffening between ECs and stromal cells. Whereas hydrogel mechanics in the angiogenic bead assay are dominated by the contribution from the embedded stromal cell (Fig 3.3A, B),

distribution of ECs throughout the matrix in a vasculogenesis model with DFs resulted in increased hydrogel stiffening compared to the angiogenesis assay (**Supplemental, Fig S2**), supporting the idea of cooperative interaction with ECs.

#### **7.4.3 DFs support enhanced vessel formation compared to MSCs and induce significant hydrogel stiffening when co-cultured with ECs in a PEG-based model of vasculogenesis.**

This replicated study compared capillary network self-assembly and hydrogel stiffening in EC/DF and EC/MSC co-cultures in a vasculogenesis model in MMP-degradable PEG hydrogels. PEG hydrogels were crosslinked with either VPMS or with the more highly degradable 2xVPMS peptides, previously compared in **Chapter 5**. In PEG-VPMS, EC/DF and EC/MSC co-cultures both exhibited significant vessel formation over time (**Fig 7.6A, B**) with EC/DF co-cultures having significantly higher vessel densities than EC/MSC co-cultures on days 7 ( $p = 0.006$ ) and days 14 ( $p = 0.0007$ ). Neither EC/DF nor EC/MSC co-cultures exhibited any significant changes in total nuclei densities over time (**Fig 7.6C**). EC/DF co-cultures significantly stiffened from day 1 to day 14 ( $p = 0.021$ ) and had significantly higher shear moduli than EC/MSC co-cultures on day 14 ( $p = 0.018$ ), whereas EC/MSC cultures exhibited insignificant softening from day 1 ( $129 \pm 12$  pa) to day 14 ( $116 \pm 57$  pa) (**Fig 7.6D**).

Hydrogels formed with 2xVPMS crosslinking peptides promote accelerated vessel formation and increased hydrogel stiffening compared to VPMS hydrogels (**Fig 5.2**) in EC/DF cocultures. Comparison of EC/DF to EC/MSC co-cultures in 2xVPMS hydrogels helps accentuate differences in morphogenetic behavior. In PEG-2xVPMS, EC/DF and EC/MSC co-cultures both exhibited significant vessel formation over time (**Fig 7.7A, B**) with EC/DF co-cultures having significantly higher vessel densities than EC/MSC co-cultures on day 14 ( $p =$

## PEG-VPMS

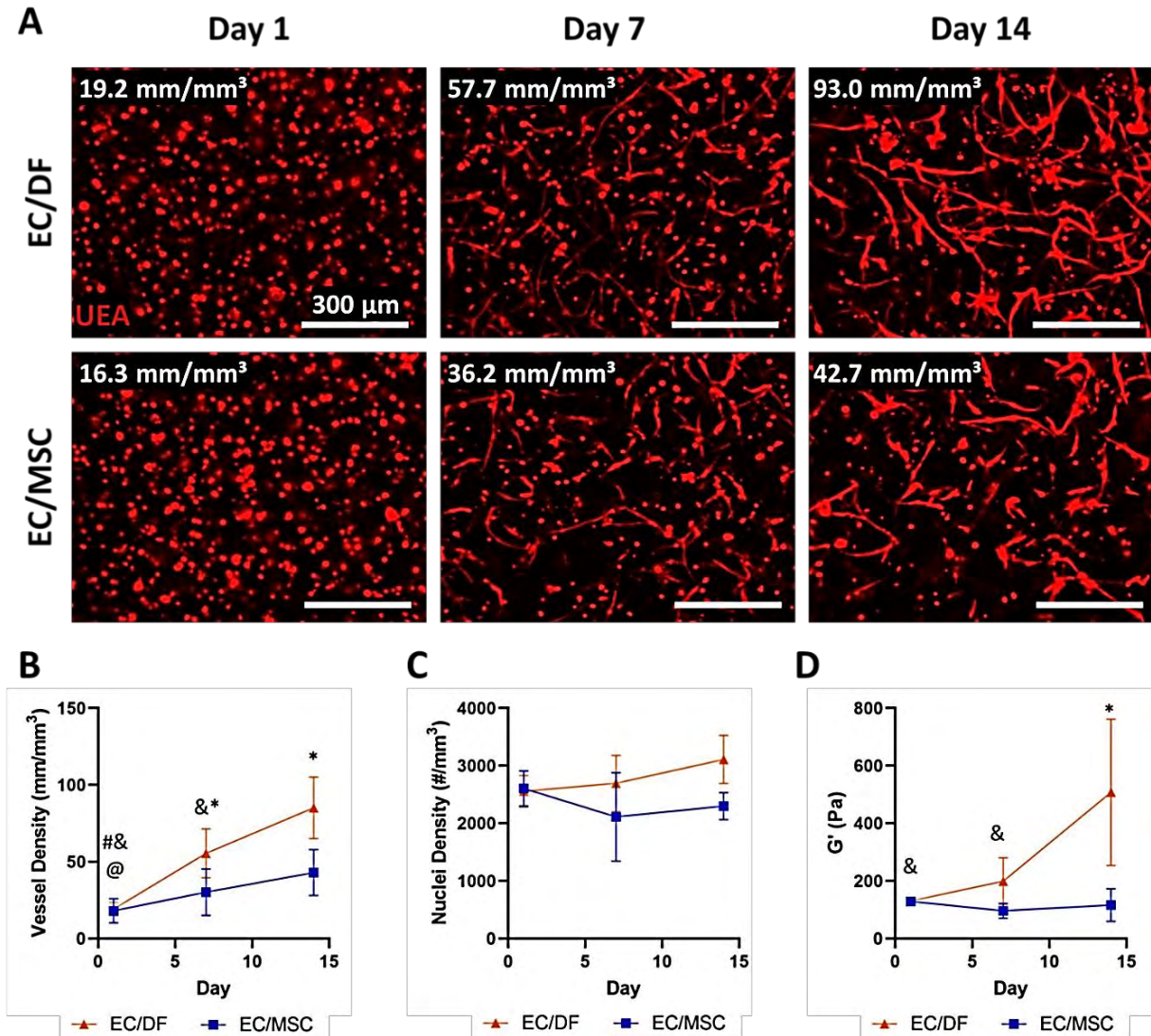


**Figure 7.6: DFs support enhanced vessel formation compared to MSCs and induce significant hydrogel stiffening when co-cultured with ECs in PEG-VPMS.** A) Representative images of maximum intensity projections of confocal sections ( $z$  height = 200  $\mu\text{m}$ ) for ECs stained with UEA on days 1, 7, & 14 from constructs seeded with  $5 \times 10^6$  ECs/mL and  $5 \times 10^6$  stromal cells/mL. Images were chosen with near average vessel densities between multiple replicates, quantification of vessel density for the specific image shown is indicated. B) Vessel density in the bulk of the constructs was estimated as described in the methods (Two-way ANOVA: time  $p = 0.008$ , cell  $p = 0.002$ , interaction  $p = 0.001$ ). C) Cell density in the constructs was quantified from DAPI stained images (Two-way ANOVA: time  $p = 0.607$ , cell  $p = 0.001$ , interaction  $p = 0.143$ ). D) Measurement of the shear storage modulus ( $G'$ ) of constructs on progressive days demonstrates that EC/DF hydrogels stiffen but not EC/MSC hydrogels (Two-way ANOVA: time  $p = 0.084$ , cell  $p = 0.083$ , interaction  $p = 0.024$ ). For all graphs: #:  $p < 0.05$ , EC/DF relative to EC/DF D7; &:  $p < 0.05$  EC/DF relative to EC/DF day 14; @:  $p < 0.05$  EC/MSC relative to EC/MSC D14; \*:  $p < 0.05$ , EC/DF relative to EC/MSC (same day).  $N=3$ .



## PEG-2xVPMS

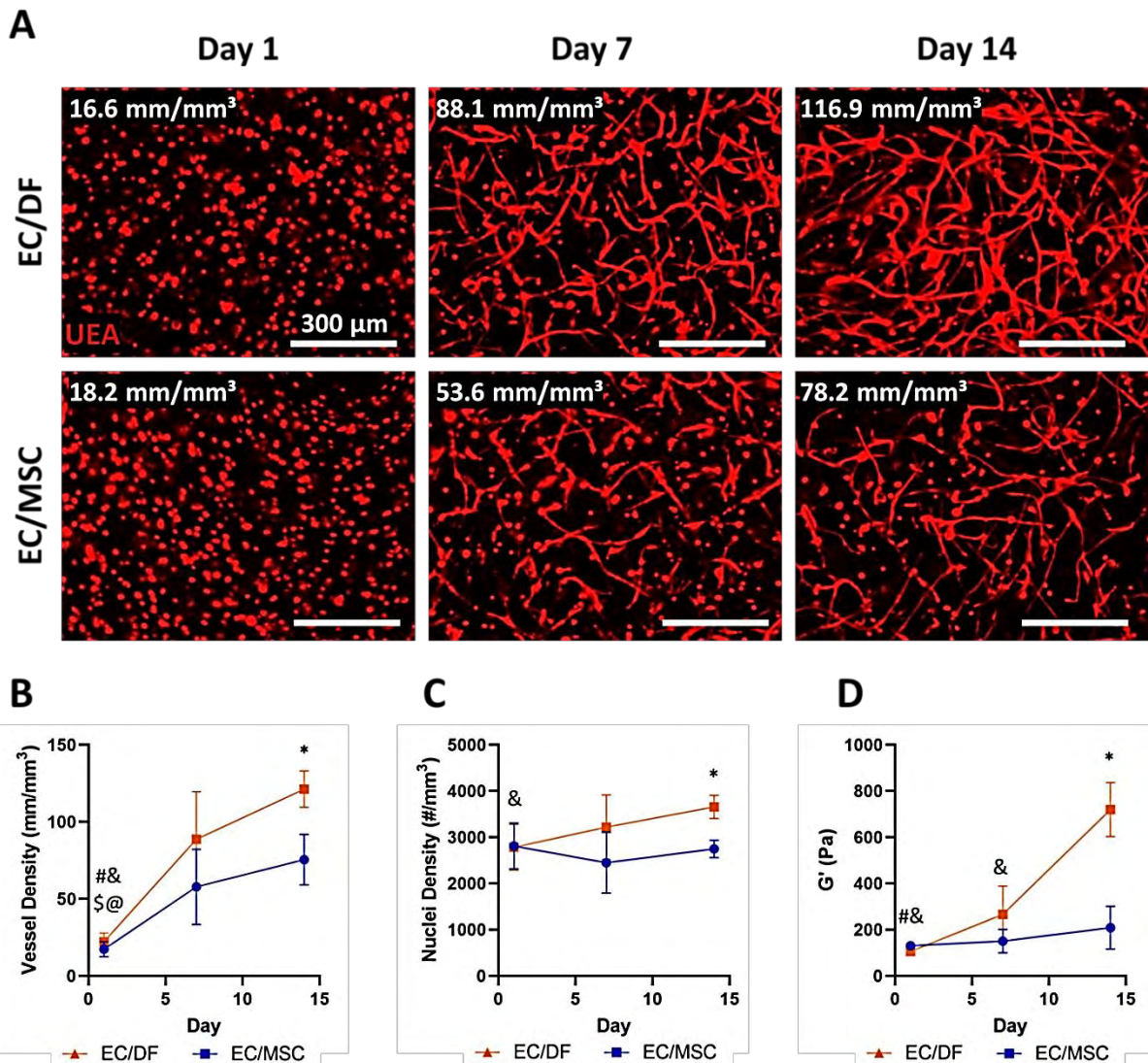


**Figure 7.7: DFs support enhanced vessel formation compared to MSCs and induce significant hydrogel stiffening when co-cultured with ECs in PEG-2xVPMS.** A) Representative images of maximum intensity projections of confocal sections ( $z$  height = 200  $\mu\text{m}$ ) for ECs stained with UEA on days 1, 7, & 14 from constructs seeded with  $5 \times 10^6$  ECs/mL and  $5 \times 10^6$  stromal cells/mL. Images were chosen with near average vessel densities between multiple replicates, quantification of vessel density for the specific image shown is indicated. B) Vessel density in the bulk of the constructs was estimated as described in the methods (Two-way ANOVA: time  $p = 0.008$ , cell  $p = 0.002$ , interaction  $p = 0.001$ ). C) Cell density in the constructs was quantified from DAPI stained images (Two-way ANOVA: time  $p = 0.607$ , cell  $p = 0.001$ , interaction  $p = 0.143$ ). D) Measurement of the shear storage modulus ( $G'$ ) of constructs on progressive days demonstrates that EC/DF hydrogels stiffen but not EC/MSC hydrogels (Two-way ANOVA: time  $p = 0.084$ , cell  $p = 0.083$ , interaction  $p = 0.024$ ). For all graphs: #:  $p < 0.05$ , EC/DF relative to EC/DF D7; &:  $p < 0.05$  EC/DF relative to EC/DF day 14; \$:  $p < 0.05$  EC/MSC relative to EC/MSC D7; @:  $p < 0.05$  EC/MSC relative to EC/MSC D14; \*:  $p < 0.05$ , EC/DF relative to EC/MSC (same day).  $N=4$ .

0.021). EC/DF co-cultures exhibited a significant increase in nuclei density from day 1 to day 14 ( $p = 0.045$ ) and significantly higher nuclei densities on day 14 than EC/MSC co-cultures ( $p = 0.038$ ), whereas nuclei densities for EC/MSC co-cultures remained statistically unchanged from day 1 to day 14 (**Fig 7.7C**). EC/DF co-cultures significantly stiffened from day 1 to day 7 ( $p = 0.40$ ), further stiffened from day 7 to day 14 ( $p = 0.0002$ ), had significantly higher shear moduli than EC/MSC co-cultures on day 14 ( $p < 0.0001$ ), whereas EC/MSC cultures exhibited insignificant stiffening from day 1 ( $131 \pm 17$  pa) to day 14 ( $209 \pm 93$  pa) (**Fig 7.7D**).

#### **7.4.4 Alpha smooth muscle actin ( $\alpha$ SMA) is upregulated overtime for EC/DF and EC/MSC co-cultures in fibrin and PEG hydrogels.**

Expression and regulation of  $\alpha$ SMA was compared between EC/DF and EC/MSC co-cultures in 2.5 mg/mL fibrin and 32 mg/mL PEG-VPMS hydrogels in this preliminary study. Cells were seeded at  $3 \times 10^5$  cells/mL for fibrin and  $3 \times 10^6$  cells/mL for PEG of each cell type (co-cultures were seeded with  $6 \times 10^5$  and  $6 \times 10^6$  cells/mL whereas monocultures were seeded at  $3 \times 10^5$  and  $3 \times 10^6$  cells/mL total, respectively). Hydrogel compaction in fibrin (**Fig 7.4B**) and hydrogel swelling in PEG (**Fig 6.14B**) from initial casting to day 1, however, resulted in roughly similar total nuclei densities between fibrin and PEG on day 1 (**Data not shown**). Immunofluorescent staining in co-cultures showed that  $\alpha$ SMA was expressed by DFs and MSCs in both fibrin and PEG hydrogels on day 7 (**Fig 7.8A**). Qualitatively,  $\alpha$ SMA expressing DFs and MSCs appeared more tightly associated with EC vessels in PEG than in fibrin, but noticeable morphologic differences between DFs and MSCs were not apparent. Gene expression analysis of ACTA2 ( $\alpha$ SMA) on days 1 and 7 suggested that  $\alpha$ SMA gene expression increases over time for both EC/MSC and EC/DF co-cultures in fibrin and PEG, but upregulation is more pronounced with MSCs (**Fig 7.8B**). Western blotting for  $\alpha$ SMA suggested similar protein expression between DFs

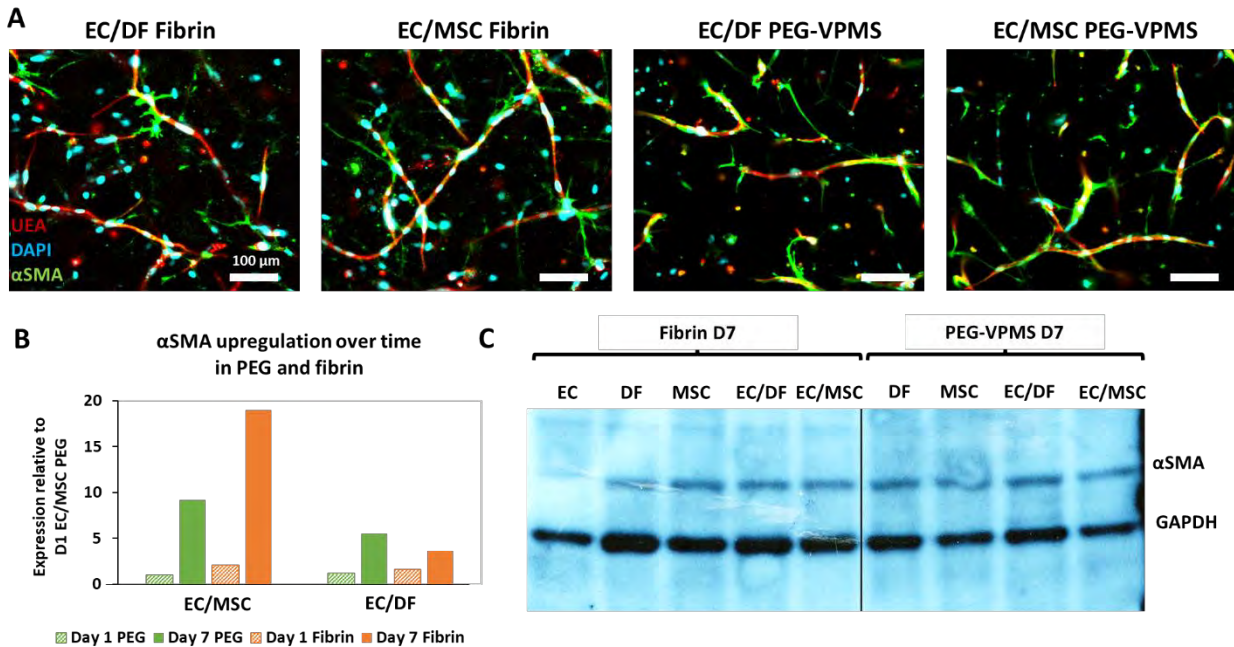


**Figure 7.8: Alpha smooth muscle actin ( $\alpha$ SMA) is upregulated overtime for EC/DF and EC/MSC co-cultures in fibrin and PEG hydrogels.** (A) Representative images of maximum intensity projections of confocal sections ( $z$  height = 50  $\mu$ m) for hydrogels fixed on day 7, stained for  $\alpha$ -smooth muscle actin ( $\alpha$ SMA), and counterstained with UEA and DAPI. (B) RNA was collected from constructs on day 1 and 7, purified, and expression of ACTA2 was determined using real time RT-PCR. Expression levels were normalized to glyceraldehyde 3-phosphate dehydrogenase (GAPDH) in each sample and then to expression in EC/MSC cultures in PEG on day 1 ( $\Delta\Delta C_t$  method). (C) Western blot image for protein expression of  $\alpha$ SMA and GAPDH on day 7 for monocultures and co-cultures in fibrin and PEG. ECs in fibrin were included as a negative control and did not exhibit  $\alpha$ SMA expression.

and MSCs whether in monoculture or co-culture with ECs in both fibrin and PEG hydrogels on day 7 (Fig 7.8C).

## 7.5 DISCUSSION

This chapter provides a characterization of differences in cell-mediated changes to hydrogel mechanics between DF and MSC supported EC cultures in three models of capillary morphogenesis. A variety of fibroblasts and MSCs have been used to support capillary morphogenesis for tissue engineering applications (7, 101, 155, 231), however, there are limited studies directly comparing the effect of stromal cell type on EC phenotype (7, 10, 11, 72, 101,

231). In this chapter accelerated vessel formation in the presence of DFs was observed, consistent with previous observations that both lung and dermal fibroblasts accelerate the rate of vessel formation compared to MSCs (7, 10, 231). Differences in proteolytic matrix remodeling has been suggested to contribute to accelerated vessel formation in the presence of fibroblasts (7), however, additional remodeling processes may also contribute. Measurements of cell-mediated changes to hydrogel mechanics during *in vitro* culture are easily obtainable and help provide insight into additional differences in ECM-remodeling depending on supportive stromal cell type which may contribute to differences in microvascular network formation.

Previous work has demonstrated multiple cellular remodeling processes that contribute to changes in hydrogel mechanics over time. Cellular traction has been shown to contribute to micro and macroscale changes in hydrogel mechanics. MSCs in collagen have been shown to locally stiffening their pericellular microenvironment, dependent on cellular contractility (205). Similarly, traction forces are necessary for EC sprouting in fibrin, and correlate with pericellular hydrogel stiffening (64). Force generation from fibroblasts has also been shown to result in hydrogel stiffening and compaction (175, 259, 261, 269), which plays a central role in wound healing (150). Hydrogel mechanics can also increase due to ECM deposition from encapsulated cells during various *in vitro* morphogenetic processes (258) including fibroblast mediated angiogenic sprouting (52), and contributes to progressive tissue stiffening in fibrotic pathologies (270). Incubation of hydrogels with appropriate proteases decreases their mechanical properties over time (231), however, proteolytic degradation of hydrogels is also necessary for morphogenetic processes to proceed that result in hydrogel stiffening (205, 238). Moreover, the contribution of cell-mediated protease secretion and hydrogel degradation may be too low to

detect with bulk rheology, as no changes were detected when fibroblasts were plated on a transwell insert spatially isolated from a fibrin hydrogel (251).

Although previous work has demonstrated differences in pro-angiogenic cytokine and protease expression (7) between fibroblasts and MSCs, which are likely to contribute to differences in the rate of vessel formation, the work presented in this chapter demonstrates that the dynamics of hydrogel mechanics also depend on stromal cell identity, suggesting differences in ECM remodeling may also contribute. Preliminary studies in fibrin suggest that EC/DF co-cultures stiffen hydrogels more than EC/MSC co-cultures in both angiogenic and vasculogenic models of capillary morphogenesis. This increased stiffening was associated with increased vessel formation for-EC-DF co-cultures in the vasculogenic model and in the angiogenesis model when the stromal cells were embedded in the hydrogel matrix allowing close cellular association, but not in the overlay condition. This may suggest that the cellular remodeling process that results in hydrogel stiffening may only contribute to enhanced vessel formation when close-cellular association between ECs and stromal cells is allowed. In PEG hydrogels, DFs similarly supported enhanced vessel formation, however the difference in hydrogel stiffening was much more pronounced between DF and MSC supported cultures than in fibrin. DF supported cultures had significantly higher vessel densities than MSC cultures, and promoted significant hydrogel stiffening, whereas the mechanics of MSC cultures remained statistically unchanged. The lack of change in hydrogel mechanics for EC/MSC co-cultures despite extensive network formation suggests that hydrogel stiffening is not an inherent result of cellular morphogenesis, but rather the result of a remodeling process that is particularly enhanced during capillary morphogenesis in the presence of fibroblasts. Moreover, we have previously shown that PEG hydrogel stiffening depends on co-culture of DFs and ECs, demonstrating that cooperative

interaction between the two cell types is necessary and DFs alone do not mediate this effect in PEG (238).

Potential differences in  $\alpha$ SMA were also assessed depending on stromal cell type in fibrin and PEG hydrogels. Expression of  $\alpha$ SMA is often associated with contractile phenotypes (271, 272) and we have previously shown that increased  $\alpha$ SMA expression in PEG hydrogels correlated with increased hydrogel stiffening in EC-DF co-cultures (238). Pericytes also express  $\alpha$ SMA but are not necessarily actively contractile (25, 44). There was a qualitative difference between fibrin and PEG hydrogels with  $\alpha$ SMA positive DFs and MSCs more tightly associated with EC vessels in PEG than in fibrin. However, there were no clear differences in  $\alpha$ SMA regulation or expression between DF and MSC cultures, with  $\alpha$ SMA being upregulated in both fibrin and PEG hydrogels containing cultures with either cell-type. Whether  $\alpha$ SMA upregulation was indicative of a pericyte-like or highly contractile myofibroblastic phenotype for either stromal cell type would need to be more closely investigated.

Taken together, the data presented in this chapter suggests that DFs and MSCs may differentially regulate EC morphogenesis in part by their innate differences in contractility and/or matrix deposition. However, previous work has shown that although ECM deposition may contribute to PEG hydrogel stiffening in EC/DF co-cultures, the contribution to hydrogel stiffening was largely dependent on active cellular contractility (238). Tractional stress applied on the ECM has been shown to provide a means of cell-cell communication through fibrillar matrices (257) and mechanical strain has been shown to promote and direct angiogenesis (67, 68, 273). Fibroblasts are well known for being highly contractile (150, 175, 274, 275) suggesting the potential hypothesis in which they enhance angiogenesis through increased mechanical strain on their local microenvironment. This interpretation would make sense in the context of wound

healing in which cellular traction helps contract wounds and rapid blood vessel formation is necessary (174).

## 7.6 SUPPLEMENTAL FIGURES

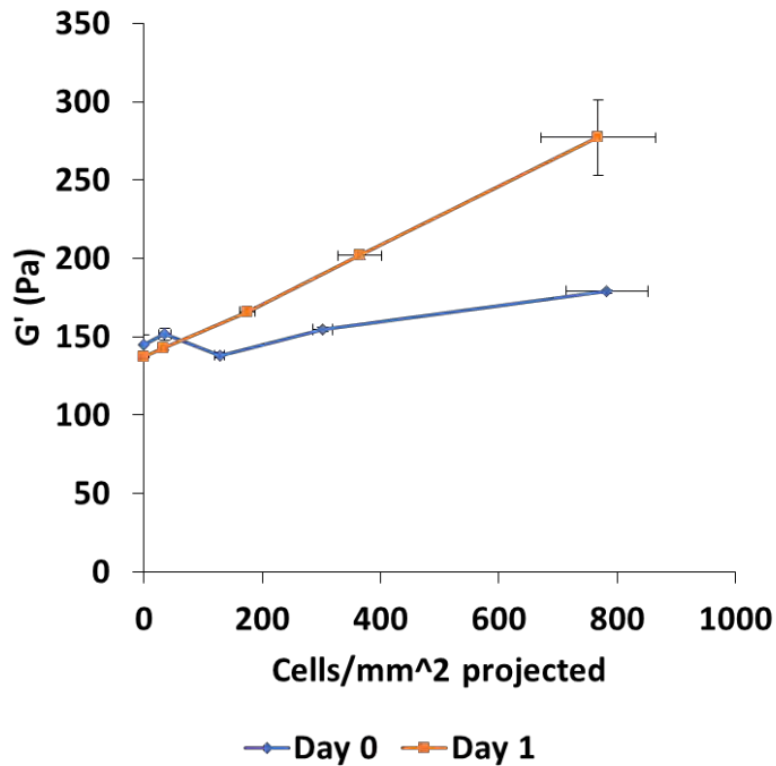


**Figure 7.9: DF monoculture stiffening of fibrin hydrogels from initial casting to day 1 is proportional to cell seeding density.** DFs were seeded in 2.5mg/mL fibrin hydrogels at 0, 25k, 100k, 250k, and 750k cells per mL and hydrogel shear modulus ( $G'$ ) and cell densities were quantified immediately after casting (Day 0) or after overnight culture (Day 1). Cell densities were calculated from confocal stacks through the full thickness of the hydrogel to compare cell densities between days without the confounding effect of hydrogel compaction. Error bars for both metrics represent intra-experimental variability between the average values obtained from 3 hydrogels.

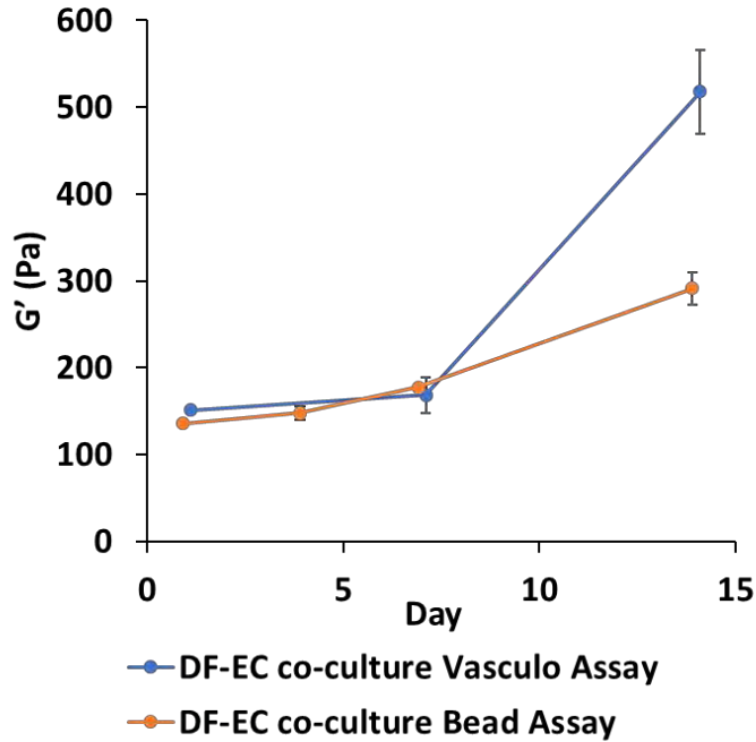


**Figure 7.10: ECs contribute to fibrin hydrogel stiffening.** In both conditions, DFs were seeded in the hydrogel at  $1.25 \times 10^4$  cells/mL. ECs were also seeded in the hydrogel at  $1.25 \times 10^4$  cells/mL for the vasculogenesis assay, whereas they were delivered on microcarrier beads embedded in the matrix for the angiogenic bead assay. Hydrogels for both conditions stiffened from day 1 to day 14, but stiffening was more pronounced when ECs were distributed throughout the matrix rather than localized to microcarrier beads.



## CHAPTER VIII

### Conclusions and Future Directions

#### 8.1 Summary of findings

The findings presented in this dissertation provide important insights on cellular remodeling processes accompanying capillary morphogenesis in engineered tissue constructs. A fundamental understanding of these processes is essential for the rational design of engineered tissues that promote extensive capillary network formation. Poly (ethylene glycol)-based hydrogels, in which proteolytic susceptibility could be modulated independent of other material properties, were used to investigate the relative contributions of plasmin- and matrix metalloproteinase (MMP)-mediated matrix degradation to capillary morphogenesis. Although pharmacological protease inhibitor studies suggested a role for plasmin in regulating vessel formation in fibrin for dermal fibroblast (DF) and lung fibroblast (LF) supported co-cultures with endothelial cells (ECs), neither co-culture exhibited a plasmin-dependent contribution to capillary morphogenesis in PEG hydrogels. Increasing MMP degradability by decreasing hydrogel density or by increasing the susceptibility of crosslinks to MMPs, without altering other material properties, however, did result in increased network formation for EC-DF co-cultures. Interestingly, EC-DF co-cultures in PEG hydrogels with enhanced susceptibility to cellular remodeling exhibited increased network formation concomitant with pronounced hydrogel stiffening overtime.

PEG hydrogel stiffening of low-density hydrogels (~50 Pa shear modulus) was dependent on active cellular contractility and correlated with upregulation of alpha smooth muscle actin

( $\alpha$ SMA) as well as upregulation and increased deposition of collagen-1 compared to high-density hydrogels (~200 Pa shear modulus) for EC-DF co-cultures. Increasing hydrogel degradability by using a crosslinker with increased susceptibility to MMP-mediated degradation similarly resulted in enhanced vessel formation concomitant with increased hydrogel stiffening for EC-DF co-cultures but not for EC co-cultures with mesenchymal stem cells (MSCs). Regardless of MMP-degradable crosslinker used, EC-MSC co-cultures in PEG hydrogels resulted in reduced vessel formation compared to EC-DF co-cultures and did not exhibit pronounced changes in hydrogel mechanics over time. The relative contributions of ECs and DFs to the dynamics of macro and micro-rheological properties of fibrin gels over time in a model of angiogenic sprouting was also investigated. Like PEG, bulk fibrin hydrogel stiffening was observed and both ECs and DFs demonstrated microscale pericellular hydrogel stiffening. Preliminary studies in fibrin between EC-DF and EC-MSC co-cultures further suggest enhanced vessel formation and hydrogel stiffening in the presence of DFs compared to MSCs.

## **8.2 Significance and impact**

Although co-delivery of ECs and supportive stromal cells in engineered tissues is a promising strategy to promote neovascular network assembly, there is little consensus on the ideal choice of cells to deliver and ECM design parameters to incorporate to promote desired morphogenetic outcomes. Our lab has previously demonstrated functional differences in neovasculature depending on the choice of stromal cells used to support vessel formation (10, 11) in fibrin hydrogels. This discrepancy in function was concomitant with differences in the rate at which vessels form, mechanism of proteolytic degradation to allow vessel invasion, and differences in pericyte association with the vessels (7).

Based on these previous findings, work presented in this dissertation addresses the dependence of capillary morphogenesis on the proteolytic susceptibility of engineered ECM hydrogels. Although the use of knock-out cells and animals is traditionally used to decipher the roles of specific proteolytic pathways (12, 56), redundancies in proteolytic ECM degradation can complicate interpretations from knock-outs. To complement these more commonly used molecular genetics approaches, we used engineered hydrogels (114) with selective degradability to MMPs or plasmin to investigate their relative importance during capillary morphogenesis. Potential plasmin-mediated contributions to angiogenesis include direct fibrin degradation (220), activation of MMP proenzymes into their active form (9, 222) and induction of cellular migration (63). Although studies have implicated plasmin as a potential regulator of capillary morphogenesis (7, 59, 62, 63), we did not observe promotion of vessel formation in plasmin-susceptible matrices, nor restriction of vessel formation with plasmin inhibition in MMP-selective matrices. These findings do not necessarily contradict findings in fibrin, however, as fibrin interacts with numerous EC integrins and receptors including  $\alpha_{11b}\beta_3$ ,  $\alpha_v\beta_1$ ,  $\alpha_M\beta_2$ ,  $\alpha_v\beta_3$ ,  $\alpha_x\beta_2$ ,  $\alpha_v\beta_1$  and  $\alpha_5\beta_1$  (74, 276), ICAM-1 and VE-cadherin (277), modulating cell behavior and signaling. PEG-hydrogels are solely functionalized with RGD adhesive peptide, and although RGD is capable of binding numerous integrins (74), it does not fully reconstitute the cell-ECM interactions present in fibrin and has even been shown to block plasmin-induced EC migration (63). Although differences between fibrin and PEG hydrogels were not fully addressed, this work does provide strong evidence for the critical dependence of capillary morphogenesis in synthetic matrices on MMP degradability.

Enhancement of PEG-hydrogels to MMP-mediated degradation increased vessel formation. Similar results have been shown in a spheroid outgrowth model (91) and EC invasion

assays (89), and incorporation of additional hydrolytic susceptibility into MMP-degradable hydrogels has also been demonstrated to facilitate endothelial invasiveness (278). Unlike native settings in which barrier function and angiogenic induction are typically anti-correlated (20, 54), our results in PEG hydrogels showing upregulation of  $\alpha$ SMA and increased collagen-1 deposition in easily remodeled hydrogels suggest that enhanced matrix degradability of synthetic hydrogels may also potentially promote vessel maturation by facilitating cellular remodeling and mural cell recruitment. Although excessive hydrogel degradation may negatively impact long-term hydrogel integrity, within the conditions tested we observed the opposite effect with increased hydrogel stiffening in more easily remodeled matrices.

PEG-hydrogel stiffening was critically dependent on active cellular contractility and correlated with enhanced collagen-1 upregulation and deposition. Although there was a correlation between degree of vessel formation and hydrogel stiffening in EC-DF co-cultures, EC-MSC co-cultures did not exhibit hydrogel stiffening regardless of degree of vessel formation. Moreover, EC-DF co-cultures exhibited enhanced vessel formation and hydrogel stiffening in both PEG- and fibrin- based hydrogels compared to EC-MSC co-cultures. The correlation between enhanced vessel formation and increased hydrogel stiffening, and dependence of hydrogel stiffening on cellular contractility, suggests increased vessel formation in the presence of DFs may partially be mediated by differences in cellular contractility. Tensile forces have been shown to contribute to capillary network formation (6, 68, 253) and fibroblasts are highly contractile (150, 175, 274, 275). Moreover, strain stiffening of fibrillar matrices due to cell traction can provide a means for cell-cell communication (257), and incorporation of nano fibers in a synthetic matrix has been shown to increase angiogenic ingrowth (279). Together these results suggest that in addition to increasing hydrogel proteolytic susceptibility to promote

capillary morphogenesis, incorporation of a nanofibrous architecture in synthetic hydrogels may be an important design consideration for achieving similar degrees of vessel formation in synthetic hydrogels as is observed in natural matrices. In addition to providing insights for the rational design of synthetic hydrogel matrices, characterization of progressive hydrogel stiffening in natural and synthetic matrices depending on encapsulated cell types is an important design consideration for regenerative medicine applications in which tissue-level mechanical changes may affect the differentiation and function of co-encapsulated functional cell types (250, 265, 280).

These findings also help illustrate the important dynamic and potentially reciprocal relationship between tissue scaffold design parameters and micro-environmental remodeling processes that contribute to vascular morphogenesis. Some of the key hydrogel properties and

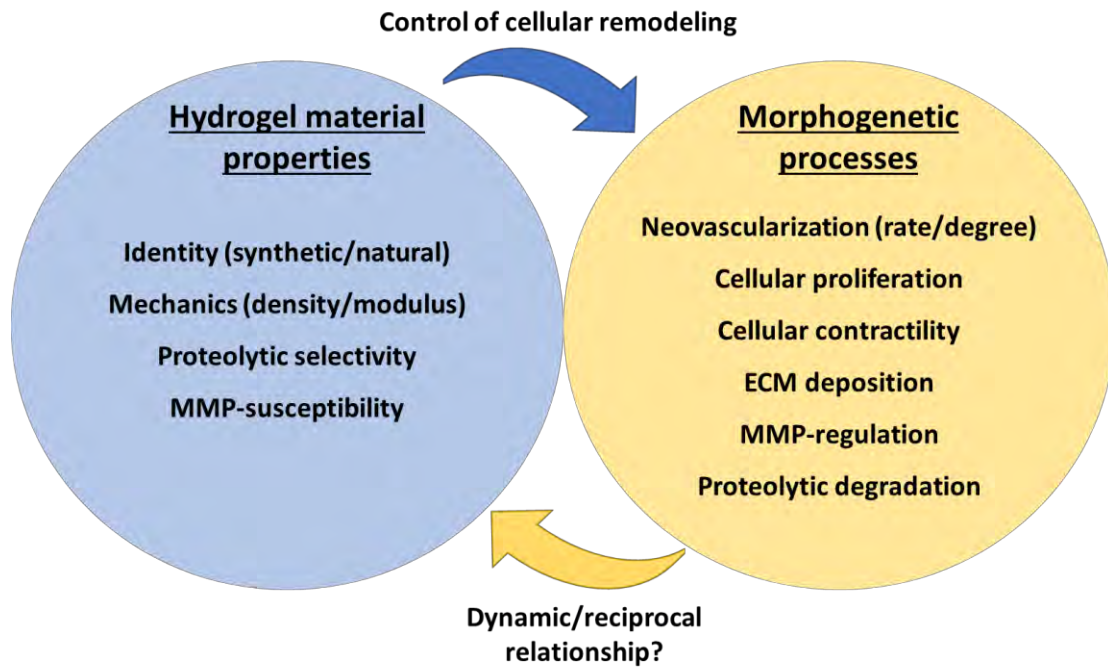


**Figure 8.1: Summary of findings.** The results presented in this dissertation demonstrate the effect of hydrogel material properties on neovascular morphogenesis and the reciprocal effect of cellular remodeling during morphogenesis on hydrogel properties. These results suggest a dynamic and reciprocal relationship during neovascular morphogenesis in engineered tissues.

morphogenetic processes investigated in this dissertation are summarized in **Figure 8.1**. Broadly, the choice of tissue scaffold hydrogel material properties controls the progression of vascular morphogenesis by dictating cellular remodeling processes and protein expression. Cellular remodeling processes such as cellular traction forces, ECM deposition, and proteolytic degradation, however in turn progressively alter hydrogel mechanics, and replace the provisional matrix with cell secreted ECM. This results in a dynamic and reciprocal relationship in certain circumstances (250), but it has yet to be documented during vascular morphogenesis. Results presented in this dissertation, however, suggest that a reciprocal relationship is likely to exist during hydrogel neovascularization. A deeper understanding of this dynamic will ultimately provide important insights to improve the design of engineered tissues for regenerative medicine applications.

### **8.3 Future directions**

This section proposes additional studies which could enhance the significance and impact of the work presented in this dissertation.

#### **8.3.1 Assess the effect of hydrogel degradability and rate of vessel formation on vessel maturity in PEG hydrogels *in vitro*.**

Additional work should be done to assess whether accelerating the rate of capillary morphogenesis by enhancing tissue scaffold degradability changes the ultimate vessel density achieved and to investigate the impact of hydrogel degradability on vessel function over time. The studies presented within this thesis were only carried out through 2 weeks, characterization of additional vessel formation for both VPMS and 2xVPMS for longer time points should be investigated to assess whether changes in matrix degradability affect the ultimate vessel densities achieved as well as the rate of vessel formation. Studies *in vitro* should investigate differences in

regulation and expression of molecular markers associated with capillary maturity for paired time points with different degrees of vessel formation, as well as for paired degrees of vessel formation at different time points. Commonly used molecular markers of vessel maturity which could be assayed by qPCR, western blotting, and immunofluorescent staining include deposition of basement membrane proteins, expression of VE- and N-cadherins, and pericyte markers. Vessel maturation is associated with enhanced deposition of fibronectin, laminins, nidogens, and collagen-4 (44, 79). Homo- and hetero-typic intercellular junctions mediated by VE- and N-cadherins are important regulators of EC barrier function (70, 72). Well-known pericyte markers include neural-glial antigen-2 (NG2),  $\alpha$ -smooth muscle actin ( $\alpha$ -SMA), desmin, and platelet derived growth factor receptor- $\beta$  (PDGFR $\beta$ ) (84–86). Lesser-used pericyte markers can also be assayed including calponin, (7) non-muscle myosin, tropomyosin, nestin, aminopeptidase A, aminopeptidase N (CD13), and sulfatide (80). However, many of these markers are shared with other cell types including smooth muscle cells, and quantification of  $\alpha$ SMA positive cells with UEA vessels could provide an additional convenient metric for assessing capillary maturity. This quantification could be easily achieved using a similar masking protocol developed in **Chapter 6** for assessing the proportion of UEA associated nuclei. Moreover, these analyses should be carried out between multiple candidate stromal support cell types, to assess the generalizability of the findings.

### **8.3.2 Assess the effect of hydrogel degradability and rate of vessel formation on vessel maturity in PEG hydrogels *in vivo*.**

Additional *in vivo* work is needed to assess the effect of hydrogel degradability on the rate and quality of vessel formation in the subcutaneous implant model, and differences in inosculation with the host vascular system. Although preliminary studies suggested a difference

in cell spreading between VPMS and 2xVPMS hydrogels, replicated studies are needed to confirm this observation, and additional experimental conditions should be investigated to achieve inosculation. The severe restriction of vessel formation *in vivo* compared to *in vitro* in intact hydrogel implants, and possible fibrous capsule formation, suggests *in situ* gelation of hydrogels should be considered to facilitate interstitial integration between implant and host tissue. Gelation of PEG hydrogels is extremely sensitive to impurities and small perturbations in stoichiometric ratio between thiol and vinyl-sulfone groups, however, suggesting great care should be taken to ensure the mechanics of hydrogels formed *in situ* are consistent to allow faithful comparisons between crosslinkers. Rheological characterization of excised hydrogels one day after *in situ* gelation would be necessary to assess potential variability in gelation. If future studies were performed using intact hydrogel implants, longer time points should be considered to allow for inosculation with the host. Angiogenic ingrowth into similar intact hydrogel implants has been observed at 2 and 4 weeks (121). Implantation of intact hydrogels after 1-week *in vitro* culture could also be considered to allow for the formation of a microvascular networks beforehand, still allowing for assessment of differences in inosculation depending on hydrogel formulation.

If intact hydrogels implantation is necessary for accurate control of hydrogel mechanics but sufficient vascularization and inosculation is not achieved in the subcutaneous space, then alternative implant sites could be considered. Implantation of intact acellular VEGF-secreting PEG-VPMS hydrogels in the epididymal fat pad and in the small bowel mesentery has provided significant improvements in vascular ingrowth compared to implantation in the subcutaneous space (121).



**Generalized equation for permeability coefficient across a membrane**

$$P_v \left( \frac{m}{sec} \right) = \frac{J_v \left( \frac{mol}{sec} \right)}{\Delta C \left( \frac{mol}{m^3} \right) S_A (m^2)}$$

P<sub>v</sub>= Solute permeability coefficient of vessel  
 J<sub>v</sub>= Flux (ΔC/Δt) of solute for known ΔC  
 ΔC = concentration difference across surface  
 S<sub>A</sub> = surface area of vessel

**Assumptions for calculating average permeability coefficient between multiple vessels within an ROI**

Linear relation between concentration and intensity:

$$Intensity (I) \propto \frac{mol}{m^3}$$

Concentration difference is proportional to vessel intensity:

$$\Delta C \propto Vessel\ intensity\ (I_0)$$

Total flux of solute equals total intensity in ROI excluding vessels:

$$J_v \propto ((I) \cdot A - I_0 \cdot \pi \cdot (R_1^2 + R_2^2 + R_3^2)) / time$$

Total surface area of vessels in ROI for example with 3 included:

$$S_A = 2\pi \cdot (R_1 + R_2 + R_3)$$

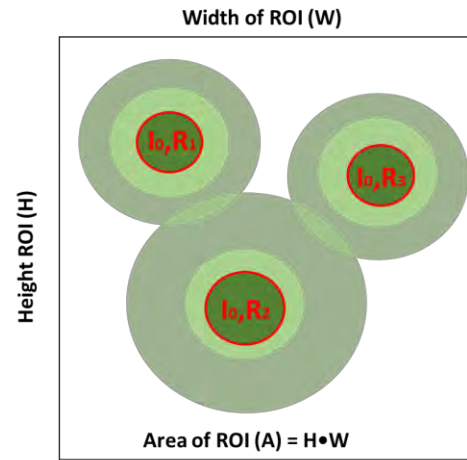


**Figure 8.2: Approximation of average vessel permeability within a region of interest from a confocal or histological cross-section containing multiple vessels.** Assumptions are put forward for approximating the average permeability between multiple vessels from the extravasation of a fluorescent marker either from confocal sections from *in vitro* confocal microscopy sections or from *in vivo* cryosections for a given region of interest. The generalized equation for the permeability coefficient of a single vessel is provided for a 2D simplification. One must work with a marker for which signal intensity is linearly proportional to its concentration and the solution can be solved using arbitrary intensity units rather than converting to concentration. Provided that the concentration of the marker within vessels remains significantly higher than the concentration of marker outside of the vessels one can also make the simplifying assumption that the concentration outside the vessel is negligible and the difference in concentration is simply proportional to the vessel intensity. The additional assumptions can be used to substitute into the general equation, an example is provided for 3 vessels within the ROI. The total flux of the solute in the region can be determined from the average intensity within the region multiplied by the area of the ROI subtracting the intensity within vessels. This flux is through the total surface area of vessels within the region.

In conditions in which inosculation is achieved, additional studies can be performed to assess functional differences in endothelial barrier function depending on hydrogel degradability such as extravasation of a fluorescent dextran (11) or labeled albumin (281, 282). Comparison of measured vessel permeability coefficients for individual vessels could be determined from cryosections (11) as has previously been done from confocal sections of *in vitro* hydrogels (72, 283). Alternatively, one could measure an average permeability coefficient for a given section as proposed in **Fig 8.2**.

In addition to functional assays of neovessel barrier function, immunohistochemical analysis for markers of vessel maturity could similarly be used *in vivo* as *in vitro* for additional qualitative assessment. Quantifying the co-localized deposition of basement membrane proteins such as fibronectin, laminins, nidogens, and collagen-4 (44, 79) as well as  $\alpha$ SMA-positive cells in histological sections with neovessels would provide additional metrics for vessel quality depending on hydrogel formulation.

### **8.3.3 Assess the effect of stromal cell contractility on rate of vessel formation and vessel maturity in fibrin and PEG hydrogels**

Additional work could be performed to assess whether differences in cellular contractility between DFs and MSCs contribute to differences in degree of vessel formation. Traction force measurement of isolated cells in 2D or 3D culture on or in elastic substrates can be achieved with traction force microscopy (TFM) (284). Tracking matrix deformations over time during complex morphogenetic processes is more difficult but has been previously achieved in our lab using spatio-temporal image correlation spectroscopy (STICS) on 3D cultures in fibrin. STICS could be used to assess whether differences in stromal cell type correlate with differences in local matrix deformations during angiogenic sprouting (64). However, this may only be achievable at early timepoints for our model of angiogenic sprouting in which stromal cells are embedded because the characteristic fibrillar architecture of fibrin, visualizable by confocal reflectance microscopy, is quickly replaced by a diffuse specular pattern without individual fibers visible (251). Alternatively, STICS could also be used to track the displacement of fluorescent fiduciary markers embedded within either PEG or fibrin hydrogels. PEG hydrogels are typically kept in floating culture to facilitate nutrient diffusion, however, thiolation of glass culture wells (285) could be used to adhere PEG-hydrogel drops to the surface and achieve a comparable ratio of

media to hydrogel size as in free-floating cultures. Constitutive RhoA-active mutants demonstrate increased cellular contractility (64, 286–288). Constitutive RhoA-active and dominant-negative fibroblast and MSC mutants could be used to assess the effect of stromal cell actomyosin contractility on rates of vessel formation for either stromal cell type. Such studies would help further illuminate potential differences between mechanisms of angiogenic induction depending on supportive stromal cells used.

In addition to investigating potential changes in rate of vessel formation, stromal and endothelial cell RhoA mutant populations could be used to investigate whether cellular hyper- or hypo-contraction impacts vessel function. The Rho-ROCK signaling pathway and associated actomyosin contractility is implicated in metastatic invasiveness for a number of cancers (289). As such, this system could also be used as a model to investigate a potential connection between cellular contractility and poor vessel quality observed in tumors (82, 290). Functional assays of vessel leakiness and biomolecular assays for markers of vessel maturity, as outlined above, could be performed with this model both *in vitro* and *in vivo* to assess morphological changes dependent on cellular contractility. Moreover, the relative effect of individual cell populations could be investigated by selectively altering expression profiles in either the endothelial or the stromal cell populations. Furthermore, an inducible promoter system (291) could be used to investigate whether any phenotypic changes compared to wild type cultures would be reversible. Such studies could provide important mechanistic insights into a potential role of cell-mediated mechanical forces on the manifestation of pathological phenotypes in oncogenic conditions.

## BIBLIOGRAPHY

1. U. Blache, M. Ehrbar, Inspired by Nature: Hydrogels as Versatile Tools for Vascular Engineering. *Adv. Wound Care* **7**, 232–246 (2018).
2. G. E. Davis, P. R. Norden, S. L. K. Bowers, Molecular Control of Capillary Morphogenesis and Maturation by Recognition and Remodeling of the Extracellular Matrix: Functional Roles of Endothelial Cells and Pericytes in Health and Disease. *Connect. Tissue Res.* **56**, 392–402 (2015).
3. D. R. Senger, G. E. Davis, Angiogenesis. *Cold Spring Harb. Perspect. Biol.* **3**, a005090–a005090 (2011).
4. G. E. Davis, Angiogenesis and Proteinases: Influence on Vascular Morphogenesis, Stabilization and Regression. *Drug Discov. Today Dis. Models* **8**, 13–20 (2011).
5. C. M. Ghajar, S. C. George, A. Putnam, Matrix metalloproteinase control of capillary morphogenesis. *Crit. Rev. Eukaryot. Gene Expr.* **18** (2008).
6. G. E. Davis, C. W. Camarillo, Regulation of Endothelial Cell Morphogenesis by Integrins, Mechanical Forces, and Matrix Guidance Pathways. *Exp. Cell Res.* **216**, 113–123 (1995).
7. C. M. Ghajar, *et al.*, Mesenchymal cells stimulate capillary morphogenesis via distinct proteolytic mechanisms. *Exp. Cell Res.* **316**, 813–825 (2010).
8. M. S. Pepper, Role of the matrix metalloproteinase and plasminogen activator–plasmin systems in angiogenesis. *Arterioscler. Thromb. Vasc. Biol.* **21**, 1104–1117 (2001).
9. G. E. Davis, K. A. Pintar, R. S. Allen, S. A. Maxwell, Matrix metalloproteinase-1 and -9 activation by plasmin regulates a novel endothelial cell-mediated mechanism of collagen gel contraction and capillary tube regression in three-dimensional collagen matrices. *J. Cell Sci.* **114**, 917–930 (2001).
10. S. J. Grainger, A. J. Putnam, Assessing the permeability of engineered capillary networks in a 3D culture. *PLoS One* **6**, e22086 (2011).
11. S. J. Grainger, B. Carrion, J. Ceccarelli, A. J. Putnam, Stromal Cell Identity Influences the *In Vivo* Functionality of Engineered Capillary Networks Formed by Co-delivery of Endothelial Cells and Stromal Cells. *Tissue Eng. Part A* **19**, 1209–1222 (2013).

12. T.-H. Chun, *et al.*, MT1-MMP–dependent neovessel formation within the confines of the three-dimensional extracellular matrix. *J. Cell Biol.* **167**, 757–767 (2004).
13. D. J. LaValley, C. A. Reinhart-King, Matrix stiffening in the formation of blood vessels. *Adv. Regen. Biol.* **1**, 25247 (2014).
14. J. M. Felner, “An Overview of the Cardiovascular System” in *Clinical Methods: The History, Physical, and Laboratory Examinations*, 3rd Ed., H. K. Walker, W. D. Hall, J. W. Hurst, Eds. (Butterworths, 1990) (April 15, 2020).
15. E. Marieb, K. Hoehn, *Human Anatomy and Physiology*, 7th Ed. (Pearson Education, 2006).
16. R. Y. Kannan, H. J. Salacinski, K. Sales, P. Butler, A. M. Seifalian, The roles of tissue engineering and vascularisation in the development of micro-vascular networks: a review. *Biomaterials* **26**, 1857–1875 (2005).
17. P. I. Aaronson, *The Cardiovascular System at a Glance* (John Wiley and Sons, Inc, 1999).
18. R. Skalak, P. I. Branemark, Deformation of Red Blood Cells in Capillaries. *Science* **164**, 717–719 (1969).
19. R. Kalluri, Basement membranes: structure, assembly and role in tumour angiogenesis. *Nat. Rev. Cancer* **3**, 422–433 (2003).
20. M. Díaz-Coránguez, C. Ramos, D. A. Antonetti, The inner blood-retinal barrier: Cellular basis and development. *Vision Res.* (2017) <https://doi.org/10.1016/j.visres.2017.05.009> (November 27, 2017).
21. L. Song, S. Ge, J. S. Pachter, Caveolin-1 regulates expression of junction-associated proteins in brain microvascular endothelial cells. *Blood* **109**, 1515–1523 (2007).
22. S. M. Stamatovic, A. M. Johnson, R. F. Keep, A. V. Andjelkovic, Junctional proteins of the blood-brain barrier: New insights into function and dysfunction. *Tissue Barriers* **4**, e1154641 (2016).
23. H. Gerhardt, H. Wolburg, C. Redies, N-cadherin mediates pericytic-endothelial interaction during brain angiogenesis in the chicken. *Dev. Dyn. Off. Publ. Am. Assoc. Anat.* **218**, 472–479 (2000).
24. J.-H. Paik, Sphingosine 1-phosphate receptor regulation of N-cadherin mediates vascular stabilization. *Genes Dev.* **18**, 2392–2403 (2004).
25. A. Armulik, Endothelial/Pericyte Interactions. *Circ. Res.* **97**, 512–523 (2005).
26. P. J. Courtoy, J. Boyles, Fibronectin in the microvasculature: localization in the pericyte-endothelial interstitium. *J. Ultrastruct. Res.* **83**, 258–273 (1983).

27. D. Bonkowski, V. Katyshev, R. D. Balabanov, A. Borisov, P. Dore-Duffy, The CNS microvascular pericyte: pericyte-astrocyte crosstalk in the regulation of tissue survival. *Fluids Barriers CNS* **8**, 8 (2011).
28. M. Fisher, Pericyte Signaling in the Neurovascular Unit. *Stroke* **40**, S13–S15 (2009).
29. W. C. Aird, Phenotypic Heterogeneity of the Endothelium: I. Structure, Function, and Mechanisms. *Circ. Res.* **100**, 158–173 (2007).
30. A. Armulik, G. Genové, C. Betsholtz, Pericytes: Developmental, Physiological, and Pathological Perspectives, Problems, and Promises. *Dev. Cell* **21**, 193–215 (2011).
31. W. G. Mayhan, D. D. Heistad, Permeability of blood-brain barrier to various sized molecules. *Am. J. Physiol.-Heart Circ. Physiol.* **248**, H712–H718 (1985).
32. O. Cleaver, P. A. Krieg, Vascular Development. *Vasc. Dev.*, 42.
33. W. Risau, I. Flamme, Vasculogenesis. *Annu. Rev. Cell Dev. Biol.* **11**, 73–91 (1995).
34. G. C. Schatteman, O. Awad, Hemangioblasts, angioblasts, and adult endothelial cell progenitors. *Anat. Rec. A. Discov. Mol. Cell. Evol. Biol.* **276A**, 13–21 (2004).
35. K. Xu, O. Cleaver, Tubulogenesis during blood vessel formation. *Semin. Cell Dev. Biol.* **22**, 993–1004 (2011).
36. B. Strilić, *et al.*, The Molecular Basis of Vascular Lumen Formation in the Developing Mouse Aorta. *Dev. Cell* **17**, 505–515 (2009).
37. R. Abdulla, G. A. Blew, M. J. Holterman, Cardiovascular Embryology. *Pediatr. Cardiol.* **25**, 191–200 (2004).
38. S. J. Mentzer, M. A. Konerding, Intussusceptive Angiogenesis: Expansion and Remodeling of Microvascular Networks. *Angiogenesis* **17**, 499–509 (2014).
39. T. Kau, *et al.*, Aortic Development and Anomalies. *Semin. Interv. Radiol.* **24**, 141–152 (2007).
40. J. Rouwkema, N. C. Rivron, C. A. van Blitterswijk, Vascularization in tissue engineering. *Trends Biotechnol.* **26**, 434–441 (2008).
41. M. Heil, I. Eitenmüller, T. Schmitz-Rixen, W. Schaper, Arteriogenesis versus angiogenesis: similarities and differences. *J. Cell. Mol. Med.* **10**, 45–55 (2006).
42. W. Cai, W. Schaper, Mechanisms of arteriogenesis. *Acta Biochim. Biophys. Sin.* **40**, 681–692 (2008).
43. R. Blanco, H. Gerhardt, VEGF and Notch in Tip and Stalk Cell Selection. *Cold Spring Harb. Perspect. Med.* **3** (2013).

44. A. N. Stratman, K. M. Malotte, R. D. Mahan, M. J. Davis, G. E. Davis, Pericyte recruitment during vasculogenic tube assembly stimulates endothelial basement membrane matrix formation. *Blood* **114**, 5091–5101 (2009).
45. B. L. Krock, N. Skuli, M. C. Simon, Hypoxia-Induced Angiogenesis. *Genes Cancer* **2**, 1117–1133 (2011).
46. X. Liu, *et al.*, Occludin S490 Phosphorylation Regulates Vascular Endothelial Growth Factor–Induced Retinal Neovascularization. *Am. J. Pathol.* **186**, 2486–2499 (2016).
47. J. Gavard, Breaking the VE-cadherin bonds. *FEBS Lett.* **583**, 1–6 (2009).
48. R. J. de Mendonça, “Angiogenesis in wound healing” in *Tissue Regeneration-From Basic Biology to Clinical Application*, (InTech, 2012).
49. K. M. Hodivala-Dilke, A. R. Reynolds, L. E. Reynolds, Integrins in angiogenesis: multitasking molecules in a balancing act. *Cell Tissue Res.* **314**, 131–144 (2003).
50. D. S. Steinbrech, *et al.*, Fibroblast Response to Hypoxia: The Relationship between Angiogenesis and Matrix Regulation. *J. Surg. Res.* **84**, 127–133 (1999).
51. J.-P. Coppé, K. Kauser, J. Campisi, C. M. Beauséjour, Secretion of Vascular Endothelial Growth Factor by Primary Human Fibroblasts at Senescence. *J. Biol. Chem.* **281**, 29568–29574 (2006).
52. A. C. Newman, M. N. Nakatsu, W. Chou, P. D. Gershon, C. C. Hughes, The requirement for fibroblasts in angiogenesis: fibroblast-derived matrix proteins are essential for endothelial cell lumen formation. *Mol. Biol. Cell* **22**, 3791–3800 (2011).
53. T. Korff, S. Kimmina, G. Martiny-Baron, H. G. Augustin, Blood vessel maturation in a 3-dimensional spheroidal coculture model: direct contact with smooth muscle cells regulates endothelial cell quiescence and abrogates VEGF responsiveness. *FASEB J.* **15**, 447–457 (2001).
54. S. Y. Yuan, R. R. Rigor, *The Endothelial Barrier* (Morgan & Claypool Life Sciences, 2010) (November 29, 2017).
55. N. Hiraoka, E. Allen, I. J. Apel, M. R. Gyetko, S. J. Weiss, Matrix metalloproteinases regulate neovascularization by acting as pericellular fibrinolysins. *Cell* **95**, 365–377 (1998).
56. S. Kachgal, B. Carrion, I. A. Janson, A. J. Putnam, Bone marrow stromal cells stimulate an angiogenic program that requires endothelial MT1-MMP. *J. Cell. Physiol.* **227**, 3546–3555 (2012).
57. A. Sacharidou, *et al.*, Endothelial lumen signaling complexes control 3D matrix–specific tubulogenesis through interdependent Cdc42- and MT1-MMP–mediated events. *Blood* **115**, 5259–5269 (2010).

58. P. Koolwijk, et al, Cooperative effect of TNFalpha, bFGF, and VEGF on the formation of tubular structures of human microvascular endothelial cells in a fibrin matrix. Role of urokinase activity. *J. Cell Biol.* **132**, 1177–1188 (1996).
59. C.-W. Oh, J. Hoover-Plow, E. F. Plow, The role of plasminogen in angiogenesis in vivo. *J. Thromb. Haemost.* **1**, 1683–1687 (2003).
60. J. M. Vogten, et al., The role of the fibrinolytic system in corneal angiogenesis. *Angiogenesis* **6**, 311–316 (2003).
61. M. S. Pepper, et al, Transforming growth factor-beta 1 modulates basic fibroblast growth factor-induced proteolytic and angiogenic properties of endothelial cells in vitro. *J. Cell Biol.* **111**, 743–755 (1990).
62. S. Mühleder, et al., The role of fibrinolysis inhibition in engineered vascular networks derived from endothelial cells and adipose-derived stem cells. *Stem Cell Res. Ther.* **9**, 35 (2018).
63. T. Tarui, M. Majumdar, L. A. Miles, W. Ruf, Y. Takada, Plasmin-induced Migration of Endothelial Cells A POTENTIAL TARGET FOR THE ANTI-ANGIOGENIC ACTION OF ANGIOSTATIN. *J. Biol. Chem.* **277**, 33564–33570 (2002).
64. E. Kniazeva, et al., Quantification of local matrix deformations and mechanical properties during capillary morphogenesis in 3D. *Integr. Biol.* **4**, 431 (2012).
65. B. M. Baker, et al., Cell-mediated fibre recruitment drives extracellular matrix mechanosensing in engineered fibrillar microenvironments. *Nat. Mater. Lond.* **14**, 1262–1268 (2015).
66. C. D. Davidson, W. Y. Wang, I. Zaimi, D. K. P. Jayco, B. M. Baker, Cell force-mediated matrix reorganization underlies multicellular network assembly. *Sci. Rep.* **9**, 1–13 (2019).
67. J. Liu, S. Agarwal, Mechanical Signals Activate Vascular Endothelial Growth Factor Receptor-2 To Upregulate Endothelial Cell Proliferation during Inflammation. *J. Immunol. Baltim. Md 1950* **185**, 1215–1221 (2010).
68. J. Ceccarelli, A. Cheng, A. J. Putnam, Mechanical strain controls endothelial patterning during angiogenic sprouting. *Cell. Mol. Bioeng.* **5**, 463–473 (2012).
69. M. V. Turturro, et al., MMP-Sensitive PEG Diacrylate Hydrogels with Spatial Variations in Matrix Properties Stimulate Directional Vascular Sprout Formation. *PLoS ONE* **8** (2013).
70. W. J. Polacheck, et al., A non-canonical Notch complex regulates adherens junctions and vascular barrier function. *Nature* (2017) <https://doi.org/10.1038/nature24998> (November 17, 2017).



71. Y. Liu, D. R. Senger, Matrix-specific activation of Src and Rho initiates capillary morphogenesis of endothelial cells. *FASEB J.* **18**, 457–468 (2004).
72. S. Alimperti, *et al.*, Three-dimensional biomimetic vascular model reveals a RhoA, Rac1, and N-cadherin balance in mural cell–endothelial cell-regulated barrier function. *Proc. Natl. Acad. Sci.* **114**, 8758–8763 (2017).
73. Y. A. Sudhakar, R. K. Verma, S. C. Pawar, Type IV collagen  $\alpha 1$ -chain noncollagenous domain blocks MMP-2 activation both in-vitro and in-vivo. *Sci. Rep.* **4**, 4136 (2014).
74. E. F. Plow, T. A. Haas, L. Zhang, J. Loftus, J. W. Smith, Ligand Binding to Integrins. *J. Biol. Chem.* **275**, 21785–21788 (2000).
75. X. Feng, R. A. Clark, D. Galanakis, M. G. Tonnesen, Fibrin and collagen differentially regulate human dermal microvascular endothelial cell integrins: stabilization of  $\alpha v/\beta 3$  mRNA by fibrin. *J. Invest. Dermatol.* **113**, 913–919 (1999).
76. S. Li, *et al.*, Hydrogels with precisely controlled integrin activation dictate vascular patterning and permeability. *Nat. Mater.* **16**, 953–961 (2017).
77. R. R. Rao, A. W. Peterson, J. Ceccarelli, A. J. Putnam, J. P. Stegemann, Matrix composition regulates three-dimensional network formation by endothelial cells and mesenchymal stem cells in collagen/fibrin materials. *Angiogenesis* **15**, 253–264 (2012).
78. G. Szulgit, *et al.*, Alterations in Fibroblast  $\alpha 1\beta 1$  Integrin Collagen Receptor Expression in Keloids and Hypertrophic Scars. *J. Invest. Dermatol.* **118**, 409–415 (2002).
79. A. N. Stratman, G. E. Davis, Endothelial cell-pericyte interactions stimulate basement membrane matrix assembly: Influence on vascular tube remodeling, maturation and stabilization. *Microsc. Microanal. Off. J. Microsc. Soc. Am. Microbeam Anal. Soc. Microsc. Soc. Can.* **18**, 68–80 (2012).
80. S. Morikawa, *et al.*, Abnormalities in Pericytes on Blood Vessels and Endothelial Sprouts in Tumors. *Am. J. Pathol.* **160**, 985–1000 (2002).
81. P. Baluk, H. Hashizume, D. M. McDonald, Cellular abnormalities of blood vessels as targets in cancer. *Curr. Opin. Genet. Dev.* **15**, 102–111 (2005).
82. D. M. McDonald, P. Baluk, Significance of Blood Vessel Leakiness in Cancer. *Cancer Res.* **62**, 5381–5385 (2002).
83. W. B. Saunders, *et al.*, Coregulation of vascular tube stabilization by endothelial cell TIMP-2 and pericyte TIMP-3. *J. Cell Biol.* **175**, 179–191 (2006).
84. G. Bergers, S. Song, The role of pericytes in blood-vessel formation and maintenance. *Neuro-Oncol.* **7**, 452–464 (2005).

85. W. L. Murfee, T. C. Skalak, S. M. Peirce, Differential Arterial/Venous Expression of NG2 Proteoglycan in Perivascular Cells Along Microvessels: Identifying a Venule-Specific Phenotype. *Microcirculation* **12**, 151–160 (2005).
86. U. Ozerdem, K. A. Grako, K. Dahlin-Huppe, E. Monosov, W. B. Stallcup, NG2 proteoglycan is expressed exclusively by mural cells during vascular morphogenesis. *Dev. Dyn.* **222**, 218–227 (2001).
87. B. Vailhé, D. Vittet, J.-J. Feige, In Vitro Models of Vasculogenesis and Angiogenesis. *Lab. Invest.* **81**, 439–452 (2001).
88. K. J. Bayless, G. E. Davis, Sphingosine-1-phosphate markedly induces matrix metalloproteinase and integrin-dependent human endothelial cell invasion and lumen formation in three-dimensional collagen and fibrin matrices. *Biochem. Biophys. Res. Commun.* **312**, 903–913 (2003).
89. B. Trappmann, *et al.*, Matrix degradability controls multicellularity of 3D cell migration. *Nat. Commun.* **8** (2017).
90. R. F. Nicosia, A. Ottinetti, Growth of microvessels in serum-free matrix culture of rat aorta. A quantitative assay of angiogenesis in vitro. *Lab. Investig. J. Tech. Methods Pathol.* **63**, 115–122 (1990).
91. S. Sokic, G. Papavasiliou, Controlled Proteolytic Cleavage Site Presentation in Biomimetic PEGDA Hydrogels Enhances Neovascularization *In Vitro*. *Tissue Eng. Part A* **18**, 2477–2486 (2012).
92. V. Nehls, D. Drenkhahn, A Novel, Microcarrier-Based in Vitro Assay for Rapid and Reliable Quantification of Three-Dimensional Cell Migration and Angiogenesis. *Microvasc. Res.* **50**, 311–322 (1995).
93. P. Allen, J. Melero-Martin, J. Bischoff, Type I collagen, fibrin and PuraMatrix matrices provide permissive environments for human endothelial and mesenchymal progenitor cells to form neovascular networks. *J. Tissue Eng. Regen. Med.* **5**, e74–e86 (2011).
94. C.-C. Lin, K. S. Anseth, PEG Hydrogels for the Controlled Release of Biomolecules in Regenerative Medicine. *Pharm. Res.* **26**, 631–643 (2009).
95. R.-Z. Lin, *et al.*, Host non-inflammatory neutrophils mediate the engraftment of bioengineered vascular networks. *Nat. Biomed. Eng.* **1**, 1–13 (2017).
96. E. B. Peters, Endothelial Progenitor Cells for the Vascularization of Engineered Tissues. *Tissue Eng. Part B Rev.* **24**, 1–24 (2018).
97. M. E. Kroon, *et al.*, Role and Localization of Urokinase Receptor in the Formation of New Microvascular Structures in Fibrin Matrices. *Am. J. Pathol.* **154**, 1731–1742 (1999).

98. J. R. Bezenah, Y. P. Kong, A. J. Putnam, Evaluating the potential of endothelial cells derived from human induced pluripotent stem cells to form microvascular networks in 3D cultures. *Sci. Rep.* **8** (2018).
99. B. Carrion, Y. P. Kong, D. Kaigler, A. J. Putnam, Bone marrow-derived mesenchymal stem cells enhance angiogenesis via their  $\alpha 6\beta 1$  integrin receptor. *Exp. Cell Res.* **319**, 2964–2976 (2013).
100. J. M. Melero-Martin, *et al.*, Engineering Robust and Functional Vascular Networks In Vivo With Human Adult and Cord Blood-Derived Progenitor Cells. *Circ. Res.* **103**, 194–202 (2008).
101. S. Kachgal, A. J. Putnam, Mesenchymal stem cells from adipose and bone marrow promote angiogenesis via distinct cytokine and protease expression mechanisms. *Angiogenesis* **14**, 47–59 (2011).
102. S. Merfeld-Clauss, N. Gollahalli, K. L. March, D. O. Traktuev, Adipose Tissue Progenitor Cells Directly Interact with Endothelial Cells to Induce Vascular Network Formation. *Tissue Eng. Part A* **16**, 2953–2966 (2010).
103. X. Chen, *et al.*, Rapid anastomosis of endothelial progenitor cell–derived vessels with host vasculature is promoted by a high density of cotransplanted fibroblasts. *Tissue Eng. Part A* **16**, 585–594 (2009).
104. M. N. Nakatsu, *et al.*, Angiogenic sprouting and capillary lumen formation modeled by human umbilical vein endothelial cells (HUVEC) in fibrin gels: the role of fibroblasts and Angiopoietin-1 $\star$ . *Microvasc. Res.* **66**, 102–112 (2003).
105. B. R. Shepherd, S. M. Jay, W. M. Saltzman, G. Tellides, J. S. Pober, Human Aortic Smooth Muscle Cells Promote Arteriole Formation by Coengrafted Endothelial Cells. *Tissue Eng. Part A* **15**, 165–173 (2009).
106. E. A. Phelps, N. Landazuri, P. M. Thule, W. R. Taylor, A. J. Garcia, Bioartificial matrices for therapeutic vascularization. *Proc. Natl. Acad. Sci.* **107**, 3323–3328 (2010).
107. A. H. Zisch, *et al.*, Cell-demanded release of VEGF from synthetic, biointeractive cell ingrowth matrices for vascularized tissue growth. *FASEB J.* **17**, 2260–2262 (2003).
108. M. M. Martino, P. S. Briquez, A. Ranga, M. P. Lutolf, J. A. Hubbell, Heparin-binding domain of fibrin(ogen) binds growth factors and promotes tissue repair when incorporated within a synthetic matrix. *Proc. Natl. Acad. Sci.* **110**, 4563–4568 (2013).
109. J. R. Bezenah, A. Y. Rioja, B. Juliar, N. Friend, A. J. Putnam, Assessing the ability of human endothelial cells derived from induced-pluripotent stem cells to form functional microvasculature in vivo. *Biotechnol. Bioeng.* **116**, 415–426 (2019).
110. C. Williams, *et al.*, Short term interactions with long term consequences: modulation of chimeric vessels by neural progenitors. *PloS One* **7** (2012).

111. Y. Zheng, *et al.*, In vitro microvessels for the study of angiogenesis and thrombosis. *Proc. Natl. Acad. Sci. U. S. A.* **109**, 9342–9347 (2012).
112. J. S. Miller, *et al.*, Rapid casting of patterned vascular networks for perfusable engineered three-dimensional tissues. *Nat. Mater.* **11**, 768–774 (2012).
113. C. K. Ozaki, *et al.*, 3D-printed vascular networks direct therapeutic angiogenesis in ischaemia. *Nat. Biomed. Eng.* **1**, s41551-017-0083–017 (2017).
114. M. Vigen, J. Ceccarelli, A. J. Putnam, Protease-Sensitive PEG Hydrogels Regulate Vascularization In Vitro and In Vivo: Protease-Sensitive PEG Hydrogels Regulate Vascularization .... *Macromol. Biosci.* **14**, 1368–1379 (2014).
115. A. Y. Rioja, R. Tiruvannamalai Annamalai, S. Paris, A. J. Putnam, J. P. Stegemann, Endothelial sprouting and network formation in collagen- and fibrin-based modular microbeads. *Acta Biomater.* **29**, 33–41 (2016).
116. S. Pashneh-Tala, S. MacNeil, F. Claeysens, The Tissue-Engineered Vascular Graft—Past, Present, and Future. *Tissue Eng. Part B Rev.* **22**, 68–100 (2016).
117. M. D. Guillemette, *et al.*, Tissue-Engineered Vascular Adventitia with Vasa Vasorum Improves Graft Integration and Vascularization Through Inosculation. *Tissue Eng. Part A* **16**, 2617–2626 (2010).
118. X. Chen, *et al.*, Prevascularization of a fibrin-based tissue construct accelerates the formation of functional anastomosis with host vasculature. *Tissue Eng. Part A* **15**, 1363–1371 (2008).
119. M. Rizzo, S. L. Moran, Vascularized Bone Grafts and Their Applications in the Treatment of Carpal Pathology. *Semin. Plast. Surg.* **22**, 213–227 (2008).
120. M. Fröhlich, *et al.*, Tissue Engineered Bone Grafts: Biological Requirements, Tissue Culture and Clinical Relevance. *Curr. Stem Cell Res. Ther.* **3**, 254–264 (2008).
121. J. D. Weaver, *et al.*, Vasculogenic hydrogel enhances islet survival, engraftment, and function in leading extrahepatic sites. *Sci. Adv.* **3** (2017).
122. T. Desai, L. D. Shea, Advances in islet encapsulation technologies. *Nat. Rev. Drug Discov.* **16**, 338–350 (2016).
123. J. D. Weaver, *et al.*, Design of a vascularized synthetic poly(ethylene glycol) macroencapsulation device for islet transplantation. *Biomaterials* **172**, 54–65 (2018).
124. T. Takebe, *et al.*, Engineering of human hepatic tissue with functional vascular networks. *Organogenesis* **10**, 260–267 (2014).
125. K. Hariharan, A. Kurtz, K. M. Schmidt-Ott, Assembling Kidney Tissues from Cells: The Long Road from Organoids to Organs. *Front. Cell Dev. Biol.* **3** (2015).

126. Y. Takahashi, T. Takebe, H. Taniguchi, Engineering pancreatic tissues from stem cells towards therapy. *Regen. Ther.* **3**, 15–23 (2016).
127. M. P. Lutolf, *et al.*, Synthetic matrix metalloproteinase-sensitive hydrogels for the conduction of tissue regeneration: engineering cell-invasion characteristics. *Proc. Natl. Acad. Sci.* **100**, 5413–5418 (2003).
128. M. P. Lutolf, J. A. Hubbell, Synthesis and Physicochemical Characterization of End-Linked Poly(ethylene glycol)-*co*-peptide Hydrogels Formed by Michael-Type Addition. *Biomacromolecules* **4**, 713–722 (2003).
129. M. P. Lutolf, J. A. Hubbell, Synthetic biomaterials as instructive extracellular microenvironments for morphogenesis in tissue engineering. *Nat. Biotechnol.* **23**, 47–55 (2005).
130. J. Patterson, J. A. Hubbell, Enhanced proteolytic degradation of molecularly engineered PEG hydrogels in response to MMP-1 and MMP-2. *Biomaterials* **31**, 7836–7845 (2010).
131. J. A. Beamish, *et al.*, Deciphering the relative roles of matrix metalloproteinase- and plasmin-mediated matrix degradation during capillary morphogenesis using engineered hydrogels: MATRIX REMODELING IN ENGINEERED HYDROGELS DURING VASCULOGENESIS. *J. Biomed. Mater. Res. B Appl. Biomater.* (2019)  
<https://doi.org/10.1002/jbm.b.34341> (February 20, 2019).
132. A. B. Pratt, F. E. Weber, H. G. Schmoekel, R. Müller, J. A. Hubbell, Synthetic extracellular matrices for in situ tissue engineering: Synthetic Extracellular Matrices for In situ Tissue Engineering. *Biotechnol. Bioeng.* **86**, 27–36 (2004).
133. J. J. Moon, *et al.*, Biomimetic hydrogels with pro-angiogenic properties. *Biomaterials* **31**, 3840–3847 (2010).
134. R. M. Schweller, Z. J. Wu, B. Klitzman, J. L. West, Stiffness of Protease Sensitive and Cell Adhesive PEG Hydrogels Promotes Neovascularization In Vivo. *Ann. Biomed. Eng.* **45**, 1387–1398 (2017).
135. A. I. Caplan, All MSCs Are Pericytes? *Cell Stem Cell* **3**, 229–230 (2008).
136. M. Crisan, *et al.*, A Perivascular Origin for Mesenchymal Stem Cells in Multiple Human Organs. *Cell Stem Cell* **3**, 301–313 (2008).
137. K. K. Hirschi, S. A. Rohovsky, P. A. D'Amore, PDGF, TGF- $\beta$ , and Heterotypic Cell–Cell Interactions Mediate Endothelial Cell–induced Recruitment of 10T1/2 Cells and Their Differentiation to a Smooth Muscle Fate. *J. Cell Biol.* **141**, 805–814 (1998).
138. F. Berthod, L. Germain, N. Tremblay, F. A. Auger, Extracellular matrix deposition by fibroblasts is necessary to promote capillary-like tube formation in vitro. *J. Cell. Physiol.* **207**, 491–498 (2006).

139. D.-Y. Lee, K.-H. Cho, The effects of epidermal keratinocytes and dermal fibroblasts on the formation of cutaneous basement membrane in three-dimensional culture systems. *Arch. Dermatol. Res.* **296**, 296–302 (2005).
140. M. Varkey, J. Ding, E. E. Tredget, Superficial Dermal Fibroblasts Enhance Basement Membrane and Epidermal Barrier Formation in Tissue-Engineered Skin: Implications for Treatment of Skin Basement Membrane Disorders. *Tissue Eng. Part A* **20**, 540–552 (2014).
141. H. Smola, *et al.*, Dynamics of Basement Membrane Formation by Keratinocyte–Fibroblast Interactions in Organotypic Skin Culture. *Exp. Cell Res.* **239**, 399–410 (1998).
142. A. Furuyama, K. Kimata, K. Mochitate, Assembly of Basement Membrane in Vitro by Cooperation between Alveolar Epithelial Cells and Pulmonary Fibroblasts. *Cell Struct. Funct.* **22**, 603–614 (1997).
143. K. F. Chambers, *et al.*, Stroma Regulates Increased Epithelial Lateral Cell Adhesion in 3D Culture: A Role for Actin/Cadherin Dynamics. *PLoS ONE* **6**, e18796 (2011).
144. W.-K. You, F. Yotsumoto, K. Sakimura, R. H. Adams, W. B. Stallcup, NG2 proteoglycan promotes tumor vascularization via integrin-dependent effects on pericyte function. *Angiogenesis* **17**, 61–76 (2014).
145. C. H. Lee, E. K. Moioli, J. J. Mao, Fibroblastic Differentiation of Human Mesenchymal Stem Cells using Connective Tissue Growth Factor. *Conf. Proc. Annu. Int. Conf. IEEE Eng. Med. Biol. Soc. IEEE Eng. Med. Biol. Soc. Annu. Conf.* **1**, 775–778 (2006).
146. K. Hosaka, *et al.*, Pericyte–fibroblast transition promotes tumor growth and metastasis. *Proc. Natl. Acad. Sci.* **113**, E5618–E5627 (2016).
147. D. Kole, S. Ambady, R. L. Page, T. Dominko, Maintenance of Multipotency in Human Dermal Fibroblasts Treated with *Xenopus laevis* Egg Extract Requires Exogenous Fibroblast Growth Factor-2. *Cell. Reprogramming* **16**, 18–28 (2014).
148. S. Sartore, *et al.*, Contribution of Adventitial Fibroblasts to Neointima Formation and Vascular Remodeling: From Innocent Bystander to Active Participant. *Circ. Res.* **89**, 1111–1121 (2001).
149. M. P. Lewis, *et al.*, Tumour-derived TGF- $\beta$ 1 modulates myofibroblast differentiation and promotes HGF/SF-dependent invasion of squamous carcinoma cells. *Br. J. Cancer* **90**, 822–832 (2004).
150. I. A. Darby, B. Laverdet, F. Bonté, A. Desmoulière, Fibroblasts and myofibroblasts in wound healing. *Clin. Cosmet. Investig. Dermatol.* (2014) (May 18, 2017).
151. B. Li, J. H.-C. Wang, Fibroblasts and Myofibroblasts in Wound Healing: Force Generation and Measurement. *J. Tissue Viability* **20**, 108–120 (2011).

152. D. Mayrand, *et al.*, Angiogenic properties of myofibroblasts isolated from normal human skin wounds. *Angiogenesis* **15**, 199–212 (2012).
153. P. J. Mishra, D. Banerjee, “Activation and Differentiation of Mesenchymal Stem Cells” in *Signal Transduction Immunohistochemistry*, Methods in Molecular Biology., (Humana Press, 2011), pp. 245–253.
154. J. C. Chapin, K. A. Hajjar, Fibrinolysis and the control of blood coagulation. *Blood Rev.* **29**, 17–24 (2015).
155. M. Ponec, *et al.*, Endothelial network formed with human dermal microvascular endothelial cells in autologous multicellular skin substitutes. *Angiogenesis* **7**, 295–305 (2004).
156. D. L. Stahl, K. M. Richard, T. J. Papadimos, Complications of bronchoscopy: A concise synopsis. *Int. J. Crit. Illn. Inj. Sci.* **5**, 189–195 (2015).
157. B. J. Bain, Bone marrow biopsy morbidity: review of 2003. *J. Clin. Pathol.* **58**, 406–408 (2005).
158. P. T. Brown, A. M. Handorf, W. B. Jeon, W.-J. Li, Stem cell-based tissue engineering approaches for musculoskeletal regeneration. *Curr. Pharm. Des.* **19**, 3429–3445 (2013).
159. D. E. Discher, P. Janmey, Y. Wang, Tissue cells feel and respond to the stiffness of their substrate. *Science* **310**, 1139–1143 (2005).
160. A. Engler, *et al.*, Substrate Compliance versus Ligand Density in Cell on Gel Responses. *Biophys. J.* **86**, 617–628 (2004).
161. S. R. Peyton, A. J. Putnam, Extracellular matrix rigidity governs smooth muscle cell motility in a biphasic fashion. *J. Cell. Physiol.* **204**, 198–209 (2005).
162. J. A. Beamish, E. Chen, A. J. Putnam, Engineered extracellular matrices with controlled mechanics modulate renal proximal tubular cell epithelialization. *PLoS ONE* **12** (2017).
163. C. B. Khatiwala, S. R. Peyton, A. J. Putnam, Intrinsic mechanical properties of the extracellular matrix affect the behavior of pre-osteoblastic MC3T3-E1 cells. *Am. J. Physiol.-Cell Physiol.* **290**, C1640–C1650 (2006).
164. C. M. Lo, H. B. Wang, M. Dembo, Y. L. Wang, Cell movement is guided by the rigidity of the substrate. *Biophys. J.* **79**, 144–152 (2000).
165. A. J. Engler, S. Sen, H. L. Sweeney, D. E. Discher, Matrix Elasticity Directs Stem Cell Lineage Specification. *Cell* **126**, 677–689 (2006).
166. C. B. Khatiwala, P. D. Kim, S. R. Peyton, A. J. Putnam, ECM Compliance Regulates Osteogenesis by Influencing MAPK Signaling Downstream of RhoA and ROCK. *J. Bone Miner. Res.* **24**, 886–898 (2009).

167. N. Huebsch, *et al.*, Harnessing traction-mediated manipulation of the cell/matrix interface to control stem-cell fate. *Nat. Mater.* **9**, 518–526 (2010).
168. S. R. Peyton, P. D. Kim, C. M. Ghajar, D. Seliktar, A. J. Putnam, The Effects of Matrix Stiffness and RhoA on the Phenotypic Plasticity of Smooth Muscle Cells in a 3-D Biosynthetic Hydrogel System. *Biomaterials* **29**, 2597–2607 (2008).
169. Ingber Donald E., Mechanical Signaling and the Cellular Response to Extracellular Matrix in Angiogenesis and Cardiovascular Physiology. *Circ. Res.* **91**, 877–887 (2002).
170. T. Korff, H. G. Augustin, Tensional forces in fibrillar extracellular matrices control directional capillary sprouting. *J. Cell Sci.* **112**, 3249–3258 (1999).
171. E. Kniazeva, A. J. Putnam, Endothelial cell traction and ECM density influence both capillary morphogenesis and maintenance in 3-D. *AJP Cell Physiol.* **297**, C179–C187 (2009).
172. C. M. Ghajar, K. S. Blevins, C. C. Hughes, S. C. George, A. J. Putnam, Mesenchymal stem cells enhance angiogenesis in mechanically viable prevascularized tissues via early matrix metalloproteinase upregulation. *Tissue Eng.* **12**, 2875–2888 (2006).
173. M. G. Tonnesen, X. Feng, R. A. F. Clark, Angiogenesis in Wound Healing. *J. Investig. Dermatol. Symp. Proc.* **5**, 40–46 (2000).
174. J. J. Tomasek, G. Gabbiani, B. Hinz, C. Chaponnier, R. A. Brown, Myofibroblasts and mechano-regulation of connective tissue remodelling. *Nat. Rev. Mol. Cell Biol.* **3**, 349–363 (2002).
175. K. A. Jansen, R. G. Bacabac, I. K. Piechocka, G. H. Koenderink, Cells Actively Stiffen Fibrin Networks by Generating Contractile Stress. *Biophys. J.* **105**, 2240–2251 (2013).
176. C. M. Ghajar, *et al.*, The Effect of Matrix Density on the Regulation of 3-D Capillary Morphogenesis. *Biophys. J.* **94**, 1930–1941 (2008).
177. M. A. Kotlarchyk, *et al.*, Concentration Independent Modulation of Local Micromechanics in a Fibrin Gel. *PLoS ONE* **6**, e20201 (2011).
178. R. R. Brau, *et al.*, Passive and active microrheology with optical tweezers. *J. Opt. Pure Appl. Opt.* **9**, S103 (2007).
179. D. Mizuno, D. A. Head, F. C. MacKintosh, C. F. Schmidt, Active and Passive Microrheology in Equilibrium and Nonequilibrium Systems. *Macromolecules* **41**, 7194–7202 (2008).
180. J. W. Weisel, Enigmas of Blood Clot Elasticity. *Science* **320**, 456–457 (2008).
181. P. Lu, Z. Werb, Patterning Mechanisms of Branched Organs. *Science* **322**, 1506–1509 (2008).



182. E. Bellas, C. S. Chen, Forms, forces, and stem cell fate. *Curr. Opin. Cell Biol.* **0**, 92–97 (2014).
183. , Mechanobiology and Developmental Control | Annual Review of Cell and Developmental Biology (March 16, 2020).
184. O. Chaudhuri, *et al.*, Hydrogels with tunable stress relaxation regulate stem cell fate and activity. *Nat. Mater.* **15**, 326–334 (2016).
185. R. T. Justin, A. J. Engler, Stiffness gradients mimicking in vivo tissue variation regulate mesenchymal stem cell fate. *PloS One* **6** (2011).
186. C. Yang, *et al.*, Spatially patterned matrix elasticity directs stem cell fate. *Proc. Natl. Acad. Sci.* **113**, E4439–E4445 (2016).
187. S. Khetan, *et al.*, Degradation-mediated cellular traction directs stem cell fate in covalently crosslinked three-dimensional hydrogels. *Nat. Mater.* **12**, 458–465 (2013).
188. C. Yang, M. W. Tibbitt, L. Basta, K. S. Anseth, Mechanical memory and dosing influence stem cell fate. *Nat. Mater.* **13**, 645–652 (2014).
189. J. Lee, A. A. Abdeen, K. A. Kilian, Rewiring mesenchymal stem cell lineage specification by switching the biophysical microenvironment. *Sci. Rep.* **4**, 1–8 (2014).
190. P.-F. Lee, A. T. Yeh, K. J. Bayless, Nonlinear optical microscopy reveals invading endothelial cells anisotropically alter three-dimensional collagen matrices. *Exp. Cell Res.* **315**, 396–410 (2009).
191. C. B. Raub, *et al.*, Noninvasive Assessment of Collagen Gel Microstructure and Mechanics Using Multiphoton Microscopy. *Biophys. J.* **92**, 2212–2222 (2007).
192. J. Steinwachs, *et al.*, Three-dimensional force microscopy of cells in biopolymer networks. *Nat. Methods N. Y.* **13**, 171–176 (2016).
193. B. Vailhé, M. Lecomte, N. Wiernsperger, L. Tranqui, The formation of tubular structures by endothelial cells is under the control of fibrinolysis and mechanical factors. *Angiogenesis* **2**, 331–344 (1998).
194. C. F. Deroanne, C. M. Lapiere, B. V. Nusgens, In vitro tubulogenesis of endothelial cells by relaxation of the coupling extracellular matrix-cytoskeleton. *Cardiovasc. Res.* **49**, 647–658 (2001).
195. L. Urech, A. G. Bittermann, Jeffrey. A. Hubbell, H. Hall, Mechanical properties, proteolytic degradability and biological modifications affect angiogenic process extension into native and modified fibrin matrices in vitro. *Biomaterials* **26**, 1369–1379 (2005).

196. E. Kniazeva, S. Kachgal, A. J. Putnam, Effects of Extracellular Matrix Density and Mesenchymal Stem Cells on Neovascularization *In Vivo*. *Tissue Eng. Part A* **17**, 905–914 (2011).
197. B. N. Mason, A. Starchenko, R. M. Williams, L. J. Bonassar, C. A. Reinhart-King, Tuning 3D Collagen Matrix Stiffness Independently of Collagen Concentration Modulates Endothelial Cell Behavior. *Acta Biomater.* **9**, 4635–4644 (2013).
198. F. Bordeleau, *et al.*, Matrix stiffening promotes a tumor vasculature phenotype. *Proc. Natl. Acad. Sci. U. S. A.* **114**, 492–497 (2017).
199. P.-F. Lee, Y. Bai, R. L. Smith, K. J. Bayless, A. T. Yeh, Angiogenic responses are enhanced in mechanically and microscopically characterized, microbial transglutaminase crosslinked collagen matrices with increased stiffness. *Acta Biomater.* **9**, 7178–7190 (2013).
200. M. E. Francis-Sedlak, *et al.*, Collagen glycation alters neovascularization in vitro and in vivo. *Microvasc. Res.* **80**, 3–9 (2010).
201. M. Kuzuya, *et al.*, Inhibition of angiogenesis on glycated collagen lattices. *Diabetologia* **41**, 491–499 (1998).
202. R. K. Singh, D. Seliktar, A. J. Putnam, Capillary morphogenesis in PEG-collagen hydrogels. *Biomaterials* **34**, 9331–9340 (2013).
203. W. R. Legant, *et al.*, Measurement of mechanical tractions exerted by cells in three-dimensional matrices. *Nat. Methods* **7**, 969–971 (2010).
204. M. Keating, A. Kurup, M. Alvarez-Elizondo, A. J. Levine, E. Botvinick, Spatial distributions of pericellular stiffness in natural extracellular matrices are dependent on cell-mediated proteolysis and contractility. *Acta Biomater.* **57**, 304–312 (2017).
205. Y. Tang, *et al.*, MT1-MMP-Dependent Control of Skeletal Stem Cell Commitment via a  $\beta$ 1-Integrin/YAP/TAZ Signaling Axis. *Dev. Cell* **25**, 402–416 (2013).
206. van Hinsbergh Victor W.M., Engelse Marten A., Quax Paul H.A., Pericellular Proteases in Angiogenesis and Vasculogenesis. *Arterioscler. Thromb. Vasc. Biol.* **26**, 716–728 (2006).
207. H. Fritz, G. Wunderer, Biochemistry and applications of aprotinin, the kallikrein inhibitor from bovine organs. *Arzneimittelforschung.* **33**, 479–494 (1983).
208. A. L. McNulty, J. B. Weinberg, F. Guilak, Inhibition of Matrix Metalloproteinases Enhances In Vitro Repair of the Meniscus. *Clin. Orthop.* **467**, 1557–1567 (2009).
209. K. R. Stevens, *et al.*, In situ expansion of engineered human liver tissue in a mouse model of chronic liver disease. *Sci. Transl. Med.* **9** (2017).

210. S. Rafii, J. M. Butler, B.-S. Ding, Angiocrine functions of organ-specific endothelial cells. *Nature* **529**, 316–325 (2016).
211. K. Pill, *et al.*, Microvascular Networks From Endothelial Cells and Mesenchymal Stromal Cells From Adipose Tissue and Bone Marrow: A Comparison. *Front. Bioeng. Biotechnol.* **6** (2018).
212. P. Nowak-Sliwinska, *et al.*, Consensus guidelines for the use and interpretation of angiogenesis assays. *Angiogenesis* **21**, 425–532 (2018).
213. I. Yana, *et al.*, Crosstalk between neovessels and mural cells directs the site-specific expression of MT1-MMP to endothelial tip cells. *J. Cell Sci.* **120**, 1607–1614 (2007).
214. B. E. Turk, L. L. Huang, E. T. Piro, L. C. Cantley, Determination of protease cleavage site motifs using mixture-based oriented peptide libraries. *Nat. Biotechnol.* **19**, 661–667 (2001).
215. V. W. Hinsbergh, A. Collen, P. Koolwijk, Role of fibrin matrix in angiogenesis. *Ann. N. Y. Acad. Sci.* **936**, 426–437 (2001).
216. T. Minami, *et al.*, Thrombin and Phenotypic Modulation of the Endothelium. *Arterioscler. Thromb. Vasc. Biol.* **24**, 41–53 (2004).
217. M. Daviran, S. M. Longwill, J. F. Casella, K. M. Schultz, Rheological characterization of dynamic remodeling of the pericellular region by human mesenchymal stem cell-secreted enzymes in well-defined synthetic hydrogel scaffolds. *Soft Matter* **14**, 3078–3089 (2018).
218. K. M. Schultz, K. A. Kyburz, K. S. Anseth, Measuring dynamic cell–material interactions and remodeling during 3D human mesenchymal stem cell migration in hydrogels. *Proc. Natl. Acad. Sci.* **112**, E3757–E3764 (2015).
219. G. P. Raeber, M. P. Lutolf, J. A. Hubbell, Molecularly Engineered PEG Hydrogels: A Novel Model System for Proteolytically Mediated Cell Migration. *Biophys. J.* **89**, 1374–1388 (2005).
220. G. Cesarman-Maus, K. A. Hajjar, Molecular mechanisms of fibrinolysis. *Br. J. Haematol.* **129**, 307–321 (2005).
221. U. Blache, *et al.*, Notch-inducing hydrogels reveal a perivascular switch of mesenchymal stem cell fate. *EMBO Rep.* **19**, e45964 (2018).
222. N. Ramos-DeSimone, *et al.*, Activation of Matrix Metalloproteinase-9 (MMP-9) via a Converging Plasmin/Stromelysin-1 Cascade Enhances Tumor Cell Invasion. *J. Biol. Chem.* **274**, 13066–13076 (1999).
223. K. Yayama, N. Kunitatsu, Y. Teranishi, M. Takano, H. Okamoto, Tissue kallikrein is synthesized and secreted by human vascular endothelial cells. *Biochim. Biophys. Acta BBA - Mol. Cell Res.* **1593**, 231–238 (2003).

224. H. Zollner, *Handbook of Enzyme Inhibitors* (Weinheim, Federal Republic of Germany, 1993) <https://doi.org/10.1002/9783527618330> (March 19, 2020).
225. E. A. Phelps, K. L. Templeman, P. M. Thulé, A. J. García, Engineered VEGF-releasing PEG-MAL hydrogel for pancreatic islet vascularization. *Drug Deliv. Transl. Res.* **5**, 125–136 (2015).
226. S. Sokic, *et al.*, Evaluation of MMP substrate concentration and specificity for neovascularization of hydrogel scaffolds. *Biomater. Sci.* **2**, 1343–1354 (2014).
227. E. B. Peters, N. Christoforou, K. W. Leong, G. A. Truskey, J. L. West, Poly(ethylene glycol) Hydrogel Scaffolds Containing Cell-Adhesive and Protease-Sensitive Peptides Support Microvessel Formation by Endothelial Progenitor Cells. *Cell. Mol. Bioeng.* **9**, 38–54 (2016).
228. L. T. Edgar, C. J. Underwood, J. E. Guilkey, J. B. Hoying, J. A. Weiss, Extracellular Matrix Density Regulates the Rate of Neovessel Growth and Branching in Sprouting Angiogenesis. *PLOS ONE* **9**, e85178 (2014).
229. Y.-C. Chen, *et al.*, Functional Human Vascular Network Generated in Photocrosslinkable Gelatin Methacrylate Hydrogels. *Adv. Funct. Mater.* **22**, 2027–2039 (2012).
230. K. Chwalek, M. V. Tsurkan, U. Freudenberg, C. Werner, Glycosaminoglycan-based hydrogels to modulate heterocellular communication in in vitro angiogenesis models. *Sci. Rep.* **4**, 1–8 (2014).
231. J. A. Beamish, *et al.*, Deciphering the relative roles of matrix metalloproteinase- and plasmin-mediated matrix degradation during capillary morphogenesis using engineered hydrogels. *J. Biomed. Mater. Res. B Appl. Biomater.* **107**, 2507–2516 (2019).
232. L. R. Nih, S. Gojgini, S. T. Carmichael, T. Segura, Dual-function injectable angiogenic biomaterial for the repair of brain tissue following stroke. *Nat. Mater.* **17**, 642–651 (2018).
233. S. Bhutani, *et al.*, Evaluation of Hydrogels Presenting Extracellular Matrix-Derived Adhesion Peptides and Encapsulating Cardiac Progenitor Cells for Cardiac Repair. *ACS Biomater. Sci. Eng.* **4**, 200–210 (2018).
234. X. Zhang, *et al.*, Integrating valve-inspired design features into poly(ethylene glycol) hydrogel scaffolds for heart valve tissue engineering. *Acta Biomater.* **14**, 11–21 (2015).
235. M. Vigen, “INVESTIGATING THE ROLE OF MATRIX ARCHITECTURE ON VASCULARIZATION IN MMP- SENSITIVE PEG HYDROGELS,” University of Michigan. (2014).
236. S. R. K. Ainavarapu, *et al.*, Contour Length and Refolding Rate of a Small Protein Controlled by Engineered Disulfide Bonds. *Biophys. J.* **92**, 225–233 (2007).

237. F. Oesterhelt, M. Rief, H. E. Gaub, Single molecule force spectroscopy by AFM indicates helical structure of poly(ethylene-glycol) in water. *New J. Phys.* **1**, 6–6 (1999).
238. B. A. Juliar, *et al.*, Cell-mediated matrix stiffening accompanies capillary morphogenesis in ultra-soft amorphous hydrogels. *Biomaterials* **230**, 119634 (2020).
239. T. Pearson, D. L. Greiner, L. D. Shultz, “Humanized SCID Mouse Models for Biomedical Research” in *Humanized Mice*, Current Topics in Microbiology and Immunology., T. Nomura, T. Watanabe, S. Habu, Eds. (Springer, 2008), pp. 25–51.
240. R. James, L. Jenkins, S. E. Ellis, K. J. Burg, Histological processing of hydrogel scaffolds for tissue-engineering applications. *J. Histotechnol.* **27**, 133–139 (2004).
241. J.-L. Ruan, *et al.*, An Improved Cryosection Method for Polyethylene Glycol Hydrogels Used in Tissue Engineering. *Tissue Eng. Part C Methods* **19**, 794–801 (2013).
242. S. Khetan, J. Burdick, Cellular Encapsulation in 3D Hydrogels for Tissue Engineering. *J. Vis. Exp. JoVE* (2009) <https://doi.org/10.3791/1590>.
243. A. D. Lynn, A. K. Blakney, T. R. Kyriakides, S. J. Bryant, Temporal progression of the host response to implanted poly(ethylene glycol)-based hydrogels. *J. Biomed. Mater. Res. A* **96**, 621–631 (2011).
244. M. D. Swartzlander, *et al.*, Linking the foreign body response and protein adsorption to PEG-based hydrogels using proteomics. *Biomaterials* **41**, 26–36 (2015).
245. S. Stevenson, A. H. Taylor, A. Meskiri, D. T. Sharpe, M. J. Thornton, Differing responses of human follicular and nonfollicular scalp cells in an in vitro wound healing assay: Effects of estrogen on vascular endothelial growth factor secretion. *Wound Repair Regen.* **16**, 243–253 (2008).
246. J. Rouwkema, A. Khademhosseini, Vascularization and Angiogenesis in Tissue Engineering: Beyond Creating Static Networks. *Trends Biotechnol.* **34**, 733–745 (2016).
247. J. E. Leslie-Barbick, J. E. Saik, D. J. Gould, M. E. Dickinson, J. L. West, The promotion of microvasculature formation in poly(ethylene glycol) diacrylate hydrogels by an immobilized VEGF-mimetic peptide. *Biomaterials* **32**, 5782–5789 (2011).
248. R. M. Schweller, J. L. West, Encoding Hydrogel Mechanics via Network Cross-Linking Structure. *ACS Biomater. Sci. Eng.* **1**, 335–344 (2015).
249. M. V. Tsurkan, *et al.*, Defined Polymer–Peptide Conjugates to Form Cell-Instructive starPEG–Heparin Matrices In Situ. *Adv. Mater.* **25**, 2606–2610 (2013).
250. R. Xu, A. Boudreau, M. J. Bissell, Tissue architecture and function: dynamic reciprocity via extra- and intra-cellular matrices. *Cancer Metastasis Rev.* **28**, 167–176 (2009).

251. B. A. Juliar, M. T. Keating, Y. P. Kong, E. L. Botvinick, A. J. Putnam, Sprouting angiogenesis induces significant mechanical heterogeneities and ECM stiffening across length scales in fibrin hydrogels. *Biomaterials* **162**, 99–108 (2018).
252. K. A. Beningo, K. Hamao, M. Dembo, Y. Wang, H. Hosoya, Traction Forces of Fibroblasts are Regulated by the Rho-Dependent Kinase but not by the Myosin Light Chain Kinase. *Arch. Biochem. Biophys.* **456**, 224–231 (2006).
253. D. Rosenfeld, *et al.*, Morphogenesis of 3D vascular networks is regulated by tensile forces. *Proc. Natl. Acad. Sci.* **113**, 3215–3220 (2016).
254. B. Hinz, *et al.*, Recent Developments in Myofibroblast Biology. *Am. J. Pathol.* **180**, 1340–1355 (2012).
255. J. Zhu, Bioactive Modification of Poly(ethylene glycol) Hydrogels for Tissue Engineering. *Biomaterials* **31**, 4639–4656 (2010).
256. W. L. Murphy, T. C. McDevitt, A. J. Engler, Materials as stem cell regulators. *Nat. Mater.* **13**, 547–557 (2014).
257. J. P. Winer, S. Oake, P. A. Janmey, Non-Linear Elasticity of Extracellular Matrices Enables Contractile Cells to Communicate Local Position and Orientation. *PLOS ONE* **4**, e6382 (2009).
258. Ahearne Mark, Introduction to cell–hydrogel mechanosensing. *Interface Focus* **4**, 20130038 (2014).
259. T. Wakatsuki, E. L. Elson, Reciprocal interactions between cells and extracellular matrix during remodeling of tissue constructs. *Biophys. Chem.* **100**, 593–605 (2002).
260. A. S. Meshel, Q. Wei, R. S. Adelstein, M. P. Sheetz, Basic mechanism of three-dimensional collagen fibre transport by fibroblasts. *Nat. Cell Biol.* **7**, 157–164 (2005).
261. D. Kesselman, O. Kossover, I. Mironi-Harpaz, D. Seliktar, Time-dependent cellular morphogenesis and matrix stiffening in proteolytically responsive hydrogels. *Acta Biomater.* **9**, 7630–7639 (2013).
262. N. C. Hunt, A. M. Smith, U. Gbureck, R. M. Shelton, L. M. Grover, Encapsulation of fibroblasts causes accelerated alginate hydrogel degradation. *Acta Biomater.* **6**, 3649–3656 (2010).
263. D. Hanjaya-Putra, *et al.*, Controlled activation of morphogenesis to generate a functional human microvasculature in a synthetic matrix. *Blood* **118**, 804–815 (2011).
264. M. Kovács, J. Tóth, C. Hetényi, A. Málnási-Csizmadia, J. R. Sellers, Mechanism of Blebbistatin Inhibition of Myosin II. *J. Biol. Chem.* **279**, 35557–35563 (2004).

265. K. M. Mabry, R. L. Lawrence, K. S. Anseth, Dynamic stiffening of poly(ethylene glycol)-based hydrogels to direct valvular interstitial cell phenotype in a three-dimensional environment. *Biomaterials* **49**, 47–56 (2015).
266. G. M. Williams, T. J. Klein, R. L. Sah, Cell density alters matrix accumulation in two distinct fractions and the mechanical integrity of alginate–chondrocyte constructs. *Acta Biomater.* **1**, 625–633 (2005).
267. J. Eyckmans, T. Boudou, X. Yu, C. S. Chen, A Hitchhiker’s Guide to Mechanobiology. *Dev. Cell* **21**, 35–47 (2011).
268. B. M. Baker, B. Trappmann, S. C. Stapleton, E. Toro, C. S. Chen, Microfluidics embedded within extracellular matrix to define vascular architectures and pattern diffusive gradients. *Lab. Chip* **13**, 3246 (2013).
269. T. Wakatsuki, M. S. Kolodney, G. I. Zahalak, E. L. Elson, Cell mechanics studied by a reconstituted model tissue. *Biophys. J.* **79**, 2353–2368 (2000).
270. R. G. Wells, Tissue Mechanics and Fibrosis. *Biochim. Biophys. Acta* **1832**, 884–890 (2013).
271. G. S. Bogatkevich, *et al.*, Contractile activity and smooth muscle  $\alpha$ -actin organization in thrombin-induced human lung myofibroblasts. *Am. J. Physiol. - Lung Cell. Mol. Physiol.* **285**, L334–L343 (2003).
272. B. Hinz, G. Celetta, J. J. Tomasek, G. Gabbiani, C. Chaponnier, Alpha-Smooth Muscle Actin Expression Upregulates Fibroblast Contractile Activity. *Mol. Biol. Cell* **12**, 2730–2741 (2001).
273. C. A. Reinhart-King, M. Dembo, D. A. Hammer, Cell-Cell Mechanical Communication through Compliant Substrates. *Biophys. J.* **95**, 6044–6051 (2008).
274. P.-J. Wipff, D. B. Rifkin, J.-J. Meister, B. Hinz, Myofibroblast contraction activates latent TGF- $\beta$ 1 from the extracellular matrix. *J. Cell Biol.* **179**, 1311–1323 (2007).
275. T. M. Freyman, I. V. Yannas, R. Yokoo, L. J. Gibson, Fibroblast Contractile Force Is Independent of the Stiffness Which Resists the Contraction. *Exp. Cell Res.* **272**, 153–162 (2002).
276. K. Suehiro, J. Gailit, E. F. Plow, Fibrinogen Is a Ligand for Integrin  $\alpha$ 5 $\beta$ 1 on Endothelial Cells. *J. Biol. Chem.* **272**, 5360–5366 (1997).
277. S. Yakovlev, L. Medved, Interaction of Fibrin(ogen) with the Endothelial Cell Receptor VE-Cadherin: Localization of the Fibrin-Binding Site within the Third Extracellular VE-Cadherin Domain. *Biochemistry* **48**, 5171–5179 (2009).
278. K. Chwalek, *et al.*, Two-tier hydrogel degradation to boost endothelial cell morphogenesis. *Biomaterials* **32**, 9649–9657 (2011).

279. X. Li, *et al.*, Nanofiber-hydrogel composite-mediated angiogenesis for soft tissue reconstruction. *Sci. Transl. Med.* **11**, eaau6210 (2019).
280. L. M. Weber, C. G. Lopez, K. S. Anseth, Effects of PEG hydrogel crosslinking density on protein diffusion and encapsulated islet survival and function. *J. Biomed. Mater. Res. A* **90A**, 720–729 (2009).
281. K. Vandoorne, Y. Addadi, M. Neeman, Visualizing vascular permeability and lymphatic drainage using labeled serum albumin. *Angiogenesis* **13**, 75–85 (2010).
282. M. Radu, J. Chernoff, An in vivo Assay to Test Blood Vessel Permeability. *J. Vis. Exp. JoVE* (2013) <https://doi.org/10.3791/50062>.
283. R. H. Adamson, J. F. Lenz, F. E. Curry, Quantitative Laser Scanning Confocal Microscopy on Single Capillaries: Permeability Measurement. *Microcirculation* **1**, 251–265 (1994).
284. B. A. Nerger, M. J. Siedlik, C. M. Nelson, Microfabricated tissues for investigating traction forces involved in cell migration and tissue morphogenesis. *Cell. Mol. Life Sci. CMLS* **74**, 1819–1834 (2017).
285. A. Bertin, H. Schlaad, Mild and Versatile (Bio-)Functionalization of Glass Surfaces via Thiol–Ene Photochemistry. *Chem. Mater.* **21**, 5698–5700 (2009).
286. S. Narumiya, T. Ishizaki, N. Watanabe, Rho effectors and reorganization of actin cytoskeleton. *FEBS Lett.* **410**, 68–72 (1997).
287. C. Zhong, M. S. Kinch, K. Burridge, Rho-stimulated Contractility Contributes to the Fibroblastic Phenotype of Ras-transformed Epithelial Cells. *Mol. Biol. Cell* **8**, 2329–2344 (1997).
288. Y. P. Kong, B. Carrion, R. K. Singh, A. J. Putnam, Matrix identity and tractional forces influence indirect cardiac reprogramming. *Sci. Rep.* **3**, 3474 (2013).
289. I. Rodriguez-Hernandez, G. Cantelli, F. Bruce, V. Sanz-Moreno, Rho, ROCK and actomyosin contractility in metastasis as drug targets. *F1000Research* **5** (2016).
290. H. Hashizume, *et al.*, Openings between defective endothelial cells explain tumor vessel leakiness. *Am. J. Pathol.* **156**, 1363–1380 (2000).
291. J. L. MacKay, S. Kumar, Simultaneous and independent tuning of RhoA and Rac1 activity with orthogonally inducible promoters. *Integr. Biol. Quant. Biosci. Nano Macro* **6**, 885–894 (2014).



## APPENDICES

### Appendix A: Unfreezing cells

Adapted from Jonathan Bezenah protocol

#### Materials

- Cryo-gloves
- Face shield
- Cryo-preserved cell vials
- Culture media
- Culture flasks
- 15ml and/or 50 ml sterile centrifuge tubes
- 70% ethanol in spray bottle

#### Procedure

1. Warm up media in water bath 37 °C.
2. Open hood sash. Open hood until set at appropriate level (alarm should stop sounding)
3. Turn on vacuum pump
4. Once airflow indicator light turns green on hood control panel, spray down and wipe down work surface with ethanol
5. Put necessary supplies into hood by first spraying with 70% ethanol and wiping down with paper towel  
\* ANYTHING that enters hood needs to be sprayed with 70% ethanol\*
6. Once media has warmed up, transfer media bottle to hood. Spray with 70% ethanol first before placing in hood
7. Press indicator light/button on liquid nitrogen tank lid and then remove lid. Let it hang from the side handle of the tank
8. Put on cryo gloves and face shield, remove respective rack where cells are stored from tank. Let all liquid nitrogen drain into tank before completely removing
9. Find cell vial in the respective box and remove from box
10. Place rack back in liquid nitrogen, close lid, and re-press indicator light/button.
11. Place vial of cells in a foam float and thaw in water bath at 37 °C
12. Immediately once cells are thawed (~ 2 minutes), transfer vial to cell culture hood
13. Using micropipetter, transfer the content of the vial to a 15 ml or 50 ml centrifuge tube.
14. Add 1 mL of respective media, using a micropipetter, to the empty vial to ensure all cells are removed from the vial and add to the centrifuge tube.
15. Add an additional 8 mL of media to the centrifuge tube bringing the total to 10 ml
16. Spin cells down at 200 X G for 5 mins. Make sure appropriate counterweight is used in centrifuge to balance machine
17. After centrifugation is complete, aspirate off supernatant.
18. Flick apart cell pellet and add 10 ml of fresh media to the centrifuge tube
19. Add the cell solution to a respective flask or well plate at the desired seeding density
20. Label flask or plate with initials, cell type/lineage, cell passage number, # of cells plated, and date

21. Change media the day after and every day thereafter until cells are confluent:  
\*5 mL for T-25, 10mL for T-75, 30 mL for T-225\*

## **Appendix B: Passaging Cells**

Adapted from Jonathan Bezenah procedure

### **Materials**

- Sterile PBS
- 0.05% Trypsin EDTA
- Trypsin Quenching media (typically DMEM + 10% FBS)
- 15 ml and/or 50 ml sterile centrifuge tube
- Culture flasks
- 70% ethanol in spray bottle

### **Procedure**

1. Warm up media and PBS and thaw trypsin and FBS in water bath
2. Prep hood by spraying with ethanol and bringing in needed supplies.
3. Aspirate off old media from culture flask
4. Rinse with equal volume of PBS to media
5. Aspirate off PBS
6. Add appropriate amount of trypsin to each flask  
\*T-25 – 2 mL, T-75 – 4 mL, T-225 – 12 mL
7. Incubate for 5 mins at 37 °C
8. Verify cells are detached from plate using microscope. If not enough cells are detached, gently tap sides of plate to detach remaining cells. If cells still seem adherent, incubate for a few more minutes
9. Once cells are detached, add quenching media to cells to neutralize trypsin such that the total volume of liquid equals amount used for culture (i.e. T75: 4ml trypsin + 6ml quench for 10 ml total)
10. Collect cells with serological pipette and add to centrifuge tube
11. Mix well and take 2 aliquots of 10ul from each cell suspension to use cell hematocytometer to do cell counts while spinning down to determine total cells recovered.
  - a. Count cells in 4 – 4x4 corners
  - b. Divide by 4
  - c. Times number by 10000, this is your cells per mL
  - d. Multiply by number of mLs used to resuspend cells
12. Spin down cells at 200 X G for 5 minutes
13. Once cells are pelleted, aspirate off supernatant
14. Flick pellet of cells to break pellet apart.
15. Resuspend cells in appropriate amount of media to achieve desired cell concentration. Ensure cells are properly resuspend by pipetting
16. Cell suspension is ready for re-plating to passage cells, to be frozen down, or to be used for vascular assays.

## **Appendix C: Freezing Cells**

Adapted from Jonathan Bezenah Protocol

### **Materials**

- Mr. Frosty
- Cell suspension to be frozen
- Cell media
- FBS
- Sterile DMSO
- Cryopreservation vials

### **Notes**

- Cryopreservation media is 70% respective media, 20% FBS, 10% DMSO
- Aliquots of FBS should not be freeze thawed more than 3x times

### **Protocol**

1. Prepare cell solution at desired concentration per the cell passaging protocol. Account for 0.7x dilution from FBS and DMSO, and determine the number of cells you want frozen per vial (typically 1 ml solution per vial)
2. Once you have determined the number of vials needed, obtain the respective number of cryopreservation vials and label them with date, initials, cell type, passage, and cell number. \* Note if cells are coming from a P2 flask label them as P3.
3. Add the appropriate amount of FBS and then DMSO such that the final solution is 70% respective cell media, 20% FBS, 10% DMSO. Flux gently to mix well, DMSO permeabilizes the cell membrane so excessive fluxing is bad for cell viability because it shears the cells
4. After adding DMSO to cells, work to aliquot out and freeze down the cells as quickly as possible because DMSO negatively affects cell viability
5. Once all vials are filled, place vials in a Mr. Frosty
6. Place Mr. Frosty in -80 °C freezer overnight
7. Within a week, move the vials from the Mr. Frosty to a box in liquid nitrogen for long term storage
8. Record the number of times the isopropanol in the Mr. Frosty has been used, replaced every 5 freezes, and top off as necessary
9. Record in lab cell log vials added to boxes in the liquid nitrogen tank

## Appendix D: Coating Cytodex microcarrier beads with HUVEC protocol

Adapted from Cyrus Ghajar protocol

### Materials:

- Cytodex microcarrier beads (Sigma C3275)
- PBS
- Scintillation vials (Fischer Sci 03-337-7)
- Endothelial cell suspension (at least 4M total cells)
- T-25 culture flasks
- Endothelial cell culture media
- Sterile 1.5 ml microcentrifuge tube

### Overview

This protocol is needed for the angiogenesis bead assay. You will also need the passaging cells protocol. See the casting fibrin hydrogels protocols to complete the assay.

### Protocol

1. Preparing dextran beads
  - a) Measure ~75 mg of powdered Cytodex dextran beads (~ 0.1 g is 200K beads)
  - b) Suspend beads in 10-15 mL of 1x – PBS in autoclavable scintillation vial
  - c) Ensure solution is well mixed then quickly, before beads begin to settle, pipette out multiple isolated 10 ul dots of bead solution onto a glass slide.
  - d) Count the number of beads per dot on the microscope to determine the bead concentration, and note on the cap
2. Autoclave beads with cap loosened to sterilize beads for cell culture use, store parafilm at 4C, good for many months.
3. Check your cell flasks on the microscope to assess whether you have enough cells to perform the assay (~80-90% confluent T75 should yield at least 4 M endothelial cells)
4. Prepare the endothelial cell suspension (per the cell passaging protocol). Resuspend at 1M cells/ml.
5. Mix beads well then pipette 10k beads (based on concentration calculated) and add to a microcentrifuge tube
6. Let beads settle by gravity
7. Aspirate off supernatant
8. Add 1 mL of endothelial media to beads
9. Repeat steps 6-8 for a total of 3 times to ensure beads are well washed
10. Add 4 M cells to a T-25 in upright position (with the neck of the flask facing up and the flask balanced on its small side, this is opposed to standard culture position in which the neck of the flask is pointing to the side and the flask is resting on its large side).  
\*at all points during coating the flask remains upright\*
11. Bring total volume in flask to 5ml by adding the 1 ml of washed bead solution (make sure to flux the bead solution well to ensure you recover all the beads)
12. Gently swish the flask side to side while holding upright for 1 minute, try not to get too many beads stuck up the side of the flask because they will not coat.
13. Place in incubator at 37 °C in upright position
14. Shake the flask again after 5 minutes and then at 20 minutes, and then every 30 minutes thereafter until 4 hours

15. After 4 hours of intermittent shaking, take beads/cell solution and add to a new T-25
16. Add 5 mL of fresh EGM-2
17. Incubate overnight in standard culture position
18. Check that beads appear well coated on the light microscope, you may also want to take a small aliquot of beads and DAPI stain to look on confocal microscope to assess bead coating. It is essential that beads are all well coated to reduce bead to bead variability in angiogenic potential. If beads do not appear well coated, increase the number of ECs added to coat the beads.
19. Transfer beads and culture media to a 15 ml centrifuge tube and allow to settle by gravity. Aspirate media
20. Resuspend beads in 1 ml of serum free DMEM, and transfer to a sterile 1.5ml microcentrifuge tube.  
\*While resuspending make sure to flux gently, shearing the beads will dislodge the endothelial cells
21. Allow beads to settle, and wash once more: aspirate and resuspend in serum free DMEM.  
\*Washing beads help remove non-adherent endothelial cells.
22. Beads are now ready angiogenesis assay. Make sure to cast gels quickly after washing, beads can start to clump if left settled for longer than 30 minutes.

## Appendix E: Casting fibrin hydrogels for vasculogenesis and/or bead assays

Adapted from Jonathan Bezenah protocol

### Materials:

- Fibrinogen (Sigma F8630)
- Thrombin (50 U/ml, Sigma T4648-1KU)
- Serum Free DMEM
- Syringes and needles (usually 10 - 20ml and 20g x 1.5")
- Millex PES membrane, 33mm diameter, 0.22 um filter
- 50 ml centrifuge tubes
- Culture media
- Appropriate cell solutions or coated Cytodex beads, resuspended in serum free DMEM.  
-often more convenient to have in 50 ml tube to make pipetting easier

### Notes:

- Hydrogels are typically 500 ul total, cast in 24-well plates, at a final concentration of 2.5 mg/ml clottable protein. If other well-plate sizes are desired, scale the hydrogel volume accordingly.
- Protocols from most previous students cast fibrin hydrogels with EGM2 and spike in FBS immediately before casting. I have found that gels cast in DMEM without any FBS added at initial casting support a similar degree of vessel formation so I simply cast my gels in DMEM
- I typically cast hydrogels with the following proportions per 500 ul gel:
  - 390 ul of fibrinogen solution (concentration accounting for % clottable and dilution)
  - 50 ul endothelial cell suspension or EC coated beads (accounting for 10x dilution)
  - 50 ul of stromal cell suspension (or media if plating stromal monolayer overlaid)
  - 10u of thrombin\*scale your total volume by number of gels to cast and include extra so you don't run out.

### Protocol

1. Prepare fibrinogen solution
  - a) Take fibrinogen out of freezer and warm up to room temperature
  - b) To determine amount of fibrinogen needed, calculate how many gels you are making, plan to make enough for 1-2 extra gels, account for dilution from cell solution and thrombin, and account for percent clottable to achieve final desired concentration of clottable fibrinogen.  
\*Percent clottable can be found on the certificate of analysis for a particular lot of fibrinogen
  - c) Measure out calculated fibrinogen and add to 50 mL centrifuge tube
  - d) In cell culture hood, add serum-free DMEM to achieve desired fibrinogen concentration
2. Place fibrinogen solution in water bath for ~5 minutes to dissolve fibrinogen, ok to vortex on medium and spin down if needed to help dissolve
3. Once fibrinogen solution has dissolved, using a needle and syringe, pull solution into syringe
4. Using a 0.22 µL filter, filter fibrinogen solution into a clean centrifuge tube

Note: filter slowly to help prevent the filter from getting clogged, you will need another filter if it gets clogged. Filters typically clog after filtering ~15ml of fibrinogen solution.

5. Prepare cell solutions and/or wash coated microcarrier beads per passaging cells protocol and/or coating Cytodex microcarrier beads protocol.
6. Add cell solutions and/or Cytodex beads and fibrinogen solution to make a master solution containing enough fibrinogen solution and cells for all the gels needed.
  - It is usually best to target 20 beads per gel if performing the angiogenesis assay.
  - Getting a consistent number of beads per gel is the difficult part. Make sure they are well mixed when adding to the master solution.
7. Label well plates for timepoints/conditions, keep in mind that each time point will require separate plates
8. Add 10  $\mu\text{L}$  of thrombin to the bottom of each for which a gel will be cast
9. Pipette 490  $\mu\text{L}$  of the fibrinogen/cell solution (using P1000) to each well.
  - \*if performing the bead assay keep in mind that beads settle quickly, to resuspend accurately I tend to tilt to just under 90 degrees then swirl every over hydrogel and pipette from the middle/bottom of the solution because off the top will have the fewest beads.
  - \*Pipette solution straight into thrombin droplet and flux once to mix, do not fully expel solution because you will trap air bubbles that are difficult to get out of your gels
  - \*work quickly to pipette all gels before solution starts to gel in the tip of your pipette.
10. Allow gels to polymerize undisturbed in the hood for 5 mins
11. Gently transfer gels to incubator for another 25 minutes at 37 °C to complete polymerization
12. Add 1 mL of media to the top of each gel after polymerization is complete
  - \*if plating a monolayer of cells over the hydrogel, seed cells at the desired concentration at this step
13. Change media on day 1 and every other day thereafter.



## Appendix F: Lyophilizing peptide and PEG aliquots

Adapted from Jeffery Beamish protocol

### Materials:

- Stock peptides to be aliquoted
- Sterile 0.5 ml and 1.5 ml microcentrifuge tubes
- Syringes and needles (typically 1 ml and 20g x 1” but other sizes are fine)
- 25 mM acetic acid
- Millex PES membrane 13mm diameter, 0.22  $\mu$ m filter
- 28g insulin syringe
- 50 ml centrifuge tubes
- Kimwipes
- Rubber bands
- Covered container for -80° freezer (typically the broken cylindrical desi-vac)
- Lyophilizer
- Parafilm

### Notes

- Aliquots and stock peptides should be stored in a desi-vac container with fresh dessicants in the -20c freezer. whenever removing peg or peptides from desi-vac container, allow desi-vac to warm to room temperature until condensation stops forming on the outside before opening to prevent getting condensation inside.
- Peptides and peg should never be lyophilized at the same time because peptides are dissolved in acidic solution that may volatize and react with vs-groups

### Protocol for peptide aliquots:

1. Plan out the needed aliquots for upcoming experiments. RGD is typically aliquoted in 1 mg per aliquot samples. Also, typically best if crosslinker aliquots are all identical to facilitate consistent hydrogel properties between batches
2. Make sure you have enough sterile 0.5 and 1.5 ml tubes to filter and aliquot in to
3. Prepare 1x 1.5 ml STERILE microcentrifuge tube per 1 ml of each type of peptide to aliquoted and 1x 0.5 ml STERILE microcentrifuge tube per peptide aliquot
4. Include in all batches at least 2 - 3x 1 mg aliquots for Ellman’s testing for each aliquot batch
5. In the culture hood: Pre-label 0.5 ml STERILE microcentrifuge tubes. Use all tubes of the same color for a particular peptide batch because it will be very helpful finding them later in the aliquot box. I write the peptide abbreviation and the mg in the aliquot on the top (e.g. “VPMS 5” for 5 mg of VPMS peptide) and on the side write the mass out fully (e.g. “5 mg”) and the date.
6. UV sterilize the outside of the tubes after labeling. Spray off a set of tweezers and set in hood as well (out of the way so they stay sterile)
7. Make fresh 25 mM acetic acid (37ul of glacial acetic acid per 25 ml Millipore water)
8. Remove stock peptide from storage (after allowing to warm to room temperature). Store stocks back a 4C immediately.
9. Weigh out appropriate amount of stock peptide, or preferably, if stock is less than 100mg just aliquot entire stock at the same time.

10. Add 25 mM acetic acid solution to the peptide to achieve 50 mg/ml (i.e 500 ul for a 25 mg stock vial). Vortex vigorously until dissolved (about 0.5-2 min). \*50 mg/ml is arbitrary but convenient for aliquoting 1-15 mg aliquots\*
11. If dissolving multiple vials of identical peptide, thoroughly exchange solution between all containers to ensure a uniform and complete dissolution for all aliquots.
12. In the culture hood:
  - Use a 1 ml syringe (or larger if needed) and a 1" needle (20-22 g) to draw up all the solution for a particular peptide.
  - Remove needle and replace with 13 mm 0.22 um filter, then filter into the sterile 1.5 ml microcentrifuge tube
  - Using sterile tips dispense the appropriate volume of the solution to each of the 0.5 ml tubes (at this stage I use the best calibrated pipettes available. It is important at this stage that you have very careful pipette technique. I ALWAYS pipette up one sample then back to the stock before dispensing into the vials to coat the inside of the tip first and I always ensure that I eject the full volume of material into each tube. IT IS ESSENTIAL THAT THIS STEP IS DONE PRECISELY! (but accuracy is less important because we can adjust for that later provided all the aliquots are exactly the same).
    - For 5 mg/tube – 100 ul
    - For 3.5 mg/tube – 70 ul
    - For 1 mg/tube – 20 ul (use 20 ul pipette)
  - Close all the lids
13. Spin all the tubes down briefly to collect all the liquid in the bottom the well. At this point be very careful with the tubes so the liquid does not splash up onto the side again. All the liquid must stay in the bottom of the tube.
14. Move the tubes to the main lab area. Wipe off the top of each tube with an alcohol wipe. Ignite a Bunsen burner. Heat the needle of a 28 g insulin needle red hot then quickly puncture a small hole in each of the 0.5 ml tubes containing the aliquots. You will need to reheat the needle between every tube. This hole will allow the sample to be lyophilized but will keep the contents relatively clean/sterile.
15. Back in the hood:
  - Use the sterile tweezers to place all the tubes in 50 ml falcon tubes as carefully as possible to prevent the aliquot from splashing onto the sides of the microcentrifuge tubes. If packed well, you can place 12x 0.5 ul tubes per 50 ml tube
  - Cover the top of the tubes with a chemwipe folded over on itself so there are 8 plys
  - Secure with rubber band.
16. Move all the covered 50 ml tubes to a covered container (typically the broken desi-vac) and place at -80C for at least 6 hr (or overnight). **The maximum number of 50 ml tubes that can be done per vacuum flask at a time is 4. Generally best to lyophilize at most 2 flasks at a time (i.e. 8x 50ml tubes, for a total of 96 individual aliquots)**  
**\*Do not seal the broken desi-vac by vacuum because the release is faulty and it will be very difficult to open- I use this mainly as a container with a lid.**
17. Remove the labels from the peptide vials and stick on a white paper with any notes. Take a photo for records.

## 18. PAUSE POINT

19. The next day prep the lyophilizer per instructions on it (or see protocol below) so it is ready to accept samples
20. Retrieve the lyophilizer flask (BE CAREFUL THESE ARE VERY EXPENSIVE DESPITE THEIR SIMPLE APPEARANCE!) and the rubber cover and prepare for quick transfer from freezer to flask.
21. Very quickly: remove the tubes from -80 C, place in the lyophilization flask, cover with rubber cover, place on lyophilizer and turn to vacuum. Maximum time to do this is about 30 s.
22. Cover flask with foil to protect peptides from light.
23. Lyophilize for at least 24 hr and ideally 48 hr, ok up to 72 hr.
24. Place a sign on the lyophilizer that **no other samples should be added while the peptides are on the machine.** They are very sensitive to melting if the lyophilizer fails and will be ruined.

## 25. PAUSE POINT

### 26. After LYOPHILIZATION:

- Get the aliquot storage box out at least 30 min prior to removing samples from lyophilizer so it will be ready to add samples to.
  - Prepare ~1 cm wide strips of parafilm
  - Remove samples from lyophilizer
  - **Quickly move to culture hood.** In hood cover each vial with parafilm. I start by covering the top (and the hole), then go around the edge of the tube then back across the top in a figure 8. Make sure hole on the top and the sides of the tube are well sealed.
  - Place aliquots in the aliquot storage Desi-vac box
  - Take a picture of the current set of aliquotes
  - Re-evacuate Desi-vac box and return to -20C freezer for storage
27. Make a note file (see example below) for this aliquot batch which contains the details of the peptide, the number and amounts of aliquots, the photo of where the aliquots were placed
  28. Update the peptide aliquot log

### **Protocol for PEG aliquots**

**\*IT IS ESSENTIAL THAT PEPTIDES AND PEG ARE NOT LYOPHILIZED AT THE SAME TIME\***

### **The procedure is essentially the same as peptide lyophilization EXCEPT:**

- 1) Dissolve the PEG in pure water at 60 mg/ml, PEG takes more time to dissolve before filtering than peptide (this concentration is arbitrary but convenient for 10 - 60 mg aliquots)
- 2) protect from light as much as possible at all steps
- 3) place aliquots in 1.5 ml (not 0.5 ml) tubes
- 4) it is even more essential that you move very quickly to move samples from -80C to lyophilizer (15 s max! PEG will melt very quickly)
- 5) samples need to be lyophilized for at least 48h, **covered with aluminum foil to protect from light**

## **Appendix G: SOP for operation of Lyophilizer (Thermo Micro Modulyo)**

Adapted from Rahul Singh protocol

### **Materials:**

- Vacuum flask with cover
- Tinfoil if samples need to be protected from light
- Samples in a container that allows them to be stood upright and exposed to vacuum

### **Notes:**

- DO NOT attach cracked or damaged glassware to this unit
- DO NOT dry organics, acids, bases or volatile compounds! Only use this unit to remove water
- DO NOT operate this unit continuously, it is designed to run for 2-3 days before the cooling coil needs to thaw and the pump needs to cool
- DO NOT operate this unit without a load. This includes 'idling' the unit without any samples (though a couple hours is ok to let it cool before loading samples).
- DO NOT allow this unit to draw air for more than a few seconds. Atmospheric water will readily clog the Micro Modulyo and overwhelm the pump.
- DO NOT use this unit to dry more than 200 ml of water. The efficiency of drying drastically decreases as the unit fills with ice and more than 200 ml will clog the ports

### **Protocol for preparing the Micro Modulyo**

1. Check that the vacuum pump has an appropriate amount of oil, refill if necessary.
2. Turn the drain valve fully counter clockwise to open the valve and to remove any water left at the bottom of the condenser chamber. If you are comfortable doing so, you can tip the chamber to help pour out remaining liquid. Dry the condenser chamber with a kimwipe and/or airhose
3. Make sure that the Micro Modulyo is clean, and that the accessory flange is clear of debris. The accessory flange should have a thin layer of vacuum grease.  
\* If grease is dirt or missing, DO NOT operate the Micro Modulyo. In this case thoroughly clean the flange by wiping with a dry kimwipe and then reapply a thin, uniform layer of vacuum grease. You can use a gloved hand to spread it evenly.
4. In stall the baffle tube by placing it inside the manifold stem (the extra tinfoil and taped end of the baffle goes inside the 8-port manifold stem, the extra padding was added so it would fit more snugly). The baffle should extend into the Micro Modulyo and the cutouts should face towards the drain.  
\* The baffle helps distribute water vapor and prevents ice from clogging the drain
5. Place the 8-port manifold on top of the condensing chamber. Carefully seat the manifold so that it is centered and the rubber sealing ring is uniform around the base. No mechanical fastening is required. DO NOT pound, twist, or shake the manifold to attach.  
\* The sealing ring should have a thin layer of vacuum grease on both sides of it. If the ring appears to be dry, cracked, or damages, DO NOT operate the Micro Modulyo before replacing the ring.

### **Protocol for turning on the Micro Modulyo**

6. All ports on the manifold should be turned to 'Vent' and no vacuum flasks should be attached.

7. Close the drain valve snugly by turning it clockwise.
8. Turn 'ON' the switch on the face of the Micro Modulyo, a soft humming noise indicates that the unit is cooling to -50°C. Once the unit has cooled, a green light will turn on indicating it is ready for use. This usually takes ~15 minutes.
9. Turn the high-vacuum pump on. It may initially make a soft gurgling noise that becomes lower to a buzz within a minute. If the Pump continues to gurgle, there is a leak and air is entering the pump. Switch off the pump and check for leaks:
  - \* Ensure the drain valve is closed
  - \* Ensure the manifold ports are all turned to 'Vent'
  - \* Ensure that the rubber sealing ring is not damaged
  - \* Ensure that the high-vacuum tubing is not loose or damaged
  - \* Ensure that all fittings are snug and lightly greased
10. Check to make sure the green light is still on. If not wait for the unit to cool back down.
11. Place your sample in a vacuum flask and attach it to a steel port on the manifold.
12. Slowly and carefully turn the associated port from 'Vent' to 'Vac'. A soft hissing can be heard as air is evacuated from the flask.
  - \* Wait 5 minutes between attaching additional flasks. Make sure the green light is still on before loading each flask. This prevents overheating and prevents overloading the high vacuum flask
13. Dry the samples for as long as needed (typically 1-2 days)

#### **Protocol for shutting down the Micro Modulyo**

14. Recover the vacuum flask by slowly and carefully turning the manifold valve from 'Vac' to 'Vent'; air can be heard entering the flask. Wait ~20 seconds to ensure the flask is re-pressurized.
15. Carefully detach the flask from the steel manifold stem, some twisting may be necessary.
16. Re-pressurize the Micro Modulyo by slowly turning the drain valve counter clockwise to open it. Air will be heard entering the unit and the pump may start to gurgle. Once the valve is fully open, immediately SHUT OFF THE PUMP.
  - \* High vacuum pumps will readily overheat if air is drawn through them for too long
  - \* Conversely, the high vacuum pump can also be damaged if the Micro Modulyo is not re-pressurized before shutting off because air will flow backwards through the system.
17. Turn 'OFF' the Micro Modulyo using the switch on the condensing chamber
18. Gently detach the 8-port manifold and place it upside-down on the table (the rubber gasket should face the ceiling). Remove the baffle and place on the table.
19. Open the drain valve and place a bucket underneath to collect water from melting ice.
20. After the ice has melted (next day) spritz down the cooling chamber with DI water to rinse then use kim wipes/air hose and air dry.

## Appendix H: Ellman's test Protocol

Adapted from Jeffery Beamish protocol

### Materials:

- Phosphate buffer: 0.1 M sodium phosphate with 1 mM EDTA, titrated to pH 8.0
- Ellman's Reagent: (5,5'-Dithio-Bis(2-Nitrobenzoic acid), DTNB, MW 396.3)
- Recently dissolved peptide solution
- 1.5 ml microcentrifuge tubes
- 15 ml centrifuge tubes
- Spectrophotometer
- Lyophilized 1 mg cysteine aliquots (L-Cysteine hydrochloride monohydrate)

### Overview

Ellman's reagent is a highly reactive disulfide compound. When Ellman's reagent is added to a sample that contains thiol, the disulfide bonds are rapidly cleaved by free thiol groups to yield a cleavage product. The cleavage product absorbs light at 412 nm and thus can be used to quantify free thiol groups because the stoichiometric ratio between the cleavage product and the thiol group is 1:1.

### Notes

- The extinction coefficient for the Ellman's reagent cleavage product at 412 nm in the phosphate buffer is  $14.15 \text{ mM}^{-1}\text{cm}^{-1}$

**Predicted absorbance** = [Thiol] (mM) \* Dilution \* 1 cm \*  $14.15 \text{ mM}^{-1}\text{cm}^{-1}$

**Purity (mg active/ mg gross)** = measured absorbance/ predicted absorbance

- Dilutions were empirically chosen to achieve an absorbance of ~0.5-1.5, which is the range over which the spectrophotometer is most accurate. This corresponds to a final thiol concentration of 0.035 – 0.106 mM. In the example of the 48mM cysteine standard the dilution of 5ul/310ul and then sub dilution of 100ul/1000ul results in a final thiol concentration of 0.0704 mM corresponding to an absorbance of 1
- The Ellman's test is typically very reproducible and has a good linear response, as a such a linear curve is generally not needed for every test. However, generating a linear curve and extracting the extinction coefficient is generally good practice well familiarizing oneself with this assay
- Thiol groups of peptides oxidize quickly after dissolved, best if the ellman's test is performed within 5 minutes of dissolving the peptide for best results, so prepare everything before dissolving peptide aliquots to be tested.
- The Ellman's test is essential for initial characterization of new batches of peptide aliquots, and important for determining active RGD concentrations for consistent conjugation between batched of aliquots, but the empirical rheological characterization when titrating the crosslinker to test crosslinking depending on the ratio of SH/VS groups

is the much more important characterization for determining how a peptide crosslinker aliquot will behave.

- When testing a new peptide, and you don't know the appropriate dilution just assume it is 100% pure and target 48mM thiol concentration (i.e. 24 mM peptide concentration for dithiol peptides)

### **Procedure**

1. Prepare large stock of identical 1 mg cysteine aliquots per the peptide lyophilization protocol. \*store stock cysteine at room temp under argon to prevent oxidation over time\*
2. Retrieve a cysteine aliquot from desi-vac box prior to starting protocol and leave in 4C fridge until ready to resuspend
3. Prepare Ellman's reagent stock (4mg/ml)
  - a) retrieve 1.5 ml tube and Ellman's reagent
  - b) pre-tare the 1.5 ml tube
  - c) use the antistatic gun on the tube and on the Ellman's reagent
  - d) carefully weigh out 10-15 mg of Ellman's reagent (Ellman's reagent sticks to the spatula and makes a mess) and record mass
  - e) in a 15 ml tube add the appropriate volume of phosphate buffer to dilute the Ellman's reagent to 4 mg/ml solution
  - f) use a 1 ml pipette to carefully transfer 1 ml of phosphate buffer from the 15 ml tube to the weighed out Ellman's reagent, vortex to resuspend. The Ellman's reagent will not fully resuspend at this point.
  - g) transfer the suspension back to the 15 ml tube, flush to rinse reagent out of the pipette tip, then using the same tip to repeat steps f and g until all of the Ellman's reagent is dissolved in the dilution
  - h) vortex the falcon tube
  - i) wrap tube in tin foil to protect from light, this Ellman's stock is good for at least 2 weeks if stored at 4C.
4. Prepare Ellman's working reagent by pipetting 200 ul of Ellman's stock into 10 ml of phosphate buffer. You will need 1 ml of working reagent for a blank, for each sample, for each standard you are testing, and a little extra to make sure you don't run out.
5. Add 1 ml of working reagent to disposable cuvettes (one for each blank, sample, standard, to be tested) in an empty cuvette box so that it can be covered and protected from light. Take note of which cuvette will be for each sample.
6. Label microcentrifuge tubes as receptacles for primary dilution, and add 305 ul of phosphate buffer to each tube
7. Dissolve cysteine stock in phosphate buffer to achieve 48mM solution as the standard
8. Dissolve peptide aliquots to be tested in phosphate buffer
  - \* ok if dissolved in HEPES buffer from making gels, will not affect absorbance because it gets diluted, but keep in mind if you do the Ellman's test a while after dissolving the peptides you will get a lower purity than expected.
9. To make primary dilutions add 5 ul of each sample to the labeled microcentrifuge tubes containing 305ul of phosphate buffer (not necessary for blank).

10. Vortex to mix well
11. Immediately transfer 100ul of primary dilution to the appropriate cuvette containing the pre-aliquoted 1000ul of working reagent and flux well to mix, the blank will be 100ul of phosphate buffer transferred to 1000ul of working reagent.
12. Keep samples covered to protect from light and wait at least 1-2 minutes to read samples to allow reaction to come to completion, but no longer than 15 minutes.
13. Turn on the spectrophotometer and make sure the wavelength of light is set to 412 nm
14. Place the blank sample in the spectrophotometer (the arrow on the cuvette should be pointed to the left or right when the cuvette is in place) and press the “cal” button to calibrate
15. Place each of the samples in the spectrophotometer and determine the absorbance (it is typical for there to be some drift in the measurement, I typically watch the value drift for ~15 seconds and take the highest value, if it keeps going up you probably didn't mix quite well enough, just wait for it to plateau.



## Appendix I: Casting PEG hydrogels: Adapted from Jeffery Beamish protocol

### Materials:

- Sterile filtered 100 mM HEPES Buffer (MW 238.3 ; 23.83 g/L) titrated to pH 8.4 with 10N NaOH
- Sterile gloves (either self-autoclaved or purchased)
- Autoclaved razor/scraper assembly in pouch with pipette tip box with aluminum foil tent cover to cut syringes in:



- Autoclaved spatulas
- Autoclaved tweezers
- RGD aliquot (s)
- PEG aliquot (s)
- Crosslinker aliquot (s)
- Sterile BD slip tip 1ml syringes (Cat. No. 14-823-434) for 50 ul hydrogel pucks
- Labeled 50 ml centrifuge tubes
- Sterile 1.5 ml microcentrifuge tubes
- Cell passaging materials if casting cellular hydrogels (0.05% Trypsin EDTA, PBS, DMEM+ 10% FBS or other quenching buffer)
- Very well calibrated micro-pipettes!

### Notes:

- This protocol is for the formation of PEG-hydrogels via a Michael-type addition reaction between cysteines on peptides and vinyl-sulfone groups on 4-arm PEG molecules. The general idea is to first conjugate RGD to PEG to functionalize the hydrogels for cellular adhesion. The hydrogels are then crosslinked with a proteolytically labile dithiol containing peptide to form a hydrogel. In principal there should be a 1:1 ratio of total SH to VS groups. As such, in theory, the concentration (in mM) of [crosslinker] =  $(4*[PEG]-[RGD])/2$ . In practice, however, the ratio of crosslinker SH to free VS after RGD conjugation is typically slightly less than 1 (~0.8-0.9) to yield maximum mechanical properties.
- See the excel work book “Example PEG Recipe book, ellman's, stoich comparison” to help with calculations and for a guide to casting gels for stoichiometric characterization
- It is very important that you have accurately calibrated pipettes. This is especially important for volumes < 20 ul where the error to pipetting can be quite large and results in significant changes in gel properties. I generally check the pipette calibration myself and include a correction in my calculations if it's off by more than 2%.

- Many of the suggestions in this protocol are intended for the purpose of forming hydrogels with very consistent mechanical properties between batches of aliquots and between sets, initial mechanical properties have a strong effect on cellular behavior, so it is important that they are well controlled and documented. These tips are also important if you are trying to form very soft hydrogels ~50pa, because small variations in the SH/VS ratio due to pipetting errors may result in failed gelation.

## **Protocol**

1. Cutting the syringes (best to do day before for convenience)
  - a) Prepare 50 ml tubes for the syringes by labeling for each condition (you can fit up to 3 syringes per 50 ml tube). Spray with ethanol then place in hood. After ethanol dries, remove all caps and place face up in the hood out of the way.
  - b) Place a sterile drape in the hood. Sterile fashion, drop the pipette tip box cover and the scraper/razor on the drape. Open and then drop the number of needed syringes out of their wrapping on to the drape in sterile fashion.
  - c) Don the sterile gloves (don't touch anything at this point that is not on the drape). You can put the gloves on outside of the hood as long as you don't touch anything.
  - d) Each gel will need a 1 cc syringe. Pull back each syringe to the ~0.2 cc mark then cut at the 0.1 cc below this. We use a razor blade in a scraper type hold to do this using an old pipette box cover as a cutting board with aluminum foil tented on one side to help catch the pipette tips as they fly off with cutting.
  - e) Group the syringes as appropriate then drop them (the entire group at the same time) into the 50 ml tubes.
  - f) UV with the lids open for at least an hour, ok to leave over night.
  - g) Recap and can be left outside the hood until needed
2. Retrieve needed aliquots from Desi-Vac making sure to let Desi-Vac warm to room temperature before opening, leave aliquots in the fridge or on ice protected from light until needed
3. If forming cellular hydrogels, get trypsin, PBS, and quenching media warming
4. Retrieve bucket of crushed ice and place microcentrifuge tube holder in it
5. Reconstitute PEG
  - a) determine the concentration of PEG desired (on excel sheet initially reconstituted at 60 mg/ml but if high concentration PEG gels are needed, will need to be higher)
  - b) protect from light as much as possible while reconstituting
  - c) Add the appropriate amount of HEPES to the PEG aliquot
  - d) Vortex vigorously for 1-2 minutes until fully dissolved
  - e) briefly spin at high speed to collect at the bottom of the tube
6. Reconstitute RGD in HEPES to achieve appropriate concentration
7. Add the appropriate amount of RGD to the PEG aliquot
 

\* I usually conjugate the entire aliquot of PEG if all gels that I will be forming have the same [PEG-VS]. If you are doing multiple formulations with different [PEG-VS], each concentration will need to be conjugated separately. When varying the stoichiometric ratio, keep in mind that the [PEG-VS] is constant, it is the [peptide] that is titrated.

8. Allow RGD to conjugate to PEG for 30 minutes at room temperature protected from light. If you need longer than 30 minutes, place in fridge or on ice until you are ready to cast gels, do not wait longer than ~1.5 hours.
9. While RGD is conjugating, if you are making cellular hydrogels, use this time to dissociate cells from culture flasks.
  - a) Rinse cells with PBS, trypsinize, quench, centrifuge, then resuspend at the final desired concentrations.
  - b) aliquot cell suspensions into sterile 1.5 ml microcentrifuge tubes for each condition (i.e. if you are forming 10 identical gels with 5M/ml ECs and 5M/ml DF seeding densities you would need 520ul of hydrogel precursor solution, then add 520ul of 5M/ml EC solution and 520ul of 5M/ml DF solution to the microcentrifuge tube)
  - c) it is best to do all of your cell suspension aliquots at the same time so that it is more accurate (i.e. if you are doing 2 peptides and 2 stromal cell types for 4 conditions, make sure your cell suspensions are well mixed then quickly aliquot them out into the 4 microcentrifuge tubes, one for each condition.
  - d) If very precise mechanical properties are required for your experiment, resuspend your cells in HEPES. If doing this, working quickly is very important to minimize time cells are in HEPES which can negatively affect viability if cells are left in it too long.
  - e) pellet each cell suspension aliquot right before casting gels at 300x g for 5 minutes using the microcentrifuge, if cells are left in pellets too long before casting hydrogels they may get clumpy and not resuspend homogenously.
  - f) very carefully aspirate pellet, use a 200ul non-filter tip on the glass pipette to minimize the aperture for aspirating. Aspirate as much media/HEPES as possible without disrupting pellet, then flick pellet to loosen.
10. For casting gels it is convenient to have 2 P200s: one for pipetting peptide and PEG solutions, and the other just set at 50ul for casting the gels.
11. Once PEG is conjugated and cells are pelleted, spray down centrifuge tubes containing syringes, bring into the hood and loosen caps to be ready to cast gels in.
12. Reconstitute the crosslinking peptide at the appropriate concentration then quickly add the appropriate amount of solution to the cell pellet.
  - \* The most important part of forming consistent gels between sets is to cast the gels very quickly after reconstituting the crosslinking peptide.
  - \*add the peptide to the side of the tube containing the pellets, expelling slowly and completely to ensure all solution but do not flux, fluxing can suck up cell pellet that gets stuck on the inside of the pipette tip
  - \*if doing multiple sets of gels from the same aliquot of peptide, parafilm the peptide and keep on ice until ready to cast next set to minimize oxidation
13. Vortex the pellet with the crosslinking solution on medium low, at just high enough of a setting that the pellet mixes but that the solution stays at the bottom at the centrifuge tube. If you lose solution up the side of the tube you can quickly spin it back down
14. Add the PEG-RGD solution to the cell suspension in crosslinking peptide solution.
  - \*PEG is highly viscous so it is important to pay close attention so that you expel it all precisely. Fully expel the PEG, then go back to the stopper position to let the PEG collect again at the end of the tip, then fully expel again directly into the cell suspension

\*at this point it is ok to quickly but gently flux 4-5 times to mix the solution instead of vortexing because if precursor gets stuck on the inside of the tip it is ok because it is not affecting the final ratios

15. Quickly switch to the 200P pipette preset to 50ul and transfer 50 ul of mixture in to the syringes in the 50 ml tubes. DO NOT depress the pipette plunger beyond the first stop as this will make bubbles.
  - \* press the pipette tip gently against the syringe stopper while expelling to make sure that you are filling the syringe from the bottom up, this helps avoid air bubbles getting trapped under the gel
16. After pipetting all gels in the set, check all the gels to make sure there are no trapped air bubbles. If there are bubbles, gently try to remove them with your pipette tip
17. Tightly cap the 50 ul tubes and move to the incubator for 60 min
18. Note the time you started for each set of gels
19. Punch the gels out directly into media. When punching out gels, they will tend to stick to the end of the plunger. They can be removed with a sterile spatula (typical lab type) but it is CRITICAL that you wet the spatula with media before trying to remove the gels or they will stick to the spatula and get destroyed (especially if the gels are very soft).
20. When changing media, take the top off and place face down in the culture hood, prop up one side of the well plate on the well top so that it is on a slant. Use a sterile spatula to hold the gel to side when aspirating off the media.
  - \*be very careful it is easy to accidently suck up you hydrogel\*

## **Appendix J: PEG and fibrin hydrogel fixing and standard fluorescent staining**

Adapted from Jonathan Bezenah protocol

### **Materials:**

- Cellular hydrogels
- Phosphate buffered saline solution (PBS)
- Z-fix (Anatech)
- Ulex Europaeus Agglutinin I (UEA-I), Rhodamine (Vector labs)
- 4',6-diamidino-2-phenylindole (DAPI, 500 ug/ml stock solution)
- Alexa Fluor 488 phalloidin (Invitrogen)

### **Overview:**

This protocol is for fixing hydrogels and staining with standard non-immunofluorescent stain. UEA is commonly used for identifying endothelial cells, DAPI stains all cell nuclei, and phalloidin stains filamental actin in all cell bodies. Phalloidin is useful for identifying cell bodies and tends to stain stromal cells more strongly than endothelial cells. Additional step are required for antibody staining, and are detailed in the immunofluorescent staining protocol. Red phalloidin and green UEA are also available but not typically used.

### **Fixation Protocol:**

1. Aspirate off culture media in cell culture hood
2. Add PBS to all wells (~2 ml per well, washes better with more)
3. Allow to rinse for 3-5 minutes at RT to wash
4. Aspirate off PBS using vacuum pump
5. Repeat wash 2x more
6. Add 1 ml Z-fix to each well in fume hood, make sure PEG hydrogels are fully submerged.
7. Let fix for 30-45 mins at room temp in hood.
8. Remove z-fix with and dispose of in appropriate waste container  
\*I typically tape a 1 ml pipette tip onto the end of a 25 ml serological pipette to remove z-fix to easily do many wells
9. Add at least 1 ml PBS to each well, more is better for more thorough washing
10. Allow to rinse for 3-5 minutes at RT
11. Remove PBS with serological pipette and dispose of in z-fix waste container for the first 2 washes
12. Repeat washes for a total of 4 washes, the 3<sup>rd</sup> and 4<sup>th</sup> washes can be aspirated with the vacuum pump in the common lab space
13. Gels are ready for storage, staining, or immunofluorescent staining.  
\*If storing, wrap with parafilm around the edges and store in the 4C fridge. Samples can be stored up to ~ 1 month before staining without noticeable detriment.

### **Standard staining procedure for UEA, DAPI, and phalloidin**

1. PEG hydrogels should be cut in half using a razor blade to accurately cut the gel in half;. Fill a petri dish with enough PBS that it barely covers the bottom of the dish. Put a single PEG hydrogel into the dish with one its flat sides down, push down with a razor blade precisely bisecting the gel and then use a scalpel while holding the razorblade down to

- finish bisecting the gel cleanly. PEG hydrogels can be further cut into quarters if needed for multiple different stains on the same gel, but halves are easier to orient for imaging
2. Prepare solution with desired stains, UEA and phalloidin are best at 100x dilutions, and DAPI at 500x dilution.
  3. Make sure all remaining PBS is removed from hydrogel wells.
  4. Add staining solution to hydrogels. For a 500 ul fibrin hydrogel I will typically stain with 750ul of solution, both halves of a PEG hydrogel can be stained in a 24-well plate with 600 ul of solution. A single half of PEG hydrogel can be stained in a 48-well plate in 400ul of solution. \*Make sure PEG hydrogels are fully submerged\*
  5. Cover well plates in foil to protect from light, samples should always be protected from light from here on to reduce photo-bleaching
  6. For best signal to noise, I typically stain over night in the 4C fridge, but 4 hours is sufficient.
  7. After staining, wash 4x with fresh PBS
  8. For best signal to noise I usually allow another rinse over night, and then another wash the next day.
  9. Samples are ready for imaging.
  10. Samples should be imaged within 2 weeks for best results.

## Appendix K: Immuno-fluorescent staining of hydrogels

### Materials:

- 10x Tris buffered Saline (TBS): 44 g NaCl, 15.75 g Tris (base), 500 ml of ddH<sub>2</sub>O, adjust pH to 7.4
- TBS-TritonX: 50 mL of 10x TBS, 2.5 ml of TritonX-100, add ddH<sub>2</sub>O to 500ml final volume, adjust pH to 7.6
- TBS-Tween20: 50 mL of 10x TBS, 0.5 ml of Tween-20, add ddH<sub>2</sub>O to 500ml final volume, adjust pH to 7.6
- Antibody dilution buffer (Abdil): 2% (2g/100mL) of bovine serum albumin (BSA) in TBS-Tween solution
- Appropriate primary and secondary antibodies
- Fixed hydrogel samples

### Notes:

- Before starting procedure, check the online data sheets for your primary and secondary antibodies by checking their catalog numbers. Take note of their species specific reactivity, host/reactivity, suggested secondary antibody, and recommended dilution. \*If samples are recommended to be stored at -20C, it is best to aliquot into microcentrifuge tubes to avoid multiple freeze thaws. I tended to aliquot 5-10 µl of antibody stock per tube
- Some procedures recommend performing all steps with TBS-TritonX100, however, TritonX is a very strong detergent and I found that prolonged periods of time in TBS-TritonX100 solutions caused gel degradation, hence the use of TBS-Tween20 for most steps: Tween20 is a milder detergent.
- Although most immuno-fluorescent staining procedures for cells in 2D culture only require ~1 hour per staining/washing steps, the large size of antibodies restricts diffusion into hydrogels, as such, all steps are performed overnight to allow complete diffusion in/out of hydrogels for optimal staining.
- Unlike DAPI, UEA, or Phalloidin staining, which are good for many weeks, antibody staining tends to fade in under a week, make sure your schedule is permissive for imaging right after staining for best results.

### Protocol:

1. Make 10x TBS solution: See components above. This solution generally does not need to be sterile filtered and is ok to store at room temp for multiple months. If significant precipitate starts to form and does not re-dissolve with mixing, then remake this stock solution.
2. Make TBS-TritonX100 solution (permeabilization buffer). See components above. This solution is 0.5% TritonX100 in TBS.
  - a) Pipette 50 ml of 10x TBS into a 1L graduated lab bottle.
  - b) Add ~200 ml of ddH<sub>2</sub>O to the 10xTBS to start dilution.
  - c) Put in a clean stir bar and start stirring on medium-low speed.  
\*TritonX100 is very viscous and difficult to pipette\*
  - d) Use a 5 ml serological pipette to slowly draw up 2.5ml of TritonX100, only put the tip of the pipette in to avoid coating the outside of the pipette with too much TritonX100. e) Expel the TritonX100 into the partially diluted TBS under constant stirring. Try to avoid expelling air, because it will create excessive bubbles.

- f) Wait for TritonX100 to recollect at the pipette tip then expel again
  - g) Repeat step (f) until significant TritonX100 stops collecting in pipette tip.
  - h) slowly draw up 5-6 ml TBS solution into the pipette tip to rinse pipette and then expel into the solution. Repeat this step multiple times until there is no longer TritonX100 visibly coating the inside of the pipette tip. Again, try to avoid expelling air to prevent excessive bubble formation.
  - i) Make up to full 500ml with ddH<sub>2</sub>O
  - j) Sterile filter this solution into an autoclaved bottle for long term storage. The solution does not necessarily need to be used/stored with proper sterile technique, but it is important to store it cleanly and use 'pseudo-sterile' technique with it for it to last multiple months. TBS-TritonX100, and TBS-Tween solutions are permissive for microbial growth, so if solutions become cloudy make a fresh stock.
3. Make TBS-Tween20 solution (rinse buffer) following an analogous procedure as outlined above for TBS-TritonX100.
  4. Make enough Abdil solution as needed for the day. It is best to make Abdil solution fresh as needed. (1 ml per well for blocking in 48-well plates, 2 ml per well for blocking in 24-well plates)
  5. Permeabilize your samples if needed, by incubating gel in TBS-TritonX100 solution at room temp for 1 hour.
    - \*Samples need to be permeabilized to stain for intracellular proteins.
    - \* Use 1 ml for 24-well plate, 0.5 ml for 48 well plate. Make sure free-floating PEG hydrogels are fully submerged.
  6. Rinse samples 4 times with TBS-Tween20 solution, waiting 3-5 minutes between rinses.
  7. Block samples overnight in Abdil solution
  8. Aspirate off Abdil solution.
    - \*For PEG hydrogels I tend to hold gels out of the well with a micro lab spoon while aspirating
  9. Stain with primary antibody overnight in Abdil solution at recommended dilution.
  10. Rinse 3x with TBS-T, 5 minutes each, then rinse overnight.
  11. The following day rinse 1x with TBS-T for 5 minutes
  12. Stain with appropriate secondary antibody at recommended dilution overnight
    - \*Make sure to choose your secondary antibody to match the host/isotype of the primary, and that the fluorophore is the appropriate wavelength, so it doesn't overlap with any intended counter stains (i.e. DAPI, UEA, Phalloidin)
    - \* Protect from light as much as possible moving forward
  13. Aspirate off secondary antibody solution.
  14. If counter staining, no rinses are necessary. Follow standard staining procedure for DAPI, UEA, and/or phalloidin for an overnight stain.
    - \*Make sure there are no fluorophores with overlapping wavelengths\*
  15. Rinse 4x with TBS-T.
  16. Rinse overnight with TBS-T
  17. Samples can be stored in either TBS-T or PBS at 4C
  18. Image samples as soon as possible.
  19. If you are making qualitative comparisons between samples, make sure to image them on the same day with the same imaging settings to avoid signal deterioration.



## Appendix L: Epifluorescent and confocal microscopy protocols

Adapted from Jonathan Bezenah protocols

### General Microscope Set-Up

1. Turn on the microscope computer
2. Login to PutnamOlympus. Password: rhoa
3. Take the cover off the microscope
4. Turn on microscope (Olympus 1x2), mercury lamp, camera controller (Hamamatsu), and slide controller (Prior)
5. Record mercury lamp “ON” hr on data sheet next to microscope
6. Open Metamorph premier on computer
7. Once open, on top tool bar, go to “ACQUIRE”. On the drop down menu, click “ACQUIRE”  
\*This opens a window which controls exposure, binning, gamma, and scaling
8. In the acquire dialogue box, the buttons do the following:
  - a) ACQUIRE – takes a picture of current field of view
  - b) SAVE IMAGE – takes a picture of the current field of view and saves to a specified location
  - c) SET SAVE – specify location to which save image button will save
  - d) SAVE W/ SEQUENCE – automatically increment next image save file after you take an image using the save image button
  - e) AUTO EXPOSE- determines optimal exposure for sample you are imaging (DO NOT USE)
  - f) IMAGE GAMMA- increase or decreases the gamma
  - g) IMAGE SCALING – set which band of light the camera will display (this can be changed after imaging if needed)
  - h) AUTO SCALING – automatically sets the best exposure limits (max and min) for image
9. Click the show live button. This will open up a new window showing you your sample live
10. The buttons on the left screen do the following:
  - a) BINOCULARS – look through the microscope eye piece
  - b) CAMERA – will look through the standard microscope camera
  - c) CIRCLE/DOT – will use the disc spinning unit
  - d) RED - for mCherry/Red filter (580  $\mu\text{m}$ )
  - e) GREEN – is for GFP/Green filter (480-560  $\mu\text{m}$ )
  - f) BLUE – is for DAPI/blue filter (405-420  $\mu\text{m}$ )
  - g) GREY – brightfield (standard lamp)
11. Set filter to desired filter and camera

## **Epifluorescent (AKA widefield) and brightfield imaging:**

### **Notes:**

- Epifluorescent imaging is a mode of fluorescent imaging where the sample is illuminated with unfocused light. This mode requires shorter exposure times than confocal imaging but yields poorer signal to noise. Illumination and imaging are both from below the sample
- Brightfield imaging is the simplest form of microscopy: The sample is illuminated from above with bright light and imaged from below. Contrast in the image is caused by differences in sample density and/or features that scatter the light.
  - Typical Exposure times for 4x imaging:  
10-20 for brightfield  
100-200 for DAPI/BLUE  
200-300 for mCHERRY/RED  
300-400 for GFP/GREEN
- On the show live screen window, on the left side there are 5 buttons. Look at the button that looks like a balance
  - The number next to the balance icon should say 12 to get best images
  - If it doesn't, increase exposure time
  - On acquire window, look at black box with green bars, this is a histogram of the image exposure, the best images will have histogram bars peaking near the middle (Adjust exposure to do so)
- All conditions within an experimental replicate should be imaged with the same exposure parameters for consistent quantification, but it is ok to change exposure settings between replicates if needed
- Epifluorescent and brightfield imaging are best for single plane images rather than z-stacks and maximum intensity projections
- I quantified the bead assay with single plane epifluorescent images, the sprouting from the beads tend to be in a single plane along the bottom of the dish so confocal imaging is not necessary, however, confocal imaging will always provide more accurate images and potential 3D reconstructions. However, confocal imaging takes at least 20 times longer because of the longer exposure times and multiple planes per image .

### **Protocol:**

1. Move stage using stage controller to desired location of sample (Press "live" in acquisition window to view streaming video)
2. Focus using the microscope dials to get the image in focus and obtain the best focal plane for analysis.
3. Check that your exposure parameters for your channels of interest are appropriate per the notes above.
4. Press "Save Image" to save your live image. Label image with all appropriate details, I usually include: Label for experiment, condition, gel #, bead #, channel color

5. For the bead assay I manually raster through the gel, keeping track of beads and imaging all beads that meet the inclusion criteria. For late time points in which networks are very extensive, the Scan Slide application may be necessary to stitch multiple images together to capture all sprouts from a single bead (see separate Scan Slide protocol below).  
\* See Jonathan Bezenah's protocol for "Multi-dimensional Acquisition" if you wish to keep track of the positions for each beads location
6. Before moving the stage, take images in all channels of interest. To adjust for the chromatic offset between different channels you may choose to adjust the Z-position a few microns to bring different channels into their sharpest focus.
7. It is usually best to image all conditions on the same day to account for differences in washing. This is especially important if you decide to image the day after staining because the signal to noise continues to improve for ~ 2 days with additional de-staining time.
8. Once complete, turn off all microscope components  
\*NOTE: Mercury lamp needs to be on for 1 hr after turning it on before turning off again. IF it hasn't been 1 hr wait to turn lamp until 1 hr has passed from turning it off  
\*NOTE: Mercury lamp needs to cool down for 1 hr after turning off. If someone else is going to use the microscope within an hour, leave the lamp on
9. On record sheet, write down lamp off hours, time turned off and your name
10. Turn of computer
11. Put microscope cover back on

### **Disk spinning (confocal) microscopy imaging**

#### **Notes:**

- In practice, spinning disk confocal microscopy significantly reduces out of focus sample illumination compared to epifluorescent imaging, resulting in reduced background and higher resolution images. However, much longer exposure times are required.
- Imaging with the disk spinning unit (DSU) is highly recommended for accurate quantification of the vasculogenesis assay, otherwise background noise adds substantial quantification artifacts.
- Generating maximum intensity projections from Z-stacks of images is also recommended to capture cellular features that may be in different Z-planes.
- Typical exposure times:  
DAPI: 2000 ms for 4x imaging, 1000 ms for 10x imaging, 500 ms for 20x imaging  
UEA-rhodamine: 6000 ms for all magnifications  
Phalloidin: 8000 ms for all magnifications  
Immunofluorescent stains: 8000+ ms  
\* The primary drawback for spinning disk microscopy is the trade off between time spent imaging (proportional to exposure time) and image quality. The exposure times I chose were to balance the need for high enough throughput with sufficient image quality for quantification. Although the DAPI signal is strong enough to provide near optimized

intensity histograms at acceptable exposure times regardless of magnification, UEA, phalloidin and immunofluorescent stains tended only to provide optimized intensity histograms at 20x magnification unless excessive exposure times were chosen.

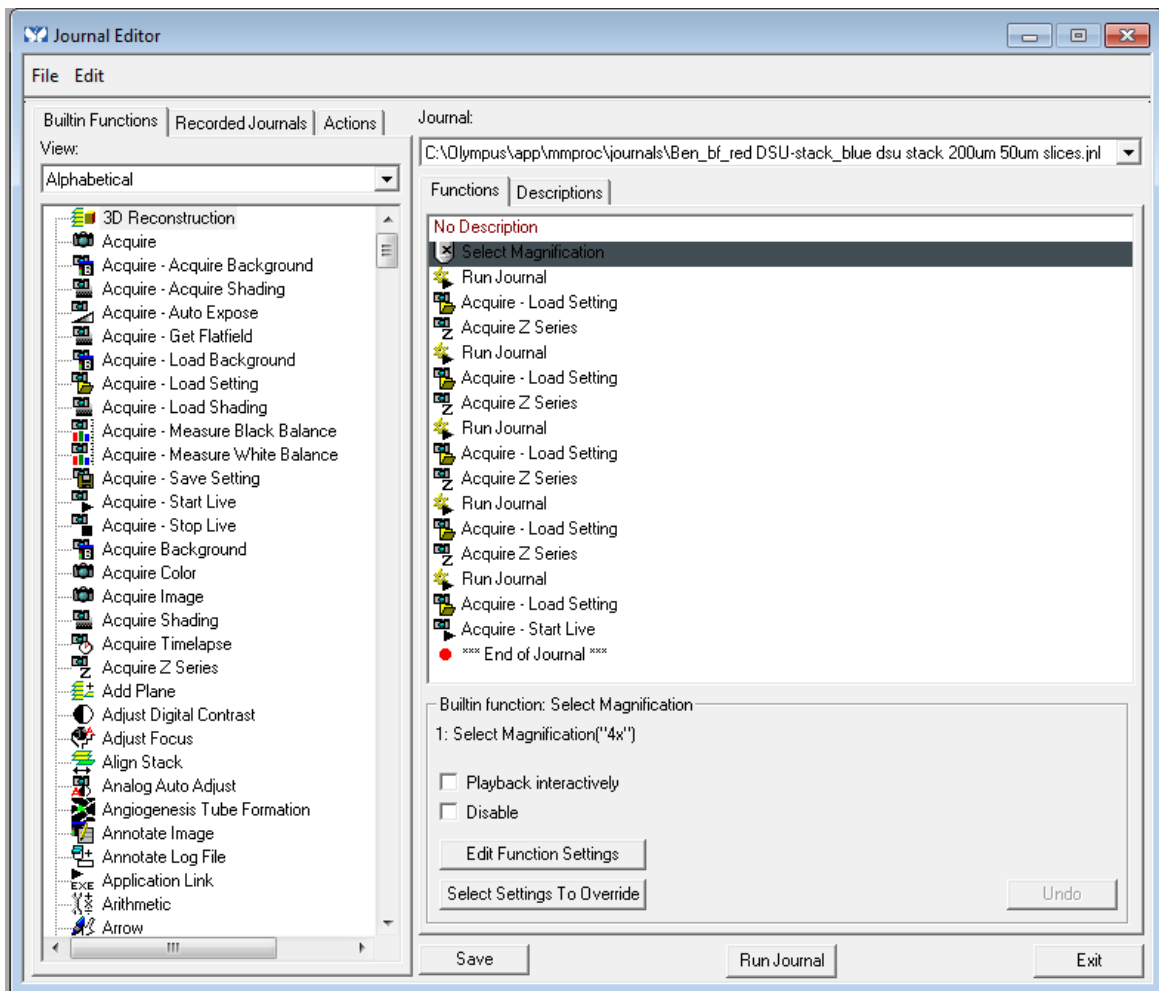
\*Higher magnifications require shorter exposure times because the light is more focused.

\*To overcome this limitation for 4x image analysis, images are post processed to remove background and enhance contrast (see protocols for ImageJ scripts)

- Typical Z-stacks:  
4x images: 200-300 micron thick stacks with 30-50 micron slices. You should optimize for your purposes but I would recommend 200 micron thick with 50 micron slices for optimal time efficiency for vessel density quantification  
20x images: 30-50 micron thick stacks with 3-5 micron slices. You should optimize for your purposes, the higher the cell density the thinner you want your stack to be to avoid many overlapping features. The thinner the slice, the higher resolution your images will be, but also the longer it will take to image.
- FOR VISUALIZATION OF LUMENS: You must image in a MatTek or similar glass bottom plate or on a microscope slide. If you image in a well-plate there will be too much background even with DSU to resolve cell lumens.  
\* Fibrin gels will need to be cultured in glass bottom plates, but PEG gels can be transferred over after culture.  
\*This is also necessary to image at 40x magnification or higher
- For 20x objective, make sure the objective collar is set to image through the appropriate thickness: 0.17 for cover glass, 2 for well plate, otherwise you will not get a crisp image.
- The shutter for the brightfield has been sticking on occasion, resulting in dim BF images for the first couple slices. If you encounter this problem, and you want BF images to complement your fluorescent images, you will need to have BF imaging live before starting the journal so the shutter is already open.

## **Protocol**

1. Get the microscope set up following the General Microscope Set-Up procedure
2. Put samples of interest on sample stage.
3. If imaging free floating PEG hydrogels it is important to orient the gel with its cut side face down.  
\*If there is too much buffer in the well with the gel then the gel will diffuse around while imaging yielding blurry images. However, if there is not enough liquid in the well then the light will diffract at the gel air interface creating excessive background and image artifact. As such, the buffer height should be exactly the same as the top of the hydrogel. You can gently push down on the gel to try to get the cut side flush with the bottom of the gel. It is also usually best to have the gel up against the side of the well to help stabilize.
4. Load or edit an existing Journal with your desired parameters for your DSU Z-stack.
  - a) Go to Journal -> Edit Journal to pull up a journal tab
  - b) If you are starting fresh it is easiest to edit a preexisting journal.
  - c) The following tab will appear after selecting a journal to edit:



d) The journal will progress in sequential order, performing the function on each line.

You can double click on each line to change its specific function.

e) First choose your desired magnification by double clicking on the Magnification line

f) All of the “Run Journal” commands in these DSU-Stack Journals are running embedded pre-established Journals for loading particular filters. Important Journals are labeled:

Brightfield camera: “BF\_Camera”

Green DSU channel: “GFP\_DSU”

Red DSU channel: “mCherry\_DSU”

Blue DSU channel: “DAPI\_DSU”

Green widefield channel: “GFP\_WF”

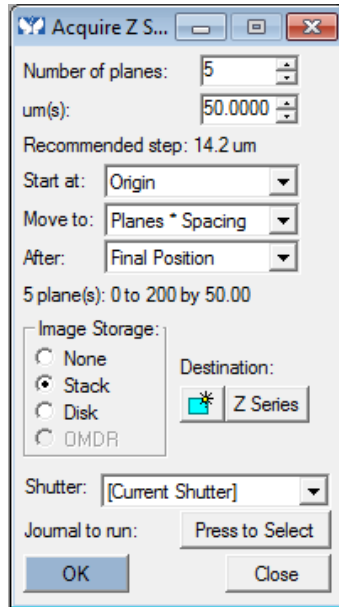
Red widefield channel: “mCherry\_WF”

Blue widefield channel: “DAPI\_WF”

g) In order, the Journal will load the proper objective, then load the proper channel, load the selected acquisition settings (exposure and thresholding), then image with the

indicated settings for the Z-stack. These Journals are set up for 4 rounds of imaging, then set to open a live acquisition window with desired acquisition settings.

5. Determine the appropriate exposure times for each of your DSU imaging channels (and BF imaging if needed)
  - a) Go to Show Live in the Acquisition window, leaving your Edit Journal window open. To determine an appropriate exposure time for DSU z-stacks first locate a region of interest with well-defined features using the wide-field fluorescence channel.
  - b) Then switch to the DSU channel and check that the DSU provides an appropriate signal to noise in the image: first adjust the Image Scaling to be able to see features, then use your mouse to scroll through the image to get an idea for the background (similar to process used for deciding threshold for Angiogenesis tube formation module. The coordinates for the mouse cursor over an image, and the intensity at the cursor, are shown at the bottom of the window: (x,y) -> Intensity.
  - c) You want there to be at least ~10% increase for signal to noise for features you intend to quantify. For instance, if the average background has an intensity of ~225 and your average vessel has an intensity of ~255 then you have ~13.3% increase in signal over noise which is sufficient for quantification. Increasing concentration and duration of staining, increasing washes, and overnight washing, and increasing exposure can all help with improving signal to noise.
  - d) You can estimate signal to noise on a live image while deciding exposure times.
  - e) The image scaling can be manually adjusted after imaging, but is convenient to set now, and you will need to adjust it to see stained cells. For DSU images there is usually a relatively narrow range selected.
  - f) After you have picked your exposure time and set your image scaling, save your image setting by clicking "Save As". It is best if you save your own individual image settings for your journals, so others don't switch them around.
  - g) repeat this to check/define the image settings for each DSU channel you intend to image.
  - h) In your Journal Window, under each "Run Journal" command, double click the "Acquire- Load Setting" to select the appropriate acquisition settings you just determined.
6. Set your Z-stack settings
  - a) Double click on each "Acquire Z Series" command and set your desired parameters. The following tab will appear:



b) Indicate your number of planes to image and the um(s) distance between slices. In this example, there are 5 slices 50um apart, for a 200um thick stack. Keep in mind that the first slice is at the origin (by default). \*If you want to make a 3D reconstruction, your steps should be smaller than the recommended step size, but for quantification of 4x max intensity projections, it is ok to be up to 50 microns without losing features\*

c) Press OK to save settings

d) CHECK THAT ALL ACQUIRE Z SERIES SETTINGS COMMANDS IN YOUR JOURNAL ARE IDENTICAL!

7. Choose the Run Journal and acquisition settings for the live window that will pop up after the journal has progressed through each Z-stack

\* I usually choose Red so it is easy to pick another ROI with good vessels, but if another channel is your primary interest (i.e. for immunofluorescent imaging) then you may choose green instead.

8. Disable any channels that you are not interested in imaging. Make sure to disable all 3 steps for that channel: 1) Channel 2) acquisition settings 3) Z-stack settings

9. MAKE SURE TO SAVE AS A NEW JOURNAL

a) If you press “Save” it will overwrite the pre-existing journal\*

b) Go to File -> Save As

c) include pertinent details in the file name

d) if your only change is disabling/enabling steps then no need to save as a new journal

10. Your Journal is now ready to run. Leave the Edit Journal window open to run the Journal when ready.

11. Open your live acquisition in Wide Field to find a ROI you want to image.

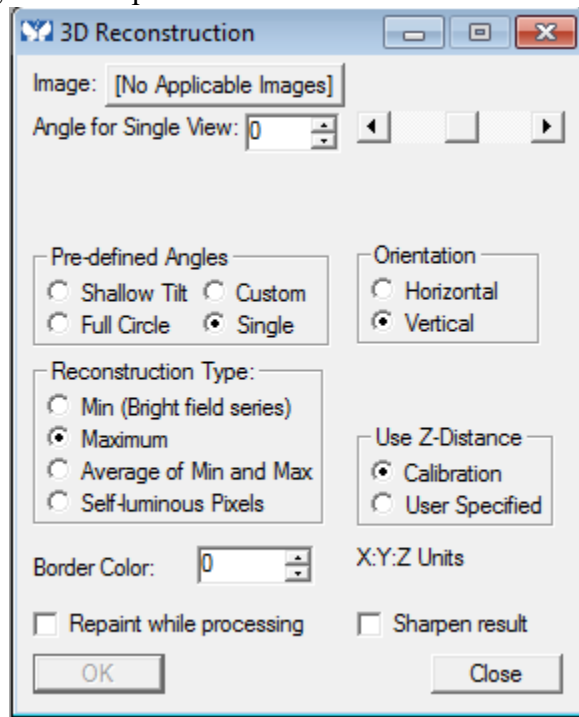
12. At your ROI of interest, adjust the Z-position on the microscope to the bottom of the Z-stack. For each ROI you will need to set the Origin in the Z direction (X,Y setting does not matter for the journal however). The default Z-stack setting is to image in the positive Z-direction for progressive slices.

- a) Resetting the origin for each ROI is especially important for PEG hydrogels where the cut side is not necessarily perfectly smooth.
  - b) You want your zero height to be the lowest plane in which vessels are in focus throughout the entire ROI. If vessels are in focus only in half your image for your first slice, then you will bias your quantification towards lower density than actual.
  - c) Also ensure that for each ROI, vessels remain in focus throughout the full thickness of the Z-stack. You will also bias your imaging if you accidentally focus over the top of your hydrogel for your last slice(s).
  - d) to set your origin: Devices-> Stage -> Move Stage to Absolute Position-> Set Origin
  - e) CHECK/SET YOUR ORIGIN FOR EVERY ROI!
13. Once your ROI and origin is set, press “Run Journal” on your Journal editor page to acquire your DSU Z-stack.
  14. Save each stack with relevant information to identify: Experiment, condition, gel #, ROI#, channel, etc...

**Generating 3D reconstructions and/or Maximum intensity projections in Metamorph**

1. You can make 3D reconstructions that you can rotate or maximum intensity projections in Metamorph if preferred to ImageJ. I will sometimes do this to quickly check the Max intensity projection instead of running the ImageJ scripts.
2. Click Stack -> 3D Reconstruction.

The following tab will open:



3. For a Maximum intensity projection, select:  
 Angle for Single View = 0  
 Predefined Angle = Single



Orientation = Vertical  
Reconstruction Type = Maximum  
Use Z-distance calibration

4. For a 3D reconstruction choose full circle and define the angles to view from. The other settings will be the same as for Maximum intensity projection.

**Acquisition of a tiled (stitched) multi-panel image in Metamorph:**

1. Go to Apps -> Scan Slide. The Scan Slide command window will open.
2. Main tab: define the name of your Scan slide and directory to save in.
3. Acquisition tab: Define the camera binning. Higher binning reduces the file size and resolution of image, typically best to leave at 1. Also indicate the number of wavelengths to image, 4 wavelengths if you want BF and all 3 fluorescent channels. Within each acquisition tab you can define the filter channel with the Illumination tab and exposure. You can auto expose to automatically define the exposure, but I tend to prefer choosing exposure myself. I also tend not to auto-focus or include a Z-offset from previous wavelength. In the Acquisition -> Run Journal tab you can combine scan slides with time course imaging or Z-stacks, however, I have never done so.
4. The Calibration automatically updates depending on magnification chosen
5. Slide Area defines the area you are going to scan. Pan over to the upper left corner for the area you would like to scan then click "Set to Current" then Pan over to the lower right corner for the area you would like to scan then click "Set to Current"
6. You are now ready to take your stitched image: Press "Scan"
7. At the end a preview will pop up at low resolution
8. To load the high resolution scan, go to the Data Review tab: Load your scan at 100%.

## Appendix M: ImageJ scripts used for image analysis:

### Notes:

- These scripts are to be used with ImageJ (you can download for free at <https://imagej.nih.gov/ij/>)
- To run the script for a macro in ImageJ, first create a text document (.txt) file containing the particular script of interest.
- Each script is written to be used to perform a function on an entire folder of either raw images, raw z-stacks, or on maximum intensity projections as indicated.
- Notes for each script are included below

### General protocol for running ImageJ macros:

1. Make a text document for the script by copy and pasting from this word document
2. Save all macros to a folder that is convenient to access
3. Download ImageJ if needed
4. Open ImageJ
5. To run a macro go to “Plugins” > “Macros” > “Run”
6. Find the text document file for the particular macro you want to run
7. This will prompt you to select the folder you want to analyze
8. Once you specify the folder the macro will automatically analyze each file within the folder and create a sub folder within the user-specified folder with the analysis.

### Automatic generation of maximum intensity projections with enhanced contrast:

### Notes:

- This macro creates maximum intensity projections of all z stacks in the user-specified folder and automatically contrast enhances them.
- Each maximum intensity projection is processed and saved to a folder created within the user-specified folder.
- Disabling the line “run(“Z Project...”, “Max Intensity”)” will result in this script enhancing contrast for a single plane image
- This script enhances contrast by normalizing the dynamic range to fill the entire range of intensities. This effectively normalizes between technical replicates because if one replicate is stained more brightly than another, they will all be similarly normalized. This is convenient for always applying the same thresholding parameters for automatic image quantification. However, this is not appropriate for qualitative comparison for immunofluorescent staining for assessing differential expression of target proteins because all images will have the same average brightnesses.

### Script:

```
dir = getDirectory("Choose a Directory");
newdir = dir + "/Recon/"
File.makeDirectory(newdir);
list = getFileList(dir);
```

```
for(i=0; i<list.length; i++) {
```

```

    if (endsWith(list[i], ".tif")){
        open(dir+list[i]);
        imgName=getTitle();
        run("Z Project...", "Max Intensity");
        run("Enhance Contrast", "saturated=0.1 normalize process_all use");
        run("Subtract Background...", "rolling=50");
        run("Despeckle");
        run("Smooth");
        saveAs("Tiff", newdir + "Recon " + imgName);
        while (nImages>0) {
            selectImage(nImages);
            close();
        }
    }
}

```

### **Quantification of DAPI nuclei density from 4x images:**

#### **Notes:**

- This macro automatically takes a folder of single plane images or maximum intensity projections, converts to a binary image, and quantifies particle metrics (i.e. particle number per image, average particle size, individual particle circularities, etc).
- It is typically used for assessing nuclei per mm<sup>2</sup> for a single plane image or nuclei per mm<sup>3</sup> for Z stacks (normalized to volume of Z-stack).
- This script works best when nuclei densities are low enough or Z-stacks are thin enough that there aren't many overlapping nuclei (there is some subjectivity to acceptable degrees of overlap).
- If there is a large degree of overlap such that binary images look like large globs instead of individual nuclei, and the watershed function is not satisfactorily dividing nuclei, you can compare total area covered with particles between conditions, normalizing to the average particle (nuclei) size for a condition with lower cell densities (such as d1 if there is a lot of proliferation over the course of the experiment), this is the approach I took for my high cell density PEG hydrogels.
- Best to run this script on a folder with only DAPI images for ease of data organization

#### **Script:**

```

dir = getDirectory("Choose a Directory");
newdir = dir + "/dapi counted/"
File.makeDirectory(newdir);
list = getFileList(dir);

for(i=0; i<list.length; i++) {
    if (endsWith(list[i], ".tif")){
        open(dir+list[i]);
        imgName=getTitle();

```

```

//run("Enhance Contrast", "saturated=0.1 normalize process_all use");
//run("Subtract Background...", "rolling=50");
//run("Despeckle");
//run("Smooth");
run("8-bit");
setAutoThreshold("Otsu dark");
run("Convert to Mask");
run("Watershed");
run("Analyze Particles...", "size=15-10000 circularity=0.00-1.00 show=Outlines
display include summarize");
saveAs("JPEG", newdir + imgName);
while (nImages>0) {
    selectImage(nImages);
    close();
}
}
}

selectWindow("Results");
saveAs("Measurements", newdir+"Results.xls");
run("Close");

selectWindow("Summary");
saveAs("Measurements", newdir+"Summary.xls");
run("Close");

```

### **Quantification of cell spreading using cell circularity and area coverage of 10x images:**

#### **Notes:**

- This script is nearly identical to the DAPI count script except a different auto threshold function was chosen that gave the most accurate binary image of cell bodies, the range of particle sizes to include is different, and this script was not updated to automatically create a folder to save images in: instead you will need to run a batch macro (details below).
- Best if used with maximum intensity projections at 10x magnification with 10 micron slices (or thinner) of total ~50 micron thick Z-stack.
- The thickness of your Z-stack should be optimized for your intended purposes based on average cell densities: The thicker your slice the more cell bodies you will have to measure so your data will be stronger, but you want to ensure that cell bodies only very rarely overlap otherwise they will not be quantified as individual cells.
- This type of quantification is most appropriate when there is large changes in cell spreading depending on condition. If changes are less pronounced, then cells need to be relatively well isolated to see subtle differences.
- This is usually used for images of phalloidin stained cell bodies, but can also be used for other stains: I usually also run this script on corresponding DAPI and UEA images from

the same ROIs to ensure I get a similar trend as observed from 4x images to verify images are not accidentally biased (assess total area covered).

### **Protocol**

1. Go to your folder containing your maximum intensity projections
2. Analysis will be most convenient if you separate each channel into separate folders
3. Within each folder create a sub folder for analyzed images, I usually label them something like “DAPI analyzed”
4. Open ImageJ, go to Process > Batch > Macro to open the batch macro dialogue box
5. Select the Input folder for images to analyze, and for the Output folder select the corresponding analyzed sub-folder that you just created.
6. Copy and paste the script below into the macro dialogue box.
7. I usually choose JPEG as the Output Format because the images are smaller and the images are just for qualitative assessment.
8. Hit Process.
9. Copy and paste data to an excel file

### **Script:**

```
run("Subtract Background...", "rolling=50");
run("Enhance Contrast", "saturated=0.4 normalize process_all use");
run("Despeckle");
run("Smooth");run("16-bit");
setAutoThreshold("Default dark");
//run("Threshold...");
run("Analyze Particles...", "size=250-Infinity circularity=0.00-1.00 show=Outlines display include summarize");
```

### **Quantifying fraction of UEA associated nuclei**

#### **Notes:**

- This set of scripts is used to determine the percentage of DAPI stained area that is overlapped by UEA stained area, giving a fractional estimate of EC nuclei compared to total nuclei.
- This is run as a combination batch macros that is input by the user (as described above for cell spreading analysis), and the masking macro.
- The output will be images that only show DAPI nuclei that are within UEA stained area

#### **Protocol:**

1. Create a text document with the script for “Create UEA masked images of DAPI binaries” provided below and save to a convenient folder.
2. Go to your folder containing DAPI maximum intensity projections and create a sub-folder labeled something like “DAPI binaries”

3. Go to your folder containing UEA maximum intensity projections and create a sub-folder labeled something like “UEA binaries”
4. Perform a batch macro with the input being your DAPI folder, the output being your DAPI binary folder and copy and paste the script below “Create binary directory of DAPI images”. Do the same for UEA images with the appropriate script (the scripts have different auto-thresholding options which were chosen to be most accurate given my standard confocal imaging technique)
5. Create directory of masked DAPI images: go to Plugins > Macros > Run and select the text document for the script “Create UEA masked images of DAPI binaries”
6. You will be prompted to select 3 directories, you need to pick them in order: 1) DAPI binaries 2) UEA binaries 3) select your whichever folder you want the masked images to be saved in (I usually pick the folder containing DAPI max projections)
7. A folder will be created called “dapi masked” that contains images for each region of interest showing dapi thresholded areas that were within UEA thresholded areas.
8. Run a batch macro for particle analysis provided below to determine the area of total nuclei and area of UEA masked nuclei for each ROI to quantify percentage of UEA associated nuclei.

Create binary directory of DAPI images

```
setAutoThreshold("Otsu dark");
//run("Threshold...");
setOption("BlackBackground", false);
run("Convert to Mask");
```

Create binary directory of UEA images

```
setAutoThreshold("Li dark");
//run("Threshold...");
setOption("BlackBackground", false);
run("Convert to Mask");
```

Create UEA masked images of DAPI binaries

```
// @File(label="source directory X",style="directory") dirX
// @File(label="source directory Y",style="directory") dirY
// @File(label="destination directory",style="directory")
```

```
dirX = getDirectory("Choose a Directory");
dirY = getDirectory("Choose a Directory");
dirZ = getDirectory("Choose a Directory");
newdir = dirZ + "/dapi masked/"
File.makeDirectory(newdir);
```

```
// get a list of all files in the two folders
listx = getFileList(dirX);
listy = getFileList(dirY);
```

```

// stop the macro if the number of images is not the same
if (listx.length != listy.length) {
    exit("number of images is not equal");
}

// set batch mode to not see the images when opened
setBatchMode(true);

// start a for loop to process all image pairs one by one
for (i=0; i<listx.length; i++) {

    // get the paths to an image pair
    incomingx = dirX+File.separator+listx[i];
    incomingy = dirY+File.separator+listy[i];

    // open the image at list position i and rename them
    open(incomingx);
    imgName = getTitle();

    rename("XX");
    open(incomingy);
    rename("Y");

    // add the images to each other
    imageCalculator("And create", "XX", "Y");
    rename("result");

    // save the image
    selectWindow("result");
    saveAs("Tiff", newdir + imgName);
    while (nImages>0) {
        selectImage(nImages);
        close();
    }
}

// close all open images
run("Close All");

Analyze total areas of DAPI binaries and UEA masked DAPI images
run("Analyze Particles...", "size=5-infinity circularity=0.00-1.00 show=Outlines display include summarize");

```

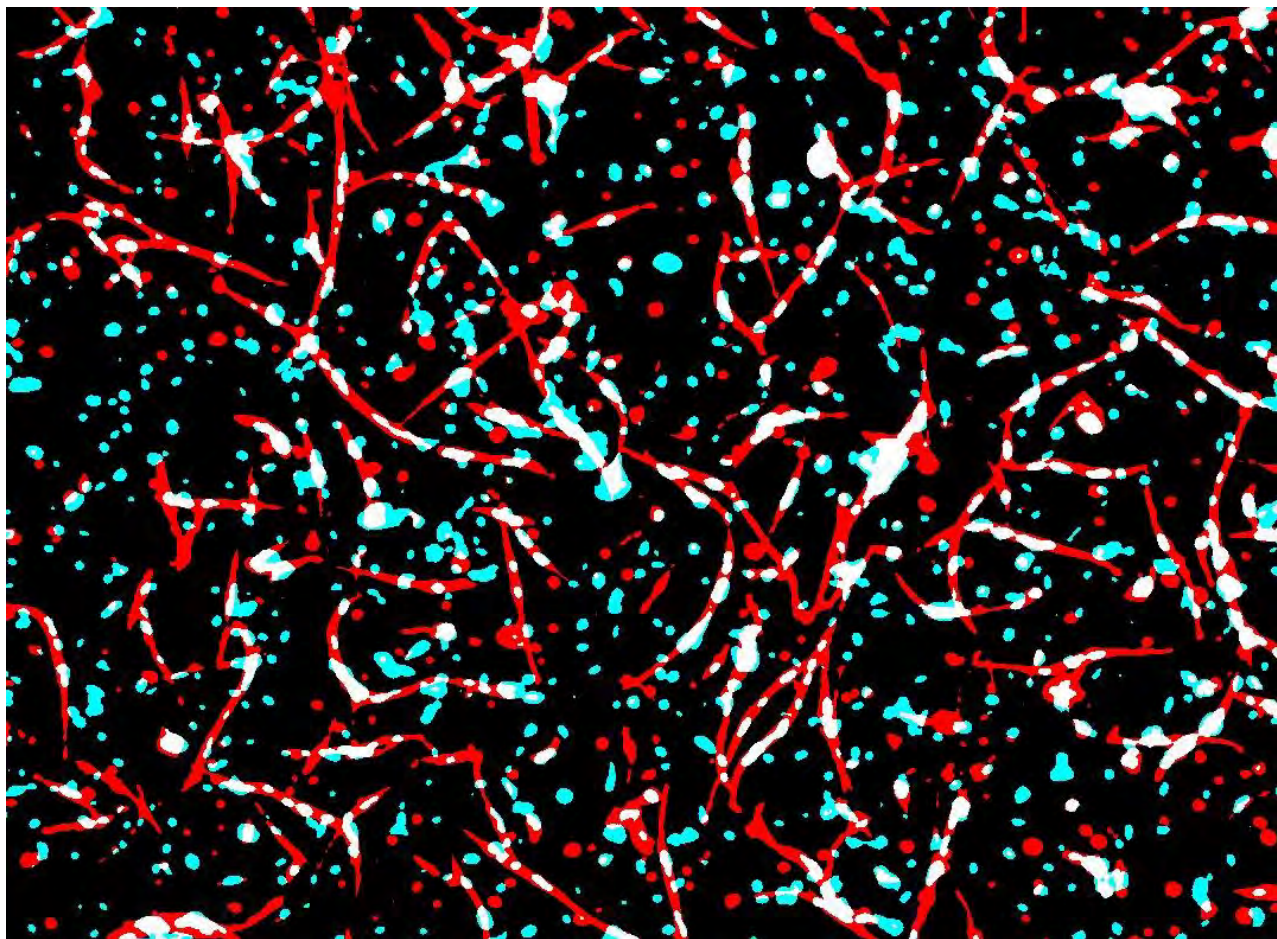


**Figure A.1 Example analysis of UEA mask on DAPI image generation for 27mg/ml hydrogel on day 7.** Masked images are generated from maximum intensity projections as described in the methods. UEA mask is shown in red. DAPI mask is shown in blue. Areas of overlap are shown in white. The analysis algorithm determines the ratio of white to blue area.



## Appendix N: Metamorph vessel quantification

Adapted from Jonathan Bezenah protocol

### Notes:

- Needs to be performed on a single plane image or a maximum intensity projection of a Z-stack
- Vessel width typically; Minimum (6 microns), Maximum (60 microns).
- For Epifluorescent imaging with optimal histogram of intensities, the intensity above background is usually 200-300
- For analysis of z-stacks that have had contrast normalization and background subtraction the intensity above background is typically 4000.

### Protocol:

1. Open Metamorph
2. Open images you want to quantify. Either:
  - \*File -> Open and find your images
  - \*Drag and drop from your folder into Metamorph
3. You will need to calibrate images if images have been processed in ImageJ at all (i.e. cropped to remove imaging artifacts or background subtracted and contrast enhanced)
  - a) Click measure -> calibrate distances
  - b) A new window will appear, select the magnification used for the image, then select apply to all images to calibrate your processed images.
4. On the top tool bar, click “APPS”
5. click “Angiogenesis Tube Formation”. A new window will appear
6. On main computer desktop, go to start menu, and open up a new excel file.
  - \*Make sure no other excel files are open
7. Once excel is open go back to Metamorph
8. On the top tool bar, go to “Log” and click “Summary log” on the drop down menu
9. A new window should appear. Click OK
10. A second window will appear. On this window make sure Microsoft excel is selected
11. In the same window, name the sheet you will write to (default is “raw”), and select the column and row you want to start writing to.
12. In the “Angiogenesis Tube” window, click the top button which says source
13. On the drop down menu, select image you want to quantify
14. Check min, and max tube width values and make sure they are set to “6” and “60” respectively. \*Or otherwise optimized values for your purposes
  - \*These values set the minimum and maximum width the program will consider a tube
  - \*You can adjust these if your vessels are smaller or wider
15. Next, you need to set the threshold value for the intensity above local background.
  - a) To determine the optimal threshold for your image, drag mouse cursor over the image. On the bottom of Metamorph, as you move the cursor, numbers will change. The first 2 are position (x,y) and the third is intensity.
  - b) Determine the intensity of the background (while moving the mouse over background take note of the average intensity value)
  - c) Place mouse cursor over dimly stained vessels and record average intensity values
  - d) The threshold you should use is intensity of vessel minus intensity of background

- e) Threshold value should be adjusted by a bit (20 – 50 lower than calculated to account for fluctuations in sprout intensity)
  - f) Do a couple practice quantifications for images from a few different conditions to make sure they all qualitatively look good
  - g) ALWAYS APPLY THE SAME THRESHOLD TO ALL IMAGES FROM ALL CONDITIONS WITHIN A EXPERIMENTAL REPLICATE TO AVOID BIAS.
16. For segment detection I indicate skeletonization, this typically provides a more conservative quantification of vessel density with reduced superfluous feathering compared to watershed. However, you should try both and decide which provides the best quantification for your purposes and then stay consistent.
  17. After the quantification parameters are set, click “start”
  18. The module will quantify the vessels and automatically import quantification metrics into the summary log.  
\*If you close your excel file before you finish quantification you can open it back up and repeat steps 8-11 but make sure to indicate a row below anything that has been written to make sure you don't overwrite data.
  19. Repeat with all the images you need to quantify.
  20. Save the excel file when you are finished and turn everything off.

## Appendix O: PEG and fibrin rheology with AR-G2 rheometer

Adapted from Yen Kong protocol

### **Materials:**

- AR-G2 shear rheometer with Peltier stage attached for standard measurements
- UV stage if performing in situ UV curing
- 8 mm measurement head with adapter and longer spindle rod for in plate or precast PEG hydrogel characterization
- 20mm measurement head for in situ gelation experiments to characterize kinetics
- Glass plate to balance well plates (if measuring directly in well)
- Double sided scotch tape
- Course grit wet sandpaper (800 grit or lower is best)
- 8mm biopsy punch and/or scalpel
- Micro lab spoon (if measuring PEG hydrogels)

### **Overview:**

The procedure described provides particular details for characterizing fibrin hydrogels cast in 24-well plates or larger, and for PEG hydrogel punch outs, in a way that can be tracked over time. However, some additional details are included for using the UV stage.


### **Notes:**


- Experiments tracking cell-mediated changes to matrix mechanics are done with the 8mm measurement head
- Experiments for characterizing the gelation kinetics, and for the UV stage, are typically best performed with the 20mm measurement head. The greater surface area provides a more accurate measurement and reduces slippage for gels that are cast in situ
- Getting a transducer initialization error has become more common over the last couple years. This error is most likely caused by a problem with the rotary optical encoder that keeps track of the displacement and velocity of the bearing spindle. If you receive this error quickly turn off the instrument because rotation of the spindle starts to accelerate out of control. Usually restarting the instrument and software a couple times will fix the problem. The error only occurs at start up. When simply restarting doesn't work, I have had some success with starting the instrument with the measurement lowered to be in contact with the measurement plate to hold it in place, which seems to allow the encoder to register the spindle more easily. You will get a magnetic bearing instability warning however, at which point, raise the measurement head and restart the software, but not the instrument.
- TA instruments suggestions for dealing with transducer initialization failure: Transducer initialization is reporting a problem with the rotary optical encoder that keeps track of the displacement and velocity of the bearing spindle. The rotary encoder is positioned at the top of the air bearing motor/transducer assembly. When it fails to report a position change the error will be posted. There could be some dust in and around the encoder, try blowing compressed air thru the opening where the draw rod sits. If you are comfortable

taking things apart you could remove the cowl cover and top encoder cover to better inspect and blow out any dust. If the error is persistent, I would recommend a service call.

- To avoid initialization failure it is ok to leave the instrument running for long periods of time, however, it is important to turn off the cooling pump when not in use because the pump will overheat if left running over night, this is bad for the pump, and also heats the water bath, such that the Peltier stage can't cool down to an appropriate temperature to perform experiments. Only leave the rheometer and air on.
- Measurement parameters for PEG hydrogels are typically at 0.05N normal force, 5% strain, 1 rad/sec using the 8 mm measurement head.
- Measurement parameters for collagen/fibrin are typically performed in a 24-well plate or larger, with the 8mm measurement head indented into the hydrogel ~300 um, 0 N normal force, 6% strain, 1 rad/sec.

### **Procedure:**

1. Turn on compressed air at the main source. Then switch the ball valve (blue handle) to the ON position and check that the supplied air pressure is 30 psi.
2. Power on the rheometer control system and water pump. Check water bath level for Peltier stage cooling pump and top off if necessary, exchange with fresh water if cleaning is needed.
3. Watch for spindle lift and rotation. Then remove the black shipping cover.
4. If a stage swap is necessary between the UV and Peltier stage swap now by removing the cooling tubes and unplug the smart swap connector. Press the right most button on the rheometer front panel twice to release the stage. Attach the cooling tubes and re-plug the smart swap connector for the desired stage.
5. Start "Instrument Control" (Icon on desktop). IF performing a UV experiment, at this point calibrate the UV irradiance with the radiometer and remote sensor (item 3). Wizard -> UV irradiance calibration.
6. Perform the inertial calibration. Options -> Instrument -> Inertia Tab.
7. Screw on the desired testing geometry components.  
\*The 8mm diameter measurement head geometry needs an adapter and a longer spindle rod.  
\*use double sided tape and biopsy punch or scalpel to apply sandpaper to the measuring face of the measurement head and cut to fit. Sandpaper is usually good for multiple days, replace when sand paper no longer seems well secured. Use a razor blade to remove.
8. Load the appropriate geometry file. Invalidate all zero point and "NO" to map when asked.
9. Calibrate geometry inertia. Settings tab -> geometry inertia calibrate
10. Calibrate bearing friction. Options -> Instrument -> Miscellaneous.
11. Zero the normal force . You may need to press the zero button several times for it to give a negligible value (< 0.01 N)
12. Prepare the stage for either PEG hydrogel or in-plate hydrogel measurement

- a) Pre-cast PEG hydrogels will be measured directly on the Peltier stage, but require sand paper on the stage to prevent it from squeezing out from under the measurement head. Put double sided tape on the back of the sandpaper, cut out an 8mm punch if you are measuring a 50ul gel or less, then carefully center the sandpaper under the measurement head.
- b) If you are measuring hydrogels directly in the well plate (typically fibrin or collagen). Find the glass plate that is kept under the rheometer (~ 0.1 x 14 x 18 cm) and place on the Peltier stage. This keeps the plate level
- c) If you are UV curing your hydrogels, make sure the UV stage is well cleaned.
13. Zero the geometry gap . If you are doing in well measurements, make sure to zero into an empty well. Say “NO” to move head to back off distance, this moves the head all the way up and wastes time.
14. Perform rotational mapping. Use ‘two’ iteration and ‘standard’ type. Instrument -> Rotational mapping.
15. Load or create new test procedure. Procedure -> open, or, Procedure -> new.  
 \*Procedures are typically “oscillation” procedures. When you click new procedure it will open the default tab to input procedure steps and test parameters. New oscillation procedures will default to have 3 steps: 1) conditioning 2) frequency sweep 3) Post-experiment. You can right click on a step to add another step to the procedure. You can uncheck the box to turn off a particular step. In addition to oscillation frequency sweep, we commonly perform an oscillation strain sweep for initial characterization of a hydrogel, then oscillation time sweeps as the primary measure for comparison between conditions for a particular type of hydrogel/material.  
 \*To input parameters for each step; click on the step in the procedure, then fill in the desired parameters for the step in the tabs that appear to the right.  
 \*to save a procedure go to File-> Save As
16. For hydrogels and new materials it is recommended to first perform an oscillation frequency sweep (0.1 -> 10 rad/sec, at least 5 points per decade) at low strain (0.5 – 1 % strain) to determine the viscoelastic limit. Then selecting an appropriate oscillation frequency based on this first test, perform a strain sweep (0.1 - 10%) to determine the strain stiffening limit. You should be ready to report these results as it is most common for materials to be characterized with frequency and strain parameters in their linear viscoelastic limit.  
 \*If you are UV curing you will need to do a time sweep first to determine how long to cure your gels before frequency and strain sweeps. Add an event step for switching on/off the UV leads to your procedure.  
 \* After determining parameters that are within the LVE range, we typically just perform a 30-60 second time sweep at the determined strain and frequency.
17. Perform oscillation mapping. Mapping needs to be done with the appropriate geometry, at the approximate gap of the test, and needs to cover all the parameters you included in your procedure. Instrument -> Oscillatory mapping.  
 \*If the instrument is not well mapped you may get inertial artifacts in your measurement, such as negative values.


18. Sample loading.

a) For Peg hydrogels, use a micro lab spoon to transfer the gel from the well plate and center on the sandpaper on the stage with a flat side face down.

b) For in-well hydrogels make sure the well of the plate is well centered under the measurement head. If the head is off to the side it will give larger than expected measurement because of the extra contact area.

c) for in situ gelation lower the head to the measurement height (typically 100 – 200 microns). The approximate volume of the sample depends on the gap value and the geometry (should be using 20 mm or larger) and can be found at the Geometry-> settings tab -> dimensions tab. Mix the precursor solution then pipette the approx. volume + 10% into the gap, then seal around the outside with mineral oil so it doesn't dry out


19. Sample measurement. Before lowering the measurement head or pipetting in sample for

in situ gelation STOP ROTATION of measurement head  to prevent shearing

a) For PEG hydrogels: zero the normal force. Manually lower the head until the normal force reads ~0.05N. IF gels are very soft and this normal force is not reached, stop at 1000 um, because you will destroy your gel if you the gap is too small.

b) For hydrogels that have a large viscous component (unlike PEG hydrogels that are primarily elastic) the normal force will quickly dissipate after lowering the measurement head onto them, so measurement at a constant normal force is not feasible. To address this, it is common to perform measurements at a constant gap height (which is appropriate for in situ gelation) but cellular hydrogels contract over time so a constant gap height is also not appropriate. To overcome these limitations while tracking mechanics over time, each gel will require measurement at sequentially decreasing gap heights: Bring the measurement head into contact with the hydrogel, then input a gap height 100um lower to start indenting into the hydrogel. Perform a 20s time sweep with parameters determined to be within the linear elastic range. After the run has completed, lower the head and repeat, continue to sequentially lower until 2 gap heights give similar moduli (typically 300-400 microns indented). Include in the file name the specific gap height of the test.

c) For in situ gelation work quickly to start measurement as soon as possible after mixing and pipetting in precursor solution.

20. When you press the start measurement button  you will be prompted to but in run information, include all important information in the file name, and make sure the it is saving to the appropriate Directory to find the file.

21. PEG hydrogels can be saved after measurement for IF staining/imaging because they are highly elastic and return to their initial shape. However, natural hydrogels become permanently compressed and are no longer suitable for accurate analysis after rheology.

22. System shut down.

a) if you are leaving the rheometer on, simply unplug the pump so it does not over heat, raise the spindle head up, put away the geometry head and loosely screw on the black shipping cover, close the software.

- b) if you are turning off the rheometer, switch OFF the power supply and close both air valves.
23. Data can be loaded from the TA data analysis program, then exported to excel for analysis. Average the values from a time sweep to get a single value for a particular hydrogel.

## Appendix P: Degradation of fibrin gels using nattokinase for cell pellet collection

Adapted from Jonathan Bezenah Protocol

### Materials:

- Ethylenediaminetetraacetic acid (EDTA, 292.24 g/mol)
- Phosphate buffered saline (PBS)
- Nattoinase (NSK-SD, Japan Bio Science Laboratory Co. Ltd., 25 FU/mg)
- Cellular hydrogels to degrade
- Sterile spatulas (optional)
- Sterile 1.5 ml microcentrifuge tubes (or 15 ml centrifuge tubes)

### Notes:

- This procedure is intended to be used with the Cell lysis for RNA isolation procedure and the Cell lysis for protein harvest procedure. Immediately after cell pelleting you will need to move forward with biomolecular isolation, so you should also prepare for that before initiating this procedure.
- To recover a decent pellet you will want at least 300k total cells per centrifuge tube (Closer to 500k is preferred). If there are not enough cells you will not be able to see your pellet to aspirate and you will get a poor yield. Keep this in mind when designing your experiments (i.e. cell seeding density and number of gels to pool together per replicate)
- Our stock of nattokinase is from a free sample received many years before my time. Its activity may diminish over time. It is a good idea to do a practice degradation on acellular fibrin hydrogels to check if you need to increase its concentration for hydrogel degradation. HYDROGELS SHOULD DEGRADE IN 30-45 MINUTES. It is no longer available from this supplier except for very large bulk orders. Conserve what we have left, or order from a new supplier and reoptimize. Others have mentioned that nattokinase from other suppliers works but doesn't completely dissolve, you may need to filter solution to remove particulates.
- This procedure does not necessarily need to be done with proper sterile technique, but it's good practice to perform as cleanly as possible.

### Protocol:

1. Prepare nattokinase solution. It is best to prepare nattokinase solution fresh each time.
  - a) Prepare/retrieve 1 mM of EDTA in PBS. Best if sterile filtered for long term storage
  - b) Calculate the amount of nattokinase solution needed (500 ul per 500 ul hydrogel)
  - c) Prepare a solution of nattokinase at 50 FU/ml (FU = fibrin degrading unit)  
\*FU/ mg varies by lot, our current lot is 25 FU/mg
2. Warm up nattokinase solution in water bath to 37 °C  
\*Do not leave in water bath longer than needed, it will start to lose activity if left for hours.
3. Aspirate media from fibrin gels
4. Rinse gels with PBS (PBS with 1 mM EDTA is best but not necessary)
5. Aspirate off PBS
6. Add nattokinase solution to gels. Volumes to add is equal to gel volume.
7. Using a pipette tip, metal measuring spoon, or other small tool, gently move/disassociate gel away from edges of well and try to mangle the gel into smaller pieces.



- \*This will ensure uniform degradation of gel and speed up degradation
8. Incubate gel in nattokinase solution at 37 °C until gel degrades. Typically, 30-45 mins, but could vary. Should not take more than 1 hr
  9. Once gel is degraded, spin down solution and cells at 500 X G for 5 minutes
  10. Aspirate off degraded fibrinogen from cells  
\*Thorough aspiration is not essential, it is more important to ensure that your pellet remains undisturbed to maximize yield.
  11. Rinse cells in PBS and spin down at 500 X G for 5 minutes.
  12. \*If your pellets are very faint, it is ok to skip the wash step to minimize the risk of losing them.
  13. Aspirate off PBS and proceed with experiment  
\*Thorough aspiration is not essential, it is more important to ensure that your pellet remains undisturbed to maximize yield.

## Appendix Q: Degradation of PEG gels using Collagenase IV for cell pellet collection

### Materials:

- Collagenase IV from *Clostridium histolyticum*
- Sterile phosphate buffered saline supplemented with 0.4 mM CaCl<sub>2</sub> and 0.1 mM MgCl<sub>2</sub>
- Hydrogels (2-3 per experimental replicate, pooled)
- Sterile micro lab spoon
- Sterile 1.5 ml microcentrifuge tubes
- Sterile surgical scissors or scalpel

### Notes:

- This procedure is intended to be used with the Cell lysis for RNA isolation procedure or the Cell lysis for protein harvest procedure. Immediately after cell pelleting you will need to move forward with biomolecular isolation, so you should also prepare for that before initiating this procedure.
- To recover a decent pellet you will want at least 300k total cells per centrifuge tube (Closer to 500k is preferred). If there are not enough cells you will not be able to see your pellet to aspirate and you will get a poor yield. Keep this in mind when designing your experiments (i.e. cell seeding density and number of gels to pool together per replicate)
- It is a good idea to do a practice degradation on acellular PEG hydrogels of the same [PEG] as your cellular gels to check if you need to increase collagenase IV concentration for hydrogel degradation. HYDROGELS SHOULD DEGRADE IN 30-45 MINUTES. If your gels do not fully degrade in this time period test higher concentrations of Collagenase IV.
- This procedure does not necessarily need to be done with proper sterile technique, but it's good practice to perform as cleanly as possible.

### Protocol

1. Prepare Collagenase IV solution. It is best to prepare solution fresh each time.
  - a) Prepare/retrieve 0.4 mM CaCl<sub>2</sub> and 0.1 mM MgCl<sub>2</sub> in PBS. Best if sterile filtered for long term storage
  - b) Calculate the amount of Collagenase IV solution needed (400 ul per 50 ul hydrogel)
  - c) Prepare a solution of Collagenase IV at 200 U/ml (U = digestion units) in PBS (0.4 mM CaCl<sub>2</sub> and 0.1 mM MgCl<sub>2</sub>)  
\*U/ mg varies by lot, check the current lot.
2. Warm up Collagenase solution in water bath to 37 °C  
\*Do not leave in water bath longer than needed, it will start to lose activity if left for hours.
3. Aspirate media from PEG gels
4. Rinse gels with PBS (0.4 mM CaCl<sub>2</sub> and 0.1 mM MgCl<sub>2</sub>). It is best to fill the wells to maximize the rinse.
5. Aspirate off PBS
6. In which ever way you find most convenient, cut up the hydrogels into quarters or smaller using surgical scissors or a scalpel, and transfer pieces to microcentrifuge tubes.  
\*You will probably need 2 gels per tube to recover enough cells for a decent pellet.

\*You may choose to transfer gels first then cut up in the microcentrifuge tube, if you find it more convenient this way.

7. Add Collagenase solution to gels in microcentrifuge tubes. Volumes to add is 400 ul per gel. Despite hydrogel swelling, you should be able to add 800 ul of collagenase solution to 2 hydrogels (50 ul hydrogels swell to ~200 ul)
8. Incubate gel in Collagenase solution at 37 °C until gel degrades. Typically, 30-45 mins, but could vary. Should not take more than 1 hr.
  - \* This step would ideally be done on a lab rotator to keep the centrifuge tube under constant spinning. If a lab rotator is not available, it is sufficient to flick/mix the gel by hand every 5-10 minutes.
9. Once gel is degraded, spin down solution and cells at 500 X G for 5 minutes
10. Aspirate off collagenase solution from cells
  - \*Thorough aspiration is not essential; it is more important to ensure that your pellet remains undisturbed to maximize yield.
11. Rinse cells in PBS and spin down at 500 X G for 5 minutes.
  - \*If your pellets are very faint, it is ok to skip the wash step to minimize the risk of losing them.
12. Aspirate off PBS and proceed with experiment
  - \*Again, thorough aspiration is not essential; it is more important to ensure that your pellet remains undisturbed to maximize yield.

## **Appendix R: Cell lysis and RNA Isolation Protocol**

Protocol adapted from Qiagen RNEasy Mini Kit [74104]

### **Materials:**

- Cell Pellet from hydrogel degradation procedure (See RNEasy mini kit or Jonathan Bezenah protocol for adaptation for recovery from 2D plated cells)
- RNase AWAY
- QIAGEN QIAshredder Kit
- RNEasy mini kit
- RNase-free pipette tips (most boxes of sterile tips come RNase free, but make sure to use boxes that have been set aside and been carefully used to avoid contamination)
- RNase free 1.5 ml microcentrifuge tubes (most bags of sterile tubes come RNase free, but make sure to use bags that have been set aside and been carefully used to avoid contamination)
- Crushed ice in bucket

### **Notes:**

- RNA is sensitive to RNases which are present on every surface. Take caution when isolating RNA and handling RNA sample to avoid contamination with RNase.
- Make sure all disposables used for RNA isolation are RNase free and have only been handled with gloves

### **Protocol:**

1. Prepare Working Area:
  - a) Ready fume hood in main lab area
  - b) Remove all contents from hood
  - c) Spray with 70% ethanol and wipe down hood
  - d) Place aluminum foil sheet down as a clean workspace within the hood and spray down with RNase away
2. Spray RNAase away on your gloves and onto a large kim-wipe
3. Wipe down necessary micro-pipettors, tube racks, micro-centrifuge tubes, markers, with RNase-away soaked kim wipe and place on foil.  
\*If in doubt just spray it down. However, you do not need to spray down tubes that have been kept in an RNase free bag.
4. Prepare buffer RLT for cell lysis:
  - a) be careful to avoid RNase contamination, and spray down the outsides of containers as necessary.
  - b) add 20 ul of  $\beta$ -mercaptoethanol to 1mL of Buffer RLT (from RNEasy mini kit) in a microcentrifuge tube.
  - c) make enough for each of your samples. Cell pellets with under 5M cells will require 350 ul of RLT buffer per pellet.
5. Gently flux the RLT buffer briefly with the pellet to lyse the cells and resuspend, then transfer to a QIA shredder tube from the QIA shredder kit.

- \* For typical RNA isolations a QIA shredder tube is optional, however, they are very convenient for removing small chunks of hydrogel that may not have fully degraded and are highly recommended for RNA isolation from cells recovered from 3D hydrogels.
6. Centrifuge for 2 minutes at the maximum speed. Remove and discard of the filter. If necessary, the procedure can be stopped here and the RNA can be stored at -80°C.  
\*If the RNA is stored at this point make sure to label tubes for easy identification and then thaw on ice or in the fridge.
  7. Add 350 ul of 70% ethanol (provided in kit) to ~350 ul of flow through and mix well. Take this ~ 700 ul of solution and add to an RNeasy Mini spin column that's in a 2 mL collection tube (provided in kit).
  8. Centrifuge for 12s at 10000 x g. Discard the flow-through (The RNA is adherent to column)
  9. Add 700 ul of Buffer RW1. Centrifuge for 15s at 10000 x g. Discard the flow through.
  10. Add 500 ul of Buffer RPE. Centrifuge for 15s at 10000 x g. Discard the flow through.
  11. Add 700 ul of Buffer RW1. Centrifuge for 2 minutes at 10000 x g. Discard the flow through.
  12. Replace bottom collection tube with new 2 mL collection centrifuge tube
  13. Spin down at max speed for 2 min to dry membrane
  14. Place spin column in new 1.5 microcentrifuge tube (provided in kit)
  15. Add 30  $\mu$ l to 50  $\mu$ l of RNase free water (provided in kit) to top of spin column (best to start at 30  $\mu$ l unless you know you will have a lot of RNA)
  16. Spin down for 1 min at 10000 x g
  17. Place samples on ice
  18. Measure RNA Concentration:
    - a) Go to nanodrop machine to measure concentration
    - b) Start up Nanodrop Program
    - c) Choose nucleic acid
    - d) Add 1  $\mu$ l of ddH<sub>2</sub>O (does not need to be RNase-free) to nanodrop sensor
    - e) Blank machine
    - f) Rinse off nanodrop sensor with DI water
    - g) Dry sensor completely with Kimwipe
    - h) Add 1  $\mu$ L of sample to sensor
    - i) Measure absorbance and record calculated RNA concentration
    - j) Repeat for each sample
  19. Store RNA samples at -80 °C if not immediately proceeding to cDNA synthesis

## **Appendix S: Protocol for cDNA Synthesis via reverse transcription of isolated RNA**

Adapted from Invitrogen High-Capacity cDNA Reverse Transcription Kit [4368814]

### **Overview:**

The High Capacity cDNA Reverse Transcription Kits contain all the reagents needed for reverse transcription (RT) of total RNA to single-stranded cDNA using a reaction size of 20  $\mu$ L. Use the kit for converting up to 2  $\mu$ g (for a 20- $\mu$ L reaction) of total RNA to cDNA for quantitative PCR applications.

### **Notes:**

- PCR assays require special laboratory practices to avoid false positive amplifications. The high throughput and repetition of these assays can lead to amplification of a single DNA molecule so careful handling of amplified PCR products is necessary.
- Wear a clean disposable lab coat (not previously worn while handling amplified PCR products or used during sample preparation) and clean gloves when preparing samples for PCR amplification. Set aside a particular disposable lab coat you only wear for setting up PCR amplifications.
- Maintain separate areas, dedicated equipment, and supplies for:
  - Sample preparation and PCR setup
  - PCR amplification and post-PCR analysis
- Never bring amplified PCR products into the PCR setup area.
- Open and close all sample tubes and reaction plates carefully. Do not splash or spray PCR samples.
- Keep reactions and components sealed as much as possible.
- Clean lab benches and equipment periodically with freshly diluted 10% chlorine bleach solution.
- Make sure all disposable used with RNA are RNase free and have only been handle with gloves

### **Materials:**

- Invitrogen High-Capacity cDNA Reverse Transcription Kit [4368814]
  - 10x RT Buffer
  - 10x RT random primers
  - 25x dNTP mix (100 mM)
  - MultiScribe Reverse Transcriptase (50 U/ $\mu$ l)
- Nuclease-free H<sub>2</sub>O
- RNase free microcentrifuge tube (0.6 or 1.5 ml depending on number of reactions)
- PCR tubes. These tubes are small, thin, and specific to PCR. Do not confuse with small (0.6 mL) Eppendorf tubes
- Example RT-PCR excel spread sheet to help with calculations
- Crushed ice in bucket

## **Procedure:**

1. Thaw purified RNA on ice.
2. Thaw components of Invitrogen High-Capacity cDNA Reverse Transcription Kit on ice
3. Prepare the 2x Reverse transcription master mix on ice:  
To a RNase free microcentrifuge tube, add the following to make the RT Master Mix:
  - a) 2 ul of 10x Reaction Buffer
  - b) 2 ul of 10x Random Primers
  - c) 0.8 ul 25x dNTP
  - d) 4.20 ul Nuclease-free H<sub>2</sub>O
  - e) 1 ul of Miltiscribe RT

\* These volumes are for a single reaction and should be scaled up depending on the number of total samples plus 1 to make sure you don't run out\*

\*See example spread sheet for automatic calculations\*

\*Good to prepare in the clean hood\*
4. Calculate amount of RNA to add for each sample. Use the example spread sheet to help with this calculation
  - a) Each experimental condition has to be the same amount of RNA loaded or results will be skewed during PCR
  - b) Depending on all concentrations of RNA, one will be limiting reagent for other conditions
  - c) Maximizing the yield of cDNA is ideal
  - d) The max amount of RNA to load is 2 ug per 10-ul reaction
  - e) The limiting RNA sample will have no extra water added
5. Get new, small clear PCR tubes, label, then put in a rack on ice.
6. Add respective amount of H<sub>2</sub>O to each PCR tube.
7. Add RNA to respective PCR tubes. Flux with water and carefully pipette to ensure all RNA is expelled
8. Then, to each individual tube of RNA, add 10 ul of the RT Master Mix. Flux carefully to mix.
9. Firmly cap each tube.
10. Briefly centrifuge the tubes to spin down contents and eliminate any air bubbles
11. Bring the tubes on ice to the thermocycler.
12. Turn machine on (switch is in back)
13. Choose run, and use the program named "JABRT".  
Program set up for this experiment is the following:
  - Step 1) 25 °C for 10 mins
  - Step 2) 37 °C for 120 mins
  - Step 3) 85 °C for 5 mins
  - Step 4) 4 °C, holdReaction volume: 20ul
14. Place small PCR blocker into machine to prevent small tubes from breaking (looks like a rectangle with small pegs in corner).

15. Place PCR tubes into small holes in block. Larger holes are used for bigger PCR tubes/reactions/
16. Close lid
17. Lock lid by turning until resistance is felt
18. Give lid an extra  $\frac{1}{4}$  turn to ensure lid is properly sealed
19. The program will run for approximately 2.5 hours.
20. Once complete, use nanodrop to quantify DNA concentration and dilute with nuclease free water to 20ng per 9 ul.
21. store cDNA at  $-20^{\circ}\text{C}$  for long term storage or at  $4^{\circ}\text{C}$  if intending to continue with qPCR within 24 hours.



## **Appendix T: Quantitative PCR (qPCR) Protocol**

Adapted from Jonathan Bezenah protocol and TaqMan® Universal Master Mix II protocol

### **Materials:**

- 7500 Fast Real-Time PCR System (Applied Biosystems)
- MicroAmp® Fast Optical 96-Well Reaction Plate with Barcode: (PN 4366932, PN 4346906)
- MicroAmp® Optical Adhesive Film (PN 4311971)
- PCR Reagent Real-Time TaqMan Universal Master Mix II With UNG [4440038]
- TaqMan Gene Expression Assay (FAM) [4331182] for appropriate gene (s) of interest and GAPDH or other appropriate internal control  
-FAM-MGB 20x
- cDNA from RT-PCR
- RNase free microcentrifuge tubes (0.6 ml)

### **Overview:**

Real time quantitative PCR is used for differential gene expression. It is essential to normalize gene expression to accepted internal controls (such as GAPDH) to assess for differential expression. Target amplification using cDNA as the template is the second step after RT-PCR to generate cDNA from RNA. In this step, the DNA polymerase (from the TaqMan® Universal Master Mix II) amplifies target cDNA using sequence-specific primers and a TaqMan® probe.

### **Notes:**

- Adhere to good PCR lab practices (outlined in rtPCR protocol) to avoid contamination
- Store Master mix in 4 C fridge and do not use if expired.
- Store TaqMan gene expression assays at -20C, protect from light, and thaw on ice as needed .
- For all sample reagents: Vortex briefly before use, and centrifuge to recollect.
- This protocol indicates 20ng of cDNA per reaction, this value is somewhat arbitrary. If you are low on cDNA you can dilute all of your samples you wish to compare; This assay is technically capable of quantifying as low as 1 ng per reaction, but I would not recommend lower than 5 ng per reaction.

### **Protocol:**

1. Primer Selection
  - Before qPCR, primers need to be selected for your gene of interest
  - TaqMan [Thermo Fisher] assay has primers specifically designed and fluorescently labeled for specific genes
  - No need to design primers
  - Purchase directly form Thermo Fisher Catalog
  - TaqMan is more specific than SYBR green PCR as fluorescent tags are associated with primers. SYBR green has fluorescent dye in reaction mix which integrates between all double strand nucleic acids

- If Thermo Fisher does not have primers, you will need to design your own for use with SYBR green
  - Protocol will work for both SYBR green and TaqMan
2. Use the example RT-PCR excel book to organize your plates for PCR.
    - Plates are relatively expensive and not intended for multiple uses so try to maximize samples per plate.
    - Print off the plate set-up so it is easier to refer to while pipetting.
  3. Thaw cDNA, and primers on ice. Keep lid on ice bucket to protect primers from light
  4. Vortex cDNA and primers then briefly centrifuge to recollect
  5. Gently vortex master mix stock solution
  6. For each gene of interest (types of primers) label an RNase-free 0.6 ml microcentrifuge tube for the gene of interest
  7. Prepare the TaqMan primer + Master mix solution for each gene of interest.
    - The ratio is 1 ul of TaqMan Primer and 10ul of Master mix per sample to be measured.
    - Best if each sample is measured in duplicate to assess pipetting error
    - Make enough for all samples to be measured twice plus an extra 11 ul in case of pipetting error.
    - e.g. if you have 3 replicates from 4 conditions per gene you are measuring: you will be measuring a total of  $3 \times 4 \times 2 = 24$  samples per gene so make  $11 \times (24+1) = 275$  ul of primer + master mix for each gene of interest
    - keep microcentrifuge tubes on ice while preparing
  8. Add 11 ul of the individual Master Mixes to their appropriate wells on Microamp reaction plate. Make sure to employ precise pipetting technique, it is essential that all wells receive precisely the same amount of master mix (accuracy is less important however). For each well, while pipetting, go to the first stop, then wait and let the master mix accumulate, then eject the rest.
  9. For each condition, take 9 ul of cDNA and add to the appropriate wells as indicated on the spread sheet. Make sure to again employ precise pipetting technique and use a different tip each time.
  10. Double check that all wells look like they have the same amount of liquid to assess if you forgot any conditions or made any mistakes.
  11. Once everything is added to the wells, seal the plate completely with MicroAmp Optical Adhesive Film
  12. Vortex the plate then take the well plate and put it in the giant centrifuge near the tissue culture hoods room and spin for 5 minutes at 5,000 rpm. You may need to swap the rotor attachment to spin the plates.
  13. Turn on PCR machine
  14. Use air or compressed duster can to remove any dirt/dust from bottom of PCR plate
    - \* Dust and debris can build up in PCR machine, leading to skewed results
  15. Place PCR plate into machine and close
  16. Run 7500 Software v 2.3
    - \*Ignore calibration and continue setup if prompted
  17. Go to advanced setup
  18. In the Experimental Properties tab:
    - a) Indicate Experiment name with details

- b) indicate 7500 Fast (96 Wells)
  - c) indicate Quantification- Comparative  $C_T$  ( $\Delta\Delta C_T$ )
  - d) indicate TaqMan Reagents
  - e) indicate standard ramp speed
19. In the plate setup tab define your targets (genes) and samples (conditions) and then assign targets and samples to particular wells.
    - Reporter (FAM), Quencher (NFQ-MGB) if using recommended TaqMan assay for this protocol
  20. In Run Method tab, check that the appropriate reaction volume is indicated (20 ul)
  21. You are ready to Run qPCR
  22. Extend cycles if needed, but if gene has not amplified by cycle 40, most likely gene of interest is not amplifying
    - \*Possible problems could be primer, cDNA integrity, machine calibration, blocked PCR well in machine, old reagents and primers, etc.
    - \*Extend cycle can only be performed once. Once an extra amount of cycle is added, you cannot add more cycle beyond that
  23. Once machine runs all of its cycle, a  $C_t$  value will be given for each sample
  24. Screen shot the amplification plot and plate set up, and export data to an excel file which can then be saved.
  25. Remove plate from machine. Plate can be reused if necessary, by carefully cutting away sealant, but this is highly discouraged. Only use wells that you did not used in previous experiments. If you accidentally spill amplified DNA into your workspace you may permanently contaminate it and jeopardize all future experiments.

### **Calculating $\Delta\Delta C_t$**

\* $\Delta\Delta C_t$  is taking the difference between two different populations to determine relative expression of one gene to another:

\* $\Delta\Delta C_t = [ (\text{Experimental Gene of interest } C_t \text{ value} - \text{experimental house keeping gene } C_t) - (\text{Control Sample gene of interest } C_t - \text{control house keeping gene } C_t) ]$

-Your chosen control is arbitrary and you will get the same relative expressions no matter what you choose, each replicate must be normalized to same control however, to conserve scaling between replicates.

-There are numerous house keeping genes (present in all cells) such as 18 s, GAPDH, and beta-actin. You should research for your intended purpose which housekeeping gene may be most appropriate to choose

-House keeping genes are generally consistently expressed at a similar level regardless of environmental condition.

-Fold change in gene expression is  $2^{(-\Delta\Delta C_t)}$ .

## Appendix U: In Vivo Subcutaneous PEG hydrogel implantation protocol

### Overview:

This procedure is for the subcutaneous implantation of PEG hydrogel pucks on the dorsal flank in a murine model of hydrogel scaffold vascularization. Pre-forming hydrogels allows for mechanical characterization of parallel hydrogels, and direct comparison to in vitro controls. Implanting pre-formed hydrogels may, however, also elicit a fibrotic response and poor integration of the scaffold with host tissue, diminishing its capacity for inosculation with the host.

### Materials:

- Puralube® Vet Ointment – Sterile ocular lubricant (Dechra, Overland Park, KS)
- Small cotton-tipped applicators Cat. No. 23-400-115 (Fisher Scientific)
- Sterile alcohol prep pads (Fisherbrand®)
- Sterling nitrile sterile powder-free exam gloves. KC300 (Kimberly-clark, Roswell, GA)
- Polylined sterile drape field. (18 in. x 26 in.) Ref No. 697 (Bosse, Hauppauge, NY)
- Isoflurane
- Carprofen
- Sterile PBS
- Sterile surgical scissors
- Sterile scissors for blunt dissection
- Sterile forceps (at least 2 pair)
- Sterile lab spoon (not micro lab spoon)
- 5-0 nylon suture and needle drivers
- Additional materials: Cap, gown, mask, shoe covers, warming pad/blanket, heating lamp, nair hair removal, hair clipper, betadine antiseptic solution, 70% ethanol.

### Notes:

- Recommended hydrogel properties to target are 100-150 pascals shear modulus to minimize hydrogel stiffness while still providing a robust enough construct to handle and implant.
- 50 ul pucks cast in a 1ml syringe, per the standard protocol, can be easily implanted through a 1 cm incision on the back of 6-8 week old CB17 mice. If a larger construct is desired you may need to switch to a different mouse strain with larger adults.
- Recommended cellular densities are 5M/ml each cell type. In a preliminary in vitro assay, cell density of 5M/ml of each cell type provided better vessel formation than either 2M/ml or 10M/ml each cell type. There appeared to be nutrient limitation for 10M/ml with a substantial proportion of ECs remaining un-spread.
- This procedure is much easier to perform **with an assistant** for the hydrogel implantation step

### Protocol:

1. Keep in mind that mice must be left in their housing facility for 3 days to acclimate prior to surgery. Check on mice when they arrive. NOTE: Appropriate gown, gloves, face

- mask, cap, and shoe covers must be worn prior to handling animals. Make sure to wear appropriate PPE before entering animal room.
2. Follow the Casting PEG hydrogels protocol to generate hydrogels for implantation the day before surgery (or other predefined period of time for your purposes)
    - Ensure that hydrogel formulations are optimized for the generation of hydrogels with shear moduli greater than 100 pascals. I target ~130 pascal hydrogels because there is decent vessel formation at this modulus and given the typical fluctuations in PEG modulus due to pipetting error it is likely that most gels will be at least 100 pascals.
    - Make sure that all parallel controls are cast from the same batch of hydrogel precursor solutions from the same cell pellet. Small pipetting errors between batches can result in large differences in hydrogel mechanical properties and resulting cellular behavior.
      - For each animal timepoint, I would recommend generating a parallel control to measure mechanical properties and cell densities (from the same gel) on day 1 (day of surgery) and another for measuring vessel density on the day of recovery. If you are not implanting on the day after casting (i.e. to implant a preformed network) I would recommend also casting an additional gel for the day of implantation. To minimize total number of controls needed for multi-time point recoveries, I would recommend casting paired gels for each time point in vivo and in vitro so the same day 1 control can be used for each time point.
    - If you are comparing multiple hydrogel formulations (different crosslinker, different RGD concentration, different modulus) I would recommend casting paired hydrogels with identical cellular pellets.
  3. The day before surgery it is also a good idea to prep your surgical space.
    - Spray down and wipe the surgical bench with Clidox spray. Turn on the snorkel and leave running over night to reduce smell.
    - Spray down the surgical room cell culture hood with ethanol and leave UV light on for at least an hour to sterilize (ok to leave on overnight)
    - Check that you have enough oxygen.
    - Check that you have enough isoflurane in unit and/or a spare bottle on hand
    - Make sure you have enough/appropriate autoclaved tools to perform surgery
  4. On the day of implantation, before preparing for surgery, measure the mechanical properties of each of your paired dl hydrogel controls. Make sure that paired conditions have similar mechanical properties. Hydrogel mechanics have a dominant effect on cellular behavior, if mechanics are not matched then you will not be able to draw any conclusions. Usually there is very little variability within a single batch, but there is often ~20% variability between batches despite good pipetting practices.
    - \*If your hydrogels do not have acceptable properties it may be smart to scrap your experiment and try again instead of moving forward with surgery.
  5. Before retrieving mice, set up isoflurane machine
    - a) Plug in active scavenging unit and turn on
    - b) Ensure isoflurane tank has enough isoflurane in it.
    - c) Attach Oxygen tube to Oxygen tank.
    - d) Turn valves to flow through inoculation chamber (plastic box next to scavenging unit.
    - e) Close valves going to nose cone
    - f) Weigh charcoal filter and record. Replace if needed. Attach to scavenging machine.

- g) Place a few paper towels in the inoculation chamber (mice tend to release excrement when under anesthesia)
  - h) Turn flow to 1 L/min
6. Set up bead sterilizer to sterilize tools between animals. It is ok to re-use the same set of tools on up to 5 animals before needing to set aside for autoclaving.
  7. Set up warming pad.
  8. Lay down a non-fenestrated drape over the heating pad to define surgical area on bench. The nose cone should easily be able to reach.
  9. Retrieve mice from housing facility and an extra cage for recovery. Place both on the table away from the surgical area and obstruct the view between cages so mice can not see littermate recover.
    - Recovery cage needs heating pad underneath
  10. Block off the gap under the door in case a mouse escapes.
  11. Place a clean plastic waste container on mini scale on the table next to the mouse cage.
  12. Remove one mouse from the cage and place on scale. Record weight on the surgical records sheet.
  13. Carefully, put mouse into the inoculation chamber by inverting weight container
  14. Turn isoflurane to 5%.
  15. Wait until mouse stops moving and breathing is slowed (~2 minutes)
  16. Record time of surgery begin on the surgical sheet.
  17. Once mouse is anesthetized, move mouse to surgical area
  18. Put nose cone over the mouse's face.
    - \*Metal bar in nose cone should be parallel to the table and positioned closest to the table.
    - \*Metal bar is to prop the mouse's head up and allow for proper breathing
  19. Work quickly to turn valves closed going to inoculation chamber and open going to the nose cone to avoid mouse waking up
  - 20. Change isoflurane to 1.5%**
  21. If mouse starts waking up during transfer wait a minute before proceeding.
  22. Using a cotton tip applicator, liberally apply Paralube Vet ointment to each eye to ensure the eyes do not dry out during surgery
  23. Prepare a 5 mg/ml solution of carprofen from stock in sterile PBS. Make enough for all surgeries for the day (assuming you will use less than 300ul per mouse).
    - Dosage of carprofen (5 mg /kg) results in injection in microliters equivalent to weight of mouse in grams (i.e. a 230 g mouse requires a 230 ul injection of 5 mg/ml carprofen)
  24. Using a 28G ½ needle (insulin syringe), inject the mouse with carprofen subcutaneously
  25. Once analgesia has been applied to mouse, shave the back of the mouse. It is best to shave the entire back of the mouse to ensure the hydrogel is implanted under a hairless region. Be careful not to abrade the skin.
  26. Apply Nair to the shaved area to remove remaining excess hair.
  27. Using PBS and ethanol, remove any excess Nair. The mice are sensitive to Nair and excess will lead to irritation and cause them to bite and scratch area around implant
  28. Apply a few drops of Betadine antiseptic solution to the surgery area and wipe away with an ethanol wipe
    - Repeat 3x to sterilize the surgical site
  29. Tape down feet and hands of mice with lab tape so that the mouse is spread out.

30. Put down fenestrated drape over the mouse
31. Drop surgical scissors and forceps onto the sterile area.
32. Have sterile PBS and sterile cotton swabs ready to wet surgical site if needed.
33. Open sterile lab spoon in hood and leave on sterilization pouch for ease of use.
34. Have assistant retrieve hydrogel(s) from incubator and put in hood while waiting to implant
35. Remove gloves and put on sterile nitrile sterile powder-free exam gloves.
36. Check depth of anesthesia by checking for slowed breathing rate and lack of withdrawal reflex from gently squeezing hind toes.
37. Use forceps to tent up skin, separating the skin and the underlying musculoskeletal system, and use the surgical scissors to cut ~ 1 cm longitudinal incision along the tensor fascia latae muscle (along the groove where the leg joins the back in the lumbar region) on one side of the mouse.
  - It is best if this incision is done with a single cut so that it is straight and clean
38. Blunt dissect along the dorsal flank of the mouse to create a sub cutaneous pocket to implant the hydrogel in.
  - You will need to blunt dissect a square pocket with proportions ~1 cm wide by ~2 cm deep.
  - Wet the incision with sterile PBS if it appears to dry at any point
39. Tent the pocket up, and have your assistant carefully retrieve the hydrogel for implantation on a lab spoon and hold the spoon flush to the incision.
40. Use a second pair of forceps to push the hydrogel into the subcutaneous pocket.
  - Be careful not to trap air in the pocket with the hydrogel. If air does become trapped, you can use your forceps to create a gap between the hydrogel and the implant to allow air to escape.
  - Make sure hydrogel is oriented with a flat side against the musculature
41. Close the surgical site with simple interrupted sutures (3-4 sutures per incision).
42. Repeat steps 36-40 on the other side if needed. Be careful to mirror your incision and blunt dissection as precisely as possible so that all implant sit in similar spots.
43. Place mouse in recovery cage and turn isoflurane to zero
44. Record time of surgery end
45. Once mouse is ambulatory, record recovery time on surgery.
46. Spray surgical tools with ethanol and sterilize with the bead sterilizer for ~1 minute. After sterilization place on sterile drape to cool down.
47. Repeat procedure for all mice, a new fenestrated drape should be used for each mouse but the same non-fenestrated drape can be re-used if it remains in good condition.
48. All cage mates should stay with the same cohort through out the experiment. Do not mix mice from different cages after surgical procedure.
49. Return all mice to housing area in fresh cage, add enrichments to cage.
50. Clean up surgical area
51. Administer another dose of carprofen ~24 hours after surgery.
52. Monitor mice each day for signs of distress or pain and note the appearance of the surgical site.

## **Appendix V: Implant retrieval and fixation protocol:**

Adapted from Jonathan Bezenah protocol.

### **Overview**

This procedure is for the recovery of PEG hydrogels implanted in subcutaneous pockets. It is appropriate for histology as well as staining for whole mount imaging.

### **Materials:**

- Z-fix
- 20 ml glass scintillation vials
- Surgical scissors
- Forceps
- PBS

### **Protocol:**

1. At the appropriate time to harvest implants, place all mice for the particular time point into a single cage (up to 12 mice can be grouped for sacrifice).  
\*group all mice together into a single cage in the hood in the animal room.
2. Check the directions for animal sacrifice. Feed the hose from the CO2 tank into the cage and turn the valve to the small mammal indicator
3. Monitor mice to ensure they are not in distress.
4. Once mice stop breathing and fall still, one at a time, move mice to hood and place on paper towel.
5. Using surgical scissors open the chest cavity to create a pneumothorax, and sever the descending aorta to ensure exsanguination.  
\*Repeat for all mice to ensure euthanasia
6. Bring mice upstairs to harvest implants
7. Clean off mice by spraying with 70% EtOH
8. Using scissors and forceps, create skin flaps cranially and caudally of implants to move excess skin out of the way for excision.
9. Use surgical scissors to cut a circle in the skin around each implant.  
\*It is best to keep skin adherent to implant and try not to disrupt the interface between the skin and implant. This will help with orienting the sample, and is important for assessing integration of the implant with host tissue and possible fibrous capsule formation.
10. Try to cut under the sample to retrieve a thin layer of muscle adhered to the sample.  
\*keeping tissue adherent to the sample on all sides will help reduce sample shrinking while dehydrating for paraffin embedding.
11. Place each implant into 20 mL vials containing Z-fix formalin.  
\*Allow samples to fix for 4 hours
12. After 4 hours in Z-fix, pipette out Z-fix to proper hazardous waste disposal container and replace with 10x diluted Z-fix in PBS and leave in fridge overnight.
13. Once implants are removed, wrap all mouse carcasses in paper towel and put into separate gloves. Tie off the gloves then place in another glove and tie off so each carcass is double gloved.
14. Write Putnam on the gloves and write the date.
15. Place in appropriate disposal area (typically fridge in surgery room)



16. After implants have been fixing in fridge for 24 hours, remove Z-fix and properly dispose
17. Rinse implants with PBS (4 times) properly disposing of rinses
18. In a petri dish trim off excess skin.
19. Add 70% ethanol to 20 mL vials containing implant and store in fridge until tissue processing.
20. If you wish to whole-mount image your construct:
  - Leave skin on to help with orientation while imaging
  - The skin will be very tough after fixation and difficult to cut with a scalpel, use a pair of surgical scissors to cut around the skin where you intend to bisect with the scalpel/razor. Try to cut superficially to avoid the hydrogel. I would recommend bisecting the implant to retrieve 2 identical halves. When viewed on the microscope one side of the hydrogel should be against skin and the other against muscle so you can qualitatively assess differences in vascularization/inosculation
  - At this point, proceed with the standard cutting and staining protocol outlined for PEG hydrogels.

## **Appendix W: PEG hydrogel explant dehydration and paraffin embedding**

Adapted from Nicole Friend protocol

### **Materials:**

- Pink or white (large) embedding cassettes (UNISLETTE cassette with lid, Simport, Canada)
- 70% ethanol
- 1L beaker

### **Notes:**

- Paraffin embedding and sectioning of PEG hydrogels is notoriously difficult and subject to substantial processing artifact. Dehydration of PEG hydrogels results in substantial hydrogel collapse and hydrogels often fall out of tissue sections while sectioning. Be aware of these limitations and take them into consideration when optimizing your procedure and analyzing your results. Most groups opt for cryo-sectioning instead, however, cryo-sectioning has its own set of difficulties. Make sure to assess the pros and cons of each method and decide what is best for you.

### **Procedure to dehydrate tissue explants**

1. Label one cassette per sample with sample information
  - \* use a pencil for labeling as embedding chemicals will remove ink and markers
  - \* pink cassettes can be used for most samples, but if samples are larger they may need a white cassette. **DO NO SQUISH SAMPLE**. If sample is squished it will collapse more, just use a white cassette.
2. Fill a 1L beaker with enough 70% ethanol to submerge all cassettes.
3. Use forceps to transfer samples from glass storage vials to cassettes
4. As each sample is transferred to a cassette, place the cassette into the 70% ethanol so they do not dry out while transferring remaining samples.
  - \*You can process up to 20 samples at a time.
5. Once all samples are ready to be dehydrated, prepare the Leica Tissue Processor
  - \*Wear a respirator (stored in drawer below) when working with the tissue processor
6. Check solution levels by raising the plastic cover/top portion of the machine by pressing the up arrow ↑ button. Check the log to see if the solutions have been changed within the last month. If solutions look low, coordinate with the Coleman lab to refill.
7. Move the grey arm (that will hold the basket) to position 4 by pressing the rotate button, which is a dashed circular arrow
  - \*This can only be done when the top component is raised
8. Put samples in metal basket and place the basket on the grey arm connector
9. Lower the top component, and basket into the first 70% ethanol bath by pressing the down ↓ arrow
10. Press “start”
11. Check the setting is program #1, P1, and if not then adjust using the + or – buttons
  - \*double check that this program is set to start in position 4 and spend 1 hour in each position (4-12)

12. Adjust the time if needed so the machine runs overnight (due to noise and chemical release)
  - a) Hit the right arrow → to show the start time
  - b) Timing can be adjusted by pressing the left and right arrows to select position and the + and – buttons to adjust the numbers
  - c) START: # - ##:##
    - \* the first # is the date (set to 0), the second ## is hour, the third ## is the minutes
  - d) Program takes ~ 10 hours to finish so start at 10 pm (0-22:00) to finish by 8 am
13. Press “start” again once desired time is set
  - \*you can press the clock button to confirm when the procedure will start, then press it again to see when the procedure will end
14. Turn on oscillations with the button that has three up and down arrows with a top and bottom border
15. Close plastic cover
16. Leave over night

### **Procedure for paraffin embedding**

1. Samples should now be in position 12 of the tissue processor, which is hot paraffin wax.
2. Before removing samples, prepare an ice bucket with on top of the ice
3. Turn on the cooling block of the embedding station by pressing the “cool” button
  - \*a red indicator light will turn on
4. Clean the station of excess wax
5. Wearing a respirator, raise the top of the machine with the up arrow button and remove the basket containing your samples, placing it on the counter next to the embedding station. Be careful to move it quickly as it will be hot to the touch
6. Lower the top component of the machine with the down button, and stop the oscillations by pressing the oscillation button. Close the plastic cover.
7. Transfer cassettes with samples in them to the paraffin bath on the right-hand side of the station.
8. Select a sample to embed, and move it to the hot block under the paraffin dispenser
  - a) If sample is in pink cassette already, remove and discard the top of the cassette.
  - b) If sample is in white cassette, label a pink cassette with the sample information and discard the white cassette.
  - \*You must mount samples onto a pink cassette as the base because the microtome does not fit the white samples.
9. Select a metal tray from the bath on the left hand side of the station that will fit your sample within the inset and move it to the hot block.
  - \* The PEG explants tended to need the deeper trays because of the large amount of skin associated. If there are not enough deep trays present, ask recent users of the embedding station if they haven’t punched their blocks out yet.
10. Transfer the sample from the cassette to the metal tray
11. Using forceps to push the lever behind the hot block, dispense enough wax to cover the sample

12. Position the sample in the center of the tray and adjust sample orientation. I oriented samples with the skin side down. What ever side is down here will be sectioned first by the microtome.
13. Place the labeled pink cassette on top of the samples, being careful not to move the sample. The hand written label should be facing upwards.
14. Add more wax to fill the cassette. Add wax adjacent to the sample instead of directly on it to help prevent it from moving.
  - \*wax should be added until there is a convex “bubble” of wax on the surface.
15. Carefully move sample to the cooling block
  - \*While one sample is cooling you can start working on the next
16. Once sample has mostly solidified, move sample from cooling block to the foil over ice
17. Once all samples are on ice, cover the bucket with a lid and leave samples to finish solidifying for at least four hours, but preferably overnight, in the 4C fridge
18. Add paraffin wax chips to the paraffin bath and paraffin reservoir at the top of the station if either is low.
19. Turn of cooling block
20. Clean any extra wax on the station using the scraper, clean wax out of the collecting trough.
21. After paraffin blocks have hardened, they need to be prepared for sectioning
22. Prepare a bucket of ice with some water
23. Using a razor blade, remove the wax around the cassette and the metal tray until you can pop the cassette with the wax block (containing sample) out to the tray
24. Place the samples in the prepared ice bath and put the metal trays back into the bath on the left-hand side of the embedding station.
25. Trim the extra wax to make a square around the around the edges of implant.
  - \*Do not trim all the way down to the surface of the cassette top, it important that you leave a layer of wax so that the sample stays firmly attached to the cassette.
  - \*Leave about 1 mm of wax around the edges of the sample
  - \*It is always safer to leave too much wax
26. Cut two corners of the block to make it more of a house shape.
  - \*You should cut the corners on the same side as the side of the cassette that is labeled.
  - \*These are just for orienting the samples, you do not want your block to be pointy. The side with the cuts should still have as much flat side as possible so there is maximum surface area to hold the ribbon together while sectioning.

## Appendix X: Paraffin sectioning

Adapted from Nicole Friend protocol

### Materials:

- Pencil
- Super frost microscope slides
- Razor blade
- Paper towels
- Static gun
- Spray bottle of 70% ethanol
- 10% ethanol bath (in 1 ml pipette box with rack removed)
- Samples in an ice bath

### Procedure:

1. Make sure to reserve time on the microtome sign up sheet (usually 3-4 hour blocks at a time)
2. Bring down all materials to the microtome bench.
3. Turn on hot blocks (s). They should be set from 39-45 C
4. Plug in and turn on the hot water bath.
  - \*The temperature nob should be set to the marked line
  - \* You can put the lid back on to speed up heating, but be careful because it may become too hot and disintegrate your initial samples
  - \*refill wter bath with MilliQ water if needed.
5. Label slides then place labeled slides on plastic slid holder. (It is typical to need at least 40 slides per sample)
6. Retrieve microtome blade from the drawer under the hot blocks and place it into the slot on the microtome.
  - a) unlock the blade holder by using the lever on the right side of the stage and slide the blade into the opening
  - b) Adjust the blade and stage so that the sample will be cute with the left most portion of the blade, so as the blade dulls or chips you can progressively slide the blade over for a fresh blade surface.
  - c) lock the blade in place using the same lever, then cover using the gold safety cover so you do not cut yourself. **THE BLADE IS EXTREMELY SHARP.**
7. Move the head of the microtome all the way backwards away from you by turning the big, lower knob on the left side clockwise.
8. Move the stage away from the head by unlocking it using the lever on the left of the stage and pulling the stage towards yourself.
9. Dry the sample and place it into the slot on the head.
  - \*This is done by pulling the silver lever on the head towards yourself, inserting the sample (with labeled side down), and releasing the lever which will secure the sample in place.
10. Unlock the large lever on the right side of the microtome by flipping the small, black lever below it up and move the sample to be centered with the blade.
11. Move the stage close to the sample surface, roughly 0.5mm away, and lock into place

12. Line up the sample surface so that the surface plane of the sample is parallel with the plane of the blade.
  - a) Remove the blade cover to make visualization easier, but be careful not to cut yourself
  - b) Unlock the head positioning using the lever on the right side of the stage, then use the nobs on the left side of the head
  - c) Lock back into place.
  - d) Move the sample up and down using the large lever on the right side to evaluate that the planes of the sample's face and blade look parallel.
  - e) unlock, adjust, then relock and assess again if needed.
13. Set your desired slice thickness using the small textured knobs on either side of the top of microtome.
  - \*5 micron thick slice are typical for most tissues, but the thinnest sections of PEG I found consistent to work with was 12 microns.
  - \*This thickness will drift over the course of sectioning so periodically check on it readjust as needed.
14. Move the stage as close as possible to the sample without the surface touching the blade and then lock into place.
15. Using the large lever on the right, start moving the sample toward the blade one rotation at a time.
  - \*it doesn't matter which direction you rotate the large lever to make the sample move forward.
16. If you have the lid on the water bath take it off at this point to let cool back down
17. Once the sample contacts the blade it will start sectioning, it will slice off one section per rotation, with each subsequent sample adhering to the previous sample creating a ribbon.
  - \*Hold up the ribbon with a pair of forceps
18. Once the ribbon is too long to hold, or tears, place it to the left of the microtome on the counter.
  - a) it is generally most time efficient to generate multiple ribbons at a time, before moving onto the next step of transferring them to slides.
  - b) Place them shiny side down, they will come off the microtome this orientation
  - c) Place them in order to keep track, and be careful not to accidentally touch the ribbons with your elbow or anything as you continue to section.
19. Find where your sample starts in your sections, i.e. when there is a different texture in the center of the section.
  - a) use some of your blank sections to test the heat of the water bath, if they disintegrate then the bath is too hot. You can add some MilliQ water to bring the temperature back down but leave knob set to mark.
  - b) Once you are sure the water bath is at the appropriate temperature, you can discard your remaining blank sections.
20. Using a razor blade cut your ribbons into strips of 4-5 sections.
  - \*keep in mind that all of these sections will be stained identically, if you want to do multiple different stains on a particular series of strips, cut into 2-3 section strips.
  - \* be careful when cutting strips to maintain order
21. Using forceps, transfer one strip of sections of sections to the 10% EtOH bath, and gently try to flatten out the sections and remove air bubbles from under them.

- \* You will not be able to get them perfectly flat; the hot bath will help flatten them, but you need to remove air bubbles here by lifting the sections with the forceps. You will not be able to remove air bubbles once the samples are softened in the hot bath.
- 22. Using the appropriate labeled slide, scoop under the section, making sure the whole section is on top of the slide, and transfer to the hot bath.
  - \*Do the transfer quickly so the sample doesn't stick to the slide in the hot bath
  - \*Come into the hot bath at 45° so the sections float off
  - \* Be careful not to touch the bottom of the water bath as this will disrupt the bubbles and they will float up under your sample ruining it.
- 23. Once the sample has flattened out, carefully collect it on the slide by positioning the slide underneath the sample and pulling up at an angle.
  - \*Be careful not to disrupt any air bubbles on the bottom of the bath
  - \*Timing is absolutely essential here to generate useable PEG sections. If you don't give it enough time to flatten then your sample will dry crinkled, if you wait too long then the PEG implant will separate from the surrounding tissue. ~10-15 seconds is good, but this will take time to practice and attention to detail for each slide.
- 24. Place slide on hot block and leave overnight for sample to dry and fully adhere to the slide.
- 25. Repeat for all remaining sections.
  - \*periodically clean out wax fro hot water bath with a blank slide
- 26. Periodically remove wax fragments on the stage/blade with paintbrushes. Always brush the blade upwards so you do not cut the bristle off and dull the blade.

**General sectioning tips:**

- You can leave white slide label overhanging on the edge of heating block allow for more slides to be processed at a time as this part does not need to be heated.
- If paraffin starts tearing as you are sectioning, try the following:
  - a) Tissue block can become too soft causing the paraffin to tear. Using a paper towel, spray the tissue block with 70% ethanol. Then Place and hold an ice cube on the tissue block for a minute
  - b) Blade can get dull causing the paraffin to tear. Adjust the blade so a fresh section of the blade is cutting the tissue block.
  - c) Avoid excess moisture around paraffin strips. Moisture will cause paraffin strips to stick resulting in loss of sections
- If the weather is particularly dry, you may want to use the static gun to reduce the likelihood of the sections sticking to the razor, counter, forceps, hands, etc.

## **Appendix Y: Hematoxylin & eosin histology staining protocol**

Protocol adapted from Ana Y. Rioja protocol

### **Materials:**

- Mayer's Hematoxylin (Electron microscopy sciences 26252)
- Eosin Y (Sigma HT 110132)
- Xylene
- 100% Ethanol
- 95% Ethanol
- 70% Ethanol
- Separate stain container for each step
- Paramount solution

### **Notes:**

- The entire procedure takes about 1 hour 15 minutes to complete for one cassette. If you want to do more than one cassette wait until the first cassette is in the hematoxylin before starting the next.
- Solutions can be reused for 4-5 cassettes, but make sure not to reuse the same solution for different steps. EACH STEP SHOULD HAVE ITS OWN WASH BATH AND NOT USED FOR ANY OTHER STEP.

### **Protocol:**

1. Determine slides of interest for staining and place into slide cassette
2. Prepare area in fume hood for staining by laying down paper towels and set up and fill all the various slide cassette baths with their appropriate solutions.  
\*Pour xylene in hood and be careful not to spill
3. Wash slides with Xylene 2X for 5 mins per wash
4. Wash slides with 100% ethanol 2X for 3 mins per wash at RT
5. Wash slides with 95% ethanol 2X for 3 mins per wash at RT
6. Wash slides with 70% ethanol 1X for 3 mins per wash at RT
7. Wash slides with DI water 1X for 3 mins at RT
8. Incubate slide in hematoxylin solution for 15 mins at RT  
\*At this point you can start the next set of slides if you are doing multiple sets
9. Place slide cassette in tap water container
10. Pour rinse down drain
11. Add new tap water to container
12. Mover slide cassette up and down to rinse slides
13. Repeat 10 – 12 until waste solution is clear
14. Add new tap water to container and rinse for 15 mins at RT
15. Wash slides with 95% Ethanol 1X for 30 seconds at RT
16. Stain slides with Eosin 1X for 1 min at RT
17. Wash slides with 95% Ethanol 1X for 1 min at RT
18. Wash slides with 100% Ethanol 2X for 1 min at RT
19. Wash slides with Xylene 2X for 3 mins at RT
20. Mounting coverslips on slides:
  - a) Double glove



- b) Remove cover slips from container and set upright leaning on wash containers for easy access (Xylene makes gloves slicky and will be hard to remove from container between slides)
  - c) One at a time, remove sample slides from cassette.
  - d) Add 3 to 4 small drops of Paramount solution using a cotton tip applicator onto coverslip and place it on top of the slides
  - e) use a kimwipe to carefully remove xylenes and excess paramount from the bottom of the slide to prevent the slide from sticking to your drying surface
  - f) Lay slides flat and let dry over night in the fume hood
21. If excess paramount has accumulated on the bottom of the slide or on top of the coverslip it can distort your images. Once the coverslip has dried you can dip a cotton applicator in xylene and rub off the excess paramount. The dry the slide with a kimwipe.